Relationships between cyanobacteria and water colour in Central North Island lakes of contrasting trophic status

A thesis

submitted partial fulfilment

of the requirements for the degree

of

Master of Science (Research) Ecology and Biodiversity

at

The University of Waikato

by

Lisa Reed

THE UNIVERSITY OF
WAIKATO
Te Whare Wānanga o Waikato

Year of submission

2022

Abstract

Nutrient enrichment of lakes and rising global temperatures promote the proliferation of cyanobacteria. Cyanobacterial blooms are becoming more widespread and increasing in frequency, size and duration, causing a cascade of detrimental changes to freshwater ecosystems. Improved lake monitoring techniques are required for early detection of bloom initiation to allow mitigation measures to be better targeted. Recent studies suggest remote sensing of the reflectance spectra of lakes can be a valuable tool to map the distribution of potentially toxic cyanobacteria in near-real time, though as yet, these are not widely used in New Zealand. In this study, three Rotorua and five Waikato Lakes were sampled to determine hyperspectral reflectance, phytoplankton composition and biovolume, chlorophyll *a*, phycocyanin concentrations, and optically active constituents. The data obtained were used to develop algorithms to examine the utility of reflectance data to aid in estimations of chlorophyll *a* and phycocyanin concentrations and phytoplankton composition with a particular focus on cyanobacteria. Results show that relationships amongst reflectance-related attributes, including chromophoric dissolved organic material, suspended solids and absorption properties of phytoplankton and pigment concentrations varied among the lakes and, to varying extents, over time. Properties of specific regions of reflectance spectra could be used to predict concentrations of these two pigments, but reflectance was not effective in separating the effects of phytoplankton composition from the other optically active variables. The two algorithms best suited these lakes for estimation of chlorophyll *a* and phycocyanin showed strong relations with the observed pigments at $R^2 = 0.83$ and $R^2 = 0.92$, respectively. This suggests reflectance spectra and the appropriate algorithm can be used to yield estimations of chlorophyll *a* and phycocyanin concentrations within inland waters with a wide variation of bio-optical characteristics. Such information could contribute to the development of an early warning system to predict cyanobacterial biovolume in New Zealand lakes using remote sensing.

Acknowledgements

I am extremely grateful to my supervisor Professor Ian Hawes for his expertise, time and patients. You helped me see the light at the end of the tunnel as daylight and not the train I secretly at times felt it was. I appreciate you taking the time to accompany me out into the field, not to mention the valuable advice and guidance in writing this thesis. To Moritz Lehmann, thank you for your expertise in all things remote sensing and your support.

Thank you to the 'Eye on Lakes' team for their regular updates and enthusiasm for the project. When part of a bigger project, it helps to know that the people on your team are committed to achieving a shared goal.

To the field staff at the Marine Research Station in Tauranga, who drove boats, booked equipment, and always had a smile to share, thank you! I would like to thank Grant Tempero for his filter analysis and Warrick Powrie for his secret supply of Lugol's iodine.

Special thanks to Cheryl Ward, the best sciences librarian a student could ask for. You were so calming and guided me through formatting this thesis via zoom due to covid restrictions. Your patience was very much appreciated.

This would not be possible without the financial assistance from the Eye on Lakes project, for which I am very grateful.

Finally, this thesis is dedicated to my fur buddies. You are always there, reminding me to live in the moment and bring perspective into my life. To Ben, Wilson, Blinky & Mr Nibbles, who passed during this thesis. *"How lucky I am to have something that makes saying goodbye so hard", A.A.Milne.*

Table of Contents

List of Figures

List of Tables

List of Abbreviations

a_{CDOM} = Absorption of CDOM

a_{NAP} = Absorption of non-algal particles

a_p = Absorption of phytoplankton

$a_p(\lambda)$ = Absorption of phytoplankton at wavelength λ

BV = Biovolume

CDOM = Chromophoric dissolved organic matter

Chl *a* = Chlorophyll *a*

NIR = Near infrared

pc = Phycocyanin

Rrs(λ) = Reflectance at a wavelength λ

Rrs(chla) = Reflectance at a waveband absorbed by chlorophyll *a*

Rrs(pc) = Reflectance at a waveband absorbed by phycocyanin

TSS = Total suspended solids

Chapter 1

Introduction

1.1 Eutrophication in lakes

The increasing human population has put immense pressure on earth's resources, with land conversion and intensification of food production leading to the deterioration of the environment across the globe (Foley *et al.*, 2005). Freshwater ecosystems are used extensively to provide goods and services; however, water quality continues to decline, caused by pollutants, increased nutrient and sediment input, water extraction, and altered flow patterns (Matson *et al.*, 1997). Combined with the global climate changes, at-risk water bodies are experiencing accelerated eutrophication, with local, regional, and global consequences (Paul *et al.*, 2012; Hamilton *et al.*, 2019).

Eutrophication is a particular problem for freshwater ecosystems and relates to the over-enrichment of nutrients, particularly nitrogen and phosphorus, usually as a consequence of industrial, agricultural or wastewater contamination. The immediate effect of nutrient enrichment is typically to promote the growth of phytoplankton. Increased phytoplankton growth can lead to algal bloom formation and a cascade of deleterious effects. For example, when blooms decrease water clarity and form surface-floating-scums, this can suppress the growth of submerged macrophytes (Zhang *et al.*, 2017) and decomposing cyanobacterial blooms may induce hypoxia, leading to the deaths of fish and other benthic biotas (Huisman *et al.*, 2018). Blooms are typically fuelled by nutrient enrichment but are also linked to a complex combination of physical (light attenuation, temperature and stratification), chemical (pH, oxygen depletion), and biological factors (shading and predation) (Harper, 1992; Paerl, 2008).

Cyanobacteria and algal blooms

Cyanobacteria are an ancient lineage of prokaryotic organisms, the majority of which fall within the Oxyphotobacteria (also known as blue-green algae), which, as their name suggests, are capable of oxygenic photosynthesis. Indeed, their evolutionary journey (dating back to

over 3.5 million years ago) is thought to have led to oxygenation of the earth's atmosphere, and through multiple symbiotic events, some of them became chloroplasts, facilitating the evolution of higher plants and the high-oxygen world that we currently inhabit (Schopf, 2000).

There are approximately 150 genera and 2000 species globally, ranging in morphology from spherical, spiral and cylindrical unicellular cells and filamentous and colonial multicellular forms (Skulberg *et al.*, 1993). Over time Cyanobacteria have evolved many adaptive eco-physiological traits that allow them to occupy a diverse range of environments, including extreme temperatures (Hawes *et al.*, 2016), light, pH and nutrient concentrations, such as glaciers and hot springs (Paerl & Otten, 2013). Many traits are genus-specific and include nitrogen fixation, phosphorus storage, gas vesicle production, akinete formation, and toxin production (Whitton & Potts, 2007; Carey *et al.*, 2012; Huisman *et al.*, 2018). Due to the range of adaptations and traits, cyanobacteria have proved able to tolerate the unusual features of eutrophic environments and can exert competitive dominance over less tolerant, sensitive species enabling planktonic or benthic bloom development (Rahel, 2007; Huisman *et al.*, 2018). Evidence shows cyanobacterial blooms are occurring more frequently, on a larger scale, with a more prolonged duration. Many studies conclude that the prevalence of cyanobacteria is likely to increase with climate change, and there is an expectation that cyanobacteria will become increasingly problematic for ecosystem management in the future (e.g. Hamilton *et al.*, 2019).

A key issue with cyanobacteria is their ability to produce toxins; indeed, for many people, the word cyanobacteria immediately conjure the phrase "toxic cyanobacterial bloom". Twenty-five genera of cyanobacteria, containing 40 species, are known to produce cyanotoxins, eight of these genera inhabit freshwater (Carmichael, 2001). The most common cyanotoxins are hepatotoxins (microcystin, nodularin and cylindrospermopsin) and neurotoxins (anatoxin and saxitoxin) and include some of the most potent biotoxins known (Carmichael, 1994). When these cyanotoxins are produced in bloom-forming species, they threaten human, animal, and aquatic life, either through consumption or contact with contaminated water (Weller, 2011).

Cyanobacteria and algal blooms in New Zealand

More than 3600 lakes over one hectare in size have been identified in New Zealand, many of cultural and economic importance, utilised for recreation, tourism, fisheries and power generation (Schallenberg & Sorrell, 2009). New Zealand is not exempt from the degradation of its freshwater lakes, with 57% of the 124 lakes monitored categorised as poor or very poor based on Trophic Level Index (TLI) (Land Air Water Aotearoa, 2020). Land modification and intensification of pastoral and forestry activities in New Zealand have pushed many lakes into a regime shift from clear macrophyte dominant states to nutrient-rich, turbid phytoplankton dominant states (Carpenter *et al.*, 1998; Abell *et al.*, 2010) and many of these eutrophic lakes have become dominated by cyanobacteria (Carmichael, 1994).

First described in New Zealand in the 1880s (Nordstedt, 1888), the number of reported terrestrial and aquatic cyanobacteria species now exceeds 339 within 65 genera (Wood *et al.*, 2005). Amongst these, cyanobacteria with potential for production of cyanotoxins are widespread in New Zealand freshwaters, with blooms recorded since the 1970s (Wood, 2004). Since 1998 cyanobacterial neurotoxins associated with *Phormidium* (now *Microcoleus*) species have been linked to over 30 reported dog deaths (Hamill, 2001; Wood *et al.*, 2010a). The 'New Zealand Guidelines for Cyanobacteria in Recreational Fresh Waters'(Table **1.1**) was created in 2009 to aid agencies responsible for monitoring and reporting water quality. Based on current research and understanding, it advises what is considered best practice when managing cyanobacteria. This document was updated in 2018 to accommodate new research and issues arising since 2009. The existing three-tier alert level framework sets down the onset and development responses for planktonic and benthic cyanobacterial events. Due to the varying size of planktonic species (some < 2 μm in diameter), the alert level uses biovolume using species-specific cell volume estimates rather than cell concentrations. By doing so, this takes into account the correlation with increased cell size to higher concentrations of chlorophyll *a* (Rigosi *et al.*, 2011), allowing for more accurate health risk evaluation.

Table 1.1. New Zealand alert level framework for planktonic cyanobacteria in recreational freshwater, indicating thresholds and recommended actions. Taken from (Ministry for the Environment and Ministry of Health, 2009).

Alert Level	Actions
Surveillance (green mode) Situation 1: The cell concentration of total cyanobacteria does not exceed 500 cells ml^{-1}. Situation 2: The biovolume equivalent for the combined total of all cyanobacteria does not exceed 0.5 mm^3 L^{-1}	Undertake weekly or fortnightly visual inspection and sampling of water bodies where cyanobacteria are known to proliferate between spring and autumn.
Alert (amber mode) Situation 1: Biovolume equivalent to 0.5 to < 1.8 mm^3 L^{-1} of potentially toxic cyanobacteria or Situation 2: 0.5 - < 10 mm^3 L^{-1} total biovolume of all cyanobacterial material	Increase sampling frequency to at least weekly. Notify the public health unit. Multiple sites should be inspected and sampled.
Action (red mode) Situation 1: ≥12 µg L^{-1} total microcystins; or biovolume equivalent to ≥ 1.8 mm^3 L^{-1} of potentially toxic cyanobacteria or Situation 2: ≥10 mm^3 L^{-1} total biovolume of all cyanobacterial material or Situation 3: cyanobacterial scum consistently present	Continue monitoring as for alert (amber mode) If potentially toxic taxa are present, consider testing samples for cyanotoxins. Notify the public of potential risk to health

Within Aotearoa New Zealand, regional councils and the Ministry for the Environment monitor cyanobacteria and establish objectives, targets, and methods to 'maintain or improve' freshwater environments. Monitoring in accordance with the above framework can be labour intensive and costly (Schaeffer *et al.*, 2013), and currently, only around 40 lakes are assessed this way in New Zealand. Other limitations of the existing site-specific, biovolume-based methods were acknowledged during the update (Wood, 2018). Examples of such issues include accessibility, with some lakes within private land boundaries, and the rapid changes in cell concentration at beach sampling sites as wind/wave action can cause surface scums to

accumulate in downwind embayment's, potentially increasing the toxic load by x1000 in a matter of hours (Ministry for the Environment and Ministry of Health, 2009). This type of monitoring fails to capture temporal and spatial phytoplankton community changes occurring within such short time frames (Reyjol *et al.*, 2014). Consistency and urgency of cell identification and counting are also of concern, with several commercial agencies and some regional councils undertaking the microscopic counting and identification of the samples. Because of different counting protocols and the difficulty with identifying and classifying taxa, this can lead to a high level of discrepancy (Willén, 1976). Under microscopic enumeration, it is also impossible to differentiate toxic and non-toxic cyanobacterial strains (Straile *et al.*, 2015), and it is now widely known that toxin quota can vary within a single species from zero to high concentrations (Wood *et al.*, 2021). In addition, the time required to complete site sampling and analysis can extend the response time if a health warning needs to be issued, making this current surveillance, alert and action procedure limited in effectiveness.

1.2 Remote sensing

New alternatives to *in situ* samplings have seen remote sensing come to the forefront for water quality monitoring. It uses a distant sensor, usually mounted on a satellite, to measure water reflectance – the light emerging from the water body within the visible and near-infrared wavelengths (400-900 nm) (Figure **1.1**). Reflectance is usually captured for a series of discreet wavelength bands (multispectral reflectance), and this is then processed with algorithms to obtain information such as suspended solids, CDOM and biota (Dörnhöfer & Oppelt, 2016).

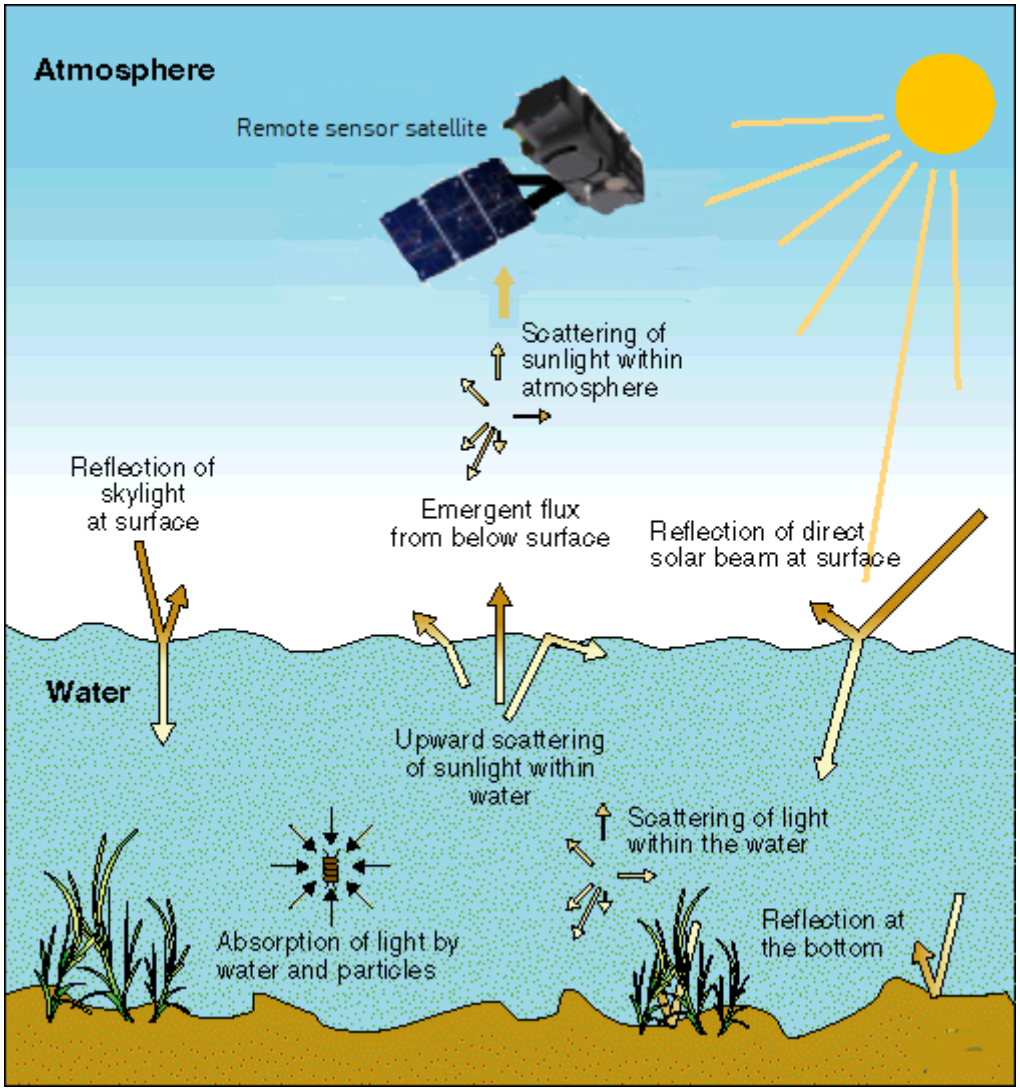

Figure 1.1. Light interactions through the atmosphere, water, and substratum, showing light origins detected by remote sensor satellite. Adapted from National Environmental Research Institute (1999).

The light reaching the remote sensing array provides information on processes that have affected it during its passage through the atmosphere, at the air-water interface and within the water column. As light passes through the atmosphere, it is affected by absorption and scattering, and when it hits the water-air interface, it can be either reflected or enter the water column. Optical active constituents within the water body such as chromophoric dissolved organic matter (CDOM), suspended solids and phytoplankton absorb or scatter this light to varying degrees, and a variable proportion of light will be backscattered back into the atmosphere from the water column depending on these optically active constituents. Light leaving the water is once again modified by absorption and scattering in the atmosphere before reaching the remote sensing satellite. Mouw *et al.* (2015) estimate that 2 – 10 % of

incident light leaves the lake surface, and it is this that is of most interest when monitoring lakes since this is the only light to have interacted with lake water constituents. The proportion and abundance of the optically active constituents absorbing light at differing wavelengths leads to variation in the reflection signal, providing information on the optical property of the water body (Odermatt *et al.*, 2012) (Figure **1.2**).

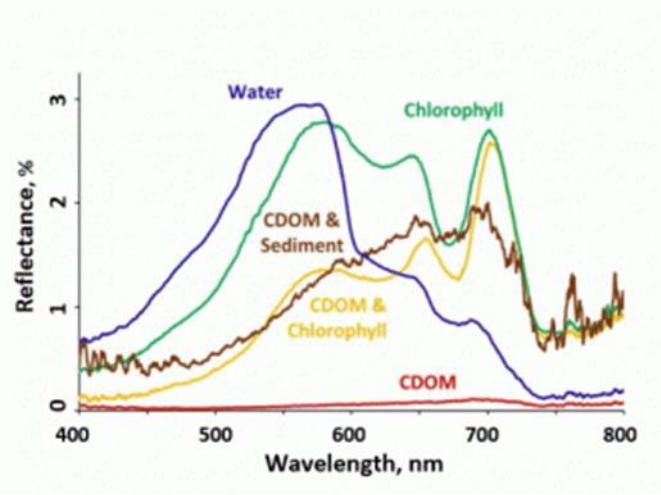

Figure 1.2. Example of reflectance spectra of different optical active constituents. Retrieved from https://water.rs.umn.edu/lwc.

CDOM is a major absorber of radiation entering lakes, with high levels impacting light availability for phytoplankton and water-leaving radiance, but does not significantly scatter or reflect light (Jones, 1998). CDOM does not display any peaks on the absorption spectra, rather, it shows an exponential decrease in absorption with increasing wavelength, often the absorption coefficient is calculated at 440 nm (Kutser *et al.*, 2005). CDOM concentrations tend to show little seasonal variation, however, temporal variation has been documented after rainfall, influenced by catchment input (Brezonik *et al.*, 2015; Kutser *et al.*, 2015).

Suspended solids, also known as suspended particulate matter, absorb and scatter light, influencing transparency and water-leaving radiance (Giardino *et al.*, 2015). These solids can enter the lake through catchment input or from resuspension of bottom sediment (Dörnhöfer & Oppelt, 2016). The spectral characteristics of suspended solids are similar to those of CDOM (Figure **1.2**) and show no specific peaks and troughs.

Phytoplankton contain pigments that absorb at known wavelengths, often with very characteristic peaks and troughs in absorptance, which can be used to estimate the overall biomass of phytoplankton. For example, chlorophyll *a* (found in all phytoplankton) absorbs

strongly in the blue wavelengths at approximately 440 nm and the red at 670 nm, while phytoplankton reflect strongly in green wavelengths (Figure **1.2**). Other pigments have different absorption characteristics, and as pigment content can vary between taxonomic groups (Hoepffner & Sathyendranath, 1993), this potentially provides a method to differentiate phytoplankton groups on the basis of their absorption spectra (Xi *et al.*, 2015).

Cyanobacteria contain phycobilin pigments, with phycocyanin, a blue coloured pigment that gives cyanobacteria its blue-green colour, often dominant in freshwater taxa (Becker *et al.*, 2009). This pigment has an absorption maximum at approximately 620 nm and is detected between 615 – 650 nm in reflectance spectra (Bryant, 1981; Ogashawara *et al.*, 2013). Therefore, it can help distinguish cyanobacterial blooms from those caused by other taxa, such as diatoms and chlorophytes that do not contain phycocyanin.

Potentially, the ability to monitor across large scales using remote sensing techniques could save time and resources and provide the ability to obtain spatial coverage of an entire lake with high temporal resolution, while the use of appropriate algorithms could allow measurement of multiple parameters simultaneously, providing advantages over *in situ* testing (Tomlinson *et al.*, 2016). Phycocyanin reflectance as a proxy for cyanobacterial bloom detection could be used to assess the need for *in situ* water collection in near real-time, resulting in quick decision making and better public health outcomes (Sharp *et al.*, 2021). However, remote sensing does have its limitations. Satellites used in remote sensing tend to be multispectral, that is, they measure radiation over a broad wavelength range in spectral bands 10-20 nm in width, which can reduce the specificity with which pigments can be identified, large pixel size can limit spatial resolution, and they depend on cloud-free conditions at the time of overpass (Dörnhöfer & Oppelt, 2016).

In addition to challenges in obtaining images at sufficient resolution, resolving phytoplankton composition by remote sensing can be difficult due to the presence of multiple pigments and associated proteins, the absorption of which can overlap (Malthus *et al.*, 1997), making it problematic to know the value each pigment contributes to the absorption spectra (Aguirre-Gomez *et al.*, 2001). For example, diatoms contain the carotenoids fucoxanthin and β

carotene, which, like chlorophyll *a,* have high absorption in the blue region, making it difficult to distinguish between them, leading to one reinforced peak (Aguirre-Gomez *et al.*, 2001).

Defining the optical signature of cyanobacteria to determine biomass is no less of a challenge. While there are already algorithms for quantifying chlorophyll *a,* phycocyanin can be more difficult to detect and quantify (Simis *et al.*, 2005). There are several reasons for this: Phycocyanin at 620 nm has a specific absorption coefficient approximately half that of chlorophyll *a*, which requires larger amounts of phycocyanin to obtain an equivalent reflectance response (Stumpf *et al.*, 2016). Phycocyanin content of cells varies with nutrient availability, light quality and species, and some rhodophytes and cryptophyte species also produce phycocyanin as well as other phycobilin's (Reuter & Müller, 1993). Cyanobacterial blooms can also display spatial irregularity due to wind and wave action (Carey *et al.*, 2014) and spatial variability with depth due to gas vacuoles (Oliver *et al.*, 2012). Both circumstances can lead to underestimating cyanobacterial biomass (Chang *et al.*, 2012) due to variation within satellite pixels (Kutser, 2009).

Despite these challenges, remote sensing is becoming increasingly used in regard to water monitoring due to its temporal and spatial coverage and can be an important tool in cyanobacterial monitoring (Schalles & Yacobi, 2000; Dörnhöfer & Oppelt, 2016; Sharp *et al.*, 2021).

1.3 Study objectives

This thesis is part of the larger "Eye on Lakes" project at the University of Waikato. The aim of the project is to develop a biovolume-related risk assessment tool to predict cyanobacteria in New Zealand lakes using satellite remote sensing. To achieve this requires (i) recognising a cyanobacterial signal within the reflectance spectrum of the lake water, (ii) quantification of that signal at a sufficiently low concentration against other changing optical properties to provide a useful lake monitoring tool and (iii) conversion to biovolume to establish a link to existing New Zealand regulations.

As part of this process, the specific aim of this thesis was to undertake an investigation into the relationships between phytoplankton biomass and community composition and optical properties of lakes in the central North Island of New Zealand. Three Rotorua lakes that vary in trophic state from oligotrophic to eutrophic were sampled over two summer seasons to address changes in optical properties as the phytoplankton populations underwent seasonal succession. In addition, single samples from five Waikato lakes to provide a more extensive range of optical water types. The goal was to determine (i) phytoplankton composition and biovolume, (ii) chlorophyll *a* and phycocyanin concentrations, (iii) absorption spectra of CDOM, algal and non-algal particles and (iv) hyperspectral *in situ* reflectance spectra.

The overall hypothesis tested was that the reflectance spectra of those lakes could be used to predict the abundance of cyanobacteria and incidentally of other phytoplankton groups. This was intended to support other research within the project to provide knowledge on how changes in phytoplankton, particularly cyanobacterial communities, can be related to satellite-based reflectance data in these New Zealand lakes.

Chapter 2

Study Sites

2.1 Overview of Sites

Field studies were designed to examine the utility of optical properties for monitoring phytoplankton populations in lakes by (a) following seasonal changes in the optical properties in three lakes of contrasting tropic conditions and relating these to phytoplankton development and (b) a series of single samples from five other lakes with contrasting phytoplankton populations.

2.2 Seasonal Study sites

The lakes selected to examine temporal variability are situated within the Rotorua District, which lies on the Central North Island of New Zealand. This region is culturally significant and internationally recognised as a tourist and trout fishing region (Paul *et al.*, 2012). Twelve major lakes lie in the district, varying in morphometry, trophic levels and catchment land use (Burns *et al.*, 2005; Trolle *et al.*, 2008). Collectively known as the Te Arawa lakes, they are situated within the Taupo Volcanic Zone, approximately 300 m above sea level. Most of the lakes were formed up to 140,000 years ago through volcanic activity, as explosive rhyolitic eruptions formed volcanic craters and lava flows that impeded river drainage, subsequently forming lakes. This region is still geothermally active, resulting in geothermal inflows into the base of Lake Rotoiti and warm phosphorus-rich surface input into Lake Rotoehu (Allan *et al.*, 2011). A paper by Rutherford *et al.* (1989) prompted public discussion around the deteriorating water quality of these lakes, suggesting the need to manage phosphorus and nitrogen inputs, which ultimately led to the establishment of target water quality values. These values are set as target Trophic level Index (TLI) values, as defined by Burns *et al.* (1999)

In 1998 Te Arawa Lakes Trust, Bay of Plenty Regional Council (BOPRC) and Rotorua Regional Council formed a Lake Management Working Group responsible for managing the lakes and their surrounding catchments. A regular water quality monitoring programme in the Rotorua

lakes was established to detect cyanobacteria after reports of blooms occurring in Lakes Rotoehu, Rotoiti, Rotorua and Okaro, which resulted in public health warnings (Deely *et al.*, 1995). Subsequently, a diverse composition of cyanobacteria have been detected within Te Arawa lakes that have changed in dominance over time, coinciding with water quality changes (Paul *et al.*, 2012). Phytoplankton in many of these lakes tend to be nitrogen-limited; this reflects their volcanic catchments, with rhyolitic pumice overlaying ignimbrite rich aquifers, ensuring groundwater is naturally high in phosphorus (Timperley, 1983; Abell *et al.*, 2010).

For this study, three Te Arawa lakes ranging in TLI values were selected (Table **2.1**); oligotrophic Lake Rotomā, mesotrophic Lake Rotoiti and eutrophic Lake Rotoehu (Figure **2.1**). This variation makes them suitable for comparative studies of algal communities and their optical properties. Two sites per lake were routinely monitored over two summer seasons, with the two sampling sites in each predetermined from other studies. GPS coordinates (Table **2.2**) allowed for consistent site location. All sites were accessed by boat.

Table 2.1. Lake attributes and water quality summary for Lakes Rotomā, Rotoiti and Rotoehu. TLI is given as the 2019/2020 value along with the target set by Council. Nitrogen, Phosphorus and Chlorophyll *a* are given as 2015 values, indicating an increase, decrease, or no change over the ten years previous. Modified from (Scholes & Hamill, 2016; Bay of Plenty Regional Council, 2020)

Lake	**Attributes**			**Trophic Level Index**	**2015 (10 Year Trend)**			
	Maximum Depth (m)	**Lake Area (ha)**	**Catchment (ha)**	**TLI 2019/2020 (target)**	**Total Nitrogen (mg m^3)**	**Total Phosphorus (mg m^3)**	**Chlorophyll *a* (mg m^3)**	**Water Clarity**
Rotomā	83	1,112	3,392	2.2 (2.3)	150 (No Change)	5.0 (Increasing)	4.1 (No Change)	(Decreasing)
Rotoiti	125	3,369	12,056	3.7 (3.5)	206 (No Change)	12 (Increasing)	7.8 (No Change)	(No Change)
Rotoehu	13	790	4,225	4.4 (3.9)	285 (Increasing)	21 (Increasing)	9.2 (Increasing)	(Decreasing)

Table 2.2. Lake's Rotomā, Rotoiti and Rotoehu sampling site location and depths.

Lake	Site number	Site	Latitude	Longitude	Depth (m)
Rotomā	1	South	38.05 ºS	176.58 ºE	54.9
Rotomā	2	North	38.02 ºS	176.58 ºE	70.8
Rotoiti	1	East	38.04 ºS	176.44 ºE	43.6
Rotoiti	2	West	38.02 ºS	176.39 ºE	33.4
Rotoehu	1	South	38.02 ºS	176.53 ºE	10.6
Rotoehu	2	North	38.01 ºS	176.53 ºE	11.0

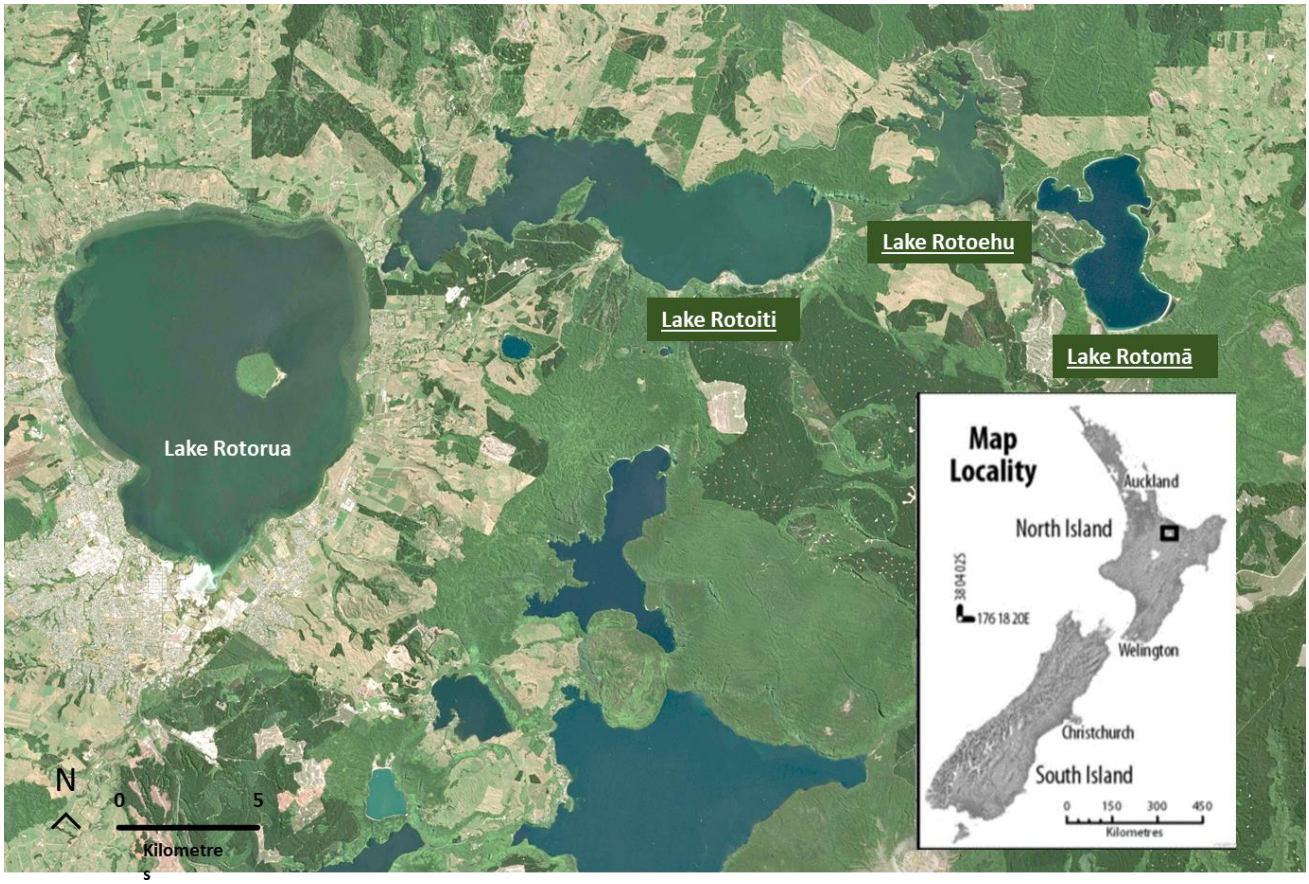

Figure 2.1: Sentinel-2 L2A satellite image of Rotorua District showing the location of lakes Rotomā, Rotoiti and Rotoehu. Insert location map from (Burns *et al.*, 2009).

2.2.2 Lake Rotomā

The most pristine of the Te Arawa lakes, Lake Rotomā, (38.04°S, 176.58°E) (Figure **2.2**), meaning 'lake of exceptionally clear water' is a deep (maximum depth 83 m, mean depth 36.9 m) monomictic, oligotrophic lake which stratifies September to June before winter mixing (Nelson, 1983; Hamilton, 2003). The lake formed after volcanic eruptions, leading to a small caldera collapse (Healy, 1975). It sits at the top of the Haroharo vent zone at an altitude of 313 m above sea level (Lowe & Green, 1987). Lake Rotomā has a total lake area of 1,112 ha consisting of three main crater basins, the northern (maximum depth of 83 m), southern (maximum depth of 73.5 m) and the shallower Matutu basin reaching a maximum of 38 m (Nelson, 1983; Scholes, 2009). A submerged pinnacle in the lake's southern basin, approximately six meters beneath the surface that once supported a Māori pa (Healy, 1975), indicative of a previous lower lake level.

Figure 2.2: Satellite image from Sentinel-2 of Lake Rotomā with sampling sites 1 and 2.

The current TLI value is 2.2, and this has not changed significantly over the last decade (Figure **2.3**). Lake Rotomā is phosphorus limited; however, total phosphorus concentrations have

doubled since 1992 (Scholes, 2009; Scholes & Hamill, 2016). In an effort to protect the water quality, the Rotorua Lakes Council in 2017 committed to replacing all current septic tanks and constructing a sewage treatment plant. By 2020 the East Rotoiti-Rotomā reticulated sewerage scheme saw all Rotomā properties connected to an out of catchment wastewater system.

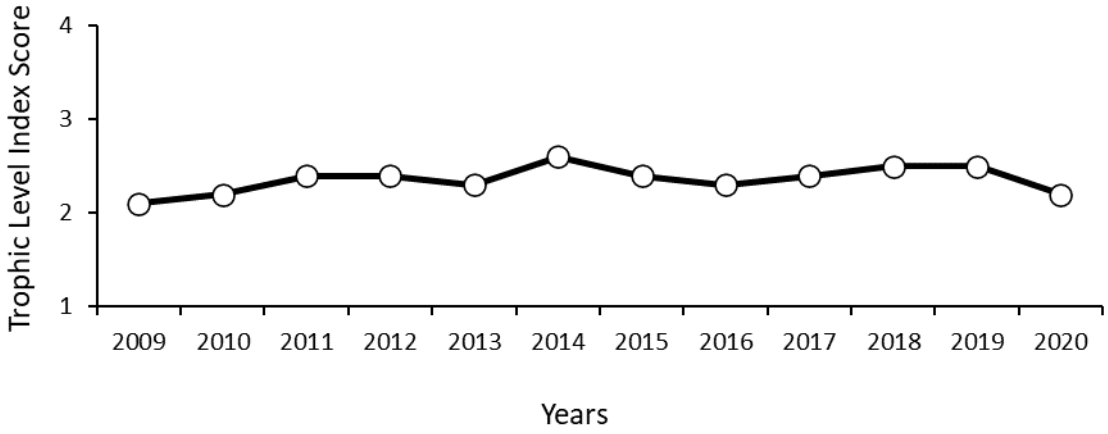

Figure 2.3. Trophic Level Index of Lake Rotomā between the years 2009 – 2020. Data from Bay of Plenty Regional Council.

The catchment area, 1,112 ha, is primarily covered in indigenous forest and exotic plantations, while the eastern side has more sheep and beef farming and lake edge communities running along the south-western side (Scholes & Hamill, 2016).

Rainfall accounts for most of the lake's inflow and significantly affects lake levels, which can fluctuate up to 6 m (Clayton *et al.*, 1981). Several small streams, springs and groundwater located around the lake's margin also contribute. There is no surface outflow; 7% of water drains annually via groundwater from the Matutu Basin through porous pumice flowing into a wetland near Lake Rotoehu (Environment Bay of Plenty, 2009). Wave and currents in the lake are created from the predominant south-westerly winds, though on occasions, winds can come from the north (Nelson, 1983).

Lake Rotomā is a popular recreational site for water-based activities, making the lake high risk of infestations from the invasive hornwort (*Ceratophyllum demersum*), and brown bullhead catfish (*Ameiurus nebulosus*) found in surrounding lakes. The lake has a diverse aquatic plant community with a mixture of native and non-native species. *Lagarosiphon major,* commonly

called oxygen weed, is the dominant invasive species thought to have been introduced into the lake on boats (Clayton *et al.*, 1981; Scholes & Hamill, 2016). A weed cordon was installed around the main boat ramps in 2008 to prevent hornwort and other aquatic pest macrophytes from entering the lake (Lass, 2012). Regular checks occur, and herbicides are used if weed is detected to prevent them from establishing outside the cordon. The lake supports an abundance of Kākahi (freshwater mussel *Echyridella menziesi*) and Kōura (freshwater crayfish *Paranephrops planifrons*), sustaining a customary tau Kōura fishery (Kusabs *et al.*, 2015). Rainbow trout (*Oncorhynchus mykiss*) and the sterile hybrid Tiger trout (*Salmo trutta* × *Salvelinus fontinalis*) were released into the lake for recreational fishers.

2.2.3 Lake Rotoiti

Lake Rotoiti's (Figure **2.4**) (38.01°S, 176.53°E) full name, Te Roto-Whaiti-i-kite-ai-a-Ihenga-i-Ariki-ai-a Kahumatamomoe means 'the small lake discovered by Ihenga'. However, with a lake surface area of 3,369 ha, it is the third-largest lake within the Rotorua Lakes District (Scholes, 2009) and the largest of the three lakes sampled for this seasonal study. It is a deep (maximum depth 125 m, mean depth 33 m) mesotrophic, monomictic lake (Hamilton, 2003). It is located 278 m above sea level, formed by lava flows damming river valleys following a volcanic eruption (Lowe & Green, 1987). The long, narrow shape accommodates three main basins. The western basin with a maximum depth of 35 m, is separated by a narrow constriction from the eastern basin (maximum depth of 125 m) and the shallower third basin, maximum depth of 6.5 m, lies in Okawa Bay which connects to the western basin via a narrow, shallow (1.5 m) constriction (Gibbs *et al.*, 2003; von Westernhagen *et al.*, 2010). On the lake's western side lies the Ohau channel inflow, connecting the lake to the adjacent nutrient-rich Lake Rotorua, which has significantly impacted water quality in Lake Rotoiti (Hamilton, 2005; Scholes & McIntosh, 2010). Stratification and deoxygenation of bottom waters occur in September – October. Thermocline deepening occurs in autumn, and the lake is thoroughly mixed by winter. Annual water temperatures range from 9 to 21 ^{o}C (Hamilton *et al.*, 2004; Beyá *et al.*, 2005), the winter supporting peak phytoplankton biomass with a community shift in summer towards cyanobacterial dominance (Vincent *et al.*, 1984).

Figure 2.4. Satellite image from Sentinel 2 of Lake Rotoiti with sampling sites 1 and 2.

Currently, BOPRC records Lake Rotoiti's TLI at 3.7, and it has remained relatively stable over the previous ten years (Figure **2.5**). The lake intermittently experiences cyanobacterial blooms, and weekly cyanobacteria monitoring occurs in Okawa Bay, Te Weta Bay, Okere Arm, Otaramarae and Hinehopu sites from November to June (Bay of Plenty Regional Council, 2020). Water quality observations in Lake Rotoiti were first reported by Jolly (1968), and these indicated there had been a deterioration of water quality since the 1950s. This is believed to be due to the increased catchment land use for agriculture and the nutrient-enriched water entering from then eutrophic Lake Rotorua through the Ohau Channel (Vincent *et al.*, 1984; Vincent *et al.*, 1991). The Channel inflow now accounts for approximately 73% nitrogen (259 t yr^{-1}) and 76% phosphorus (31.1 t yr^{-1}) entering Lake Rotoiti (Scholes & McIntosh, 2010), making it the predominant nutrient source. The temperature of this channel inflow plays a significant role in the dynamics of Lake Rotoiti. Warm summer inflows from the channel remain on the surface of the receiving Lake Rotoiti as overflow and, with the help of easterly winds, directed it towards the Okere Arm and into the Kaituna river outlet. However, if exposed to a westerly wind, this overflow can be propelled into the eastern basin. In the winter months, the colder, denser inflow forms an underflow moving along the bottom of the lake from the western basin towards the eastern region of the lake (Vincent *et al.*, 1986). To achieve the 3.5 TLI target, Rotorua and Rotoiti lake's action plan set strategies to reduce

nutrient inputs into both lakes to improve water quality. Upgrades to the Rotorua district's wastewater treatment plant and Rotoiti's reticulated sewerage scheme are ongoing but have removed approximately 5.9 t yr^{-1} of nitrogen and 0.21 t yr^{-1} phosphorus from Lake Rotoiti within two years, increasing water clarity by 25% (Scholes & McIntosh, 2010). In further attempts to protect and improve water quality in Lake Rotoiti, the Ohau Channel Wall was constructed to divert the eutrophic water entering from Lake Rotorua toward Lake Rotoiti's outlet, Kaituna River 2.6 km away. It was predicted to prevent 180 t yr^{-1} of nitrogen and 15 t yr^{-1} of phosphorus from entering the lake's main body, leading to improved water quality within five years (Gillies, 2010). Construction of the 1,275 m long wall that runs parallel to the lake's edge took approximately one year and was completed in July 2008.

Figure 2.5. Trophic Level Index for Lake Rotoiti from 2009 – 2020. Data from Bay of Plenty Regional Council.

Lake Rotoiti's catchment, 12,056 ha (excluding Lake Rotorua catchment), is covered mainly in indigenous vegetation, exotic plantations and pasture (Scholes & Hamill, 2016). Urban settlements make up a comparatively small percentage of the catchment, and there has been a gradual conversion of pasture to forestry and indigenous vegetation over the last three decades (Beyá *et al.*, 2005).

The lake's primary input is from Lake Rotorua via the Ohau channel (mean discharge 18.04 m^3s^{-1}) (Vincent *et al.*, 1991). Several small cold surface streams from the eastern and southern catchment contribute, along with multiple warm geothermal springs, the main vent in the

eastern basin. The Kaituna River, situated in the Okere Arm north-western region of the lake, is the only surface outflow (mean discharge 21.35 $m^3 s^{-1}$). The lake's average residence time is 1.5 years; weeks to months in the shallow western basin, and exceeds 1.5 years in the deeper eastern basin (Beyá *et al.*, 2005). The Okere gates lie on the Kaituna River, constructed in 1982 and regulate Lake Rotoiti's water level, prior to this, the water level was controlled by a rock ledge weir further downstream (Muraoka *et al.*, 2010).

The lake is a popular site for sailing, water skiing and birdwatching. A survey in the early 1980s showed Lake Rotoiti provides a diverse range of wildlife habitats for plants, fish and birds, particularly for the many waterbird species (Rasch, 1989). It is also a popular recreational site to fish for rainbow trout and brown trout (*Salmo trutta*), which were introduced in 1888 – 1898 (Burstall, 1880). Other non-native introductions include brown bullhead catfish (*Ameiurus nebulosus*), gambusia (*Gambusia affinis*), and goldfish (*Carassius auratus*). Native fish species residing in the lake include Longfin eels (*Anguilla dieffenbachia*), kōaro (*Galaxias brevipinnis*), common bullies (*Gobiomorphus cotidianus*), and common smelt (*Retropinna retropinna*) (Kusabs & Quinn, 2009). The common smelt were introduced to the lake as a food source to ease the predation of kōaro by trout (McDowall, 2011). Kōura can also be found here in significant numbers and is considered a valued mahinga kai species for Māori (Devcich, 1979; Kusabs & Quinn, 2009). Lake Rotoiti contains several invasive non-native pest plant species; hornwort, oxygen weed, Canadian pondweed (*Elodea canadensis*) and Egeria (Egeria densa). These invasive species have been found to compete with and displace native species (Clayton & Edwards, 2006). Harvesting of hornwort, which established in the lake in the 1970s, has been undertaken along with the application of the herbicide diquat (Mille, 2020) in an attempt to reduce nutrient loads.

2.2.4 Lake Rotoehu

Lake Rotoehu (Figure **2.6**) (38.02°S, 176.41°E) translates to 'murky water' and is the most nutrient-enriched of the three Te Arawa lakes in this study. It is a shallow (mean depth 8.2 m Maximum depth 13 m) eutrophic lake, recorded as nitrogen-limited due to high phosphorus inflows (Burns *et al.*, 2009). The 790 ha lake sits 295 m above sea level and was formed by lava deposition damming rivers from the same eruption episode as Lake Rotomā

approximately 8,500 years ago (Healy, 1975). The mixing regime tends to be polymictic, with water well mixed most of the time. The lake has seven arms radiating out to the north, housing multiple bays, while the southern side is a rounded open basin. A combination of catchment intensification, fluctuations in water level and geothermal inflows naturally high in phosphorus have contributed to substantial cyanobacterial blooms, frequently reaching red alert levels and promoting public health warnings (Burns *et al.*, 2005).

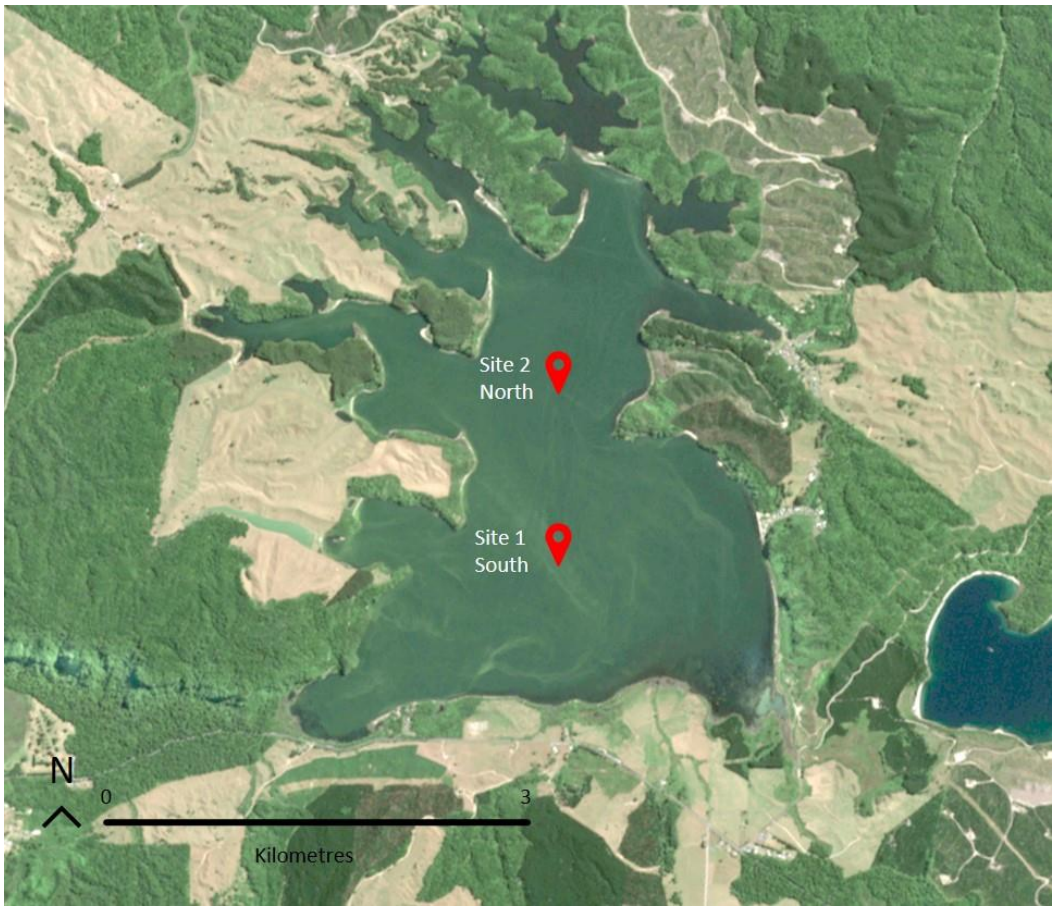

Figure 2.6. Sentinel 2 satellite image of Lake Rotoehu with cyanobacterial surface scum and an indication of sampling sites 1 and 2

The catchment has an area of 4,255 ha and is evenly covered with forestry, pasture (predominantly sheep and beef), and indigenous vegetation (Scholes & Hamill, 2016). Small pockets of urban settlements are located around the lake, with a small wetland on the southern shoreline.

In 1992 the lake was classified as mesotrophic with a TLI value of 3.7; by 1993, that had spiked at 5.2 (supertrophic). The increase of TLI was put down to a 4.2 m drop in lake level, warm summer temperatures and very little wind resulting in prolonged stratification and deoxygenation of the bottom waters. These conditions subsequently lead to increased internal nutrient loading, which the lake has never fully recovered from (Cronin *et al.*, 2007; Burns *et al.*, 2009). The current TLI is 4.4, prompting the change from supertrophic to eutrophic status (Figure **2.7**). To address the poor water quality, BOPRC in 2007 published the Lake Rotoehu Action Plan, setting a TLI target of 3.9. The plan outlines a series of catchment and in-lake restoration strategies to achieve the annual reduction of 130 tonnes of nitrogen and 19 tonnes of phosphorus required to reach the target (Cronin *et al.*, 2007). In-lake remedial methods include harvesting the nitrogen and phosphorus sequestered in hornwort. This began in 2006, intending to harvest 1000 tonnes annually. Additionally, in 2011 a floating wetland was formed in the southern region of the lake to enhance nitrogen removal, and in 2012 lake aeration devices were deployed to the lake bed to prevent stratification (McBride *et al.*, 2019). Catchment initiatives included conversion from pastoral to forestry, riparian planting and a phosphorus locking plant (operational from 2011) to release a low dose alum to remove up to 0.7 tonnes of phosphorus annually.

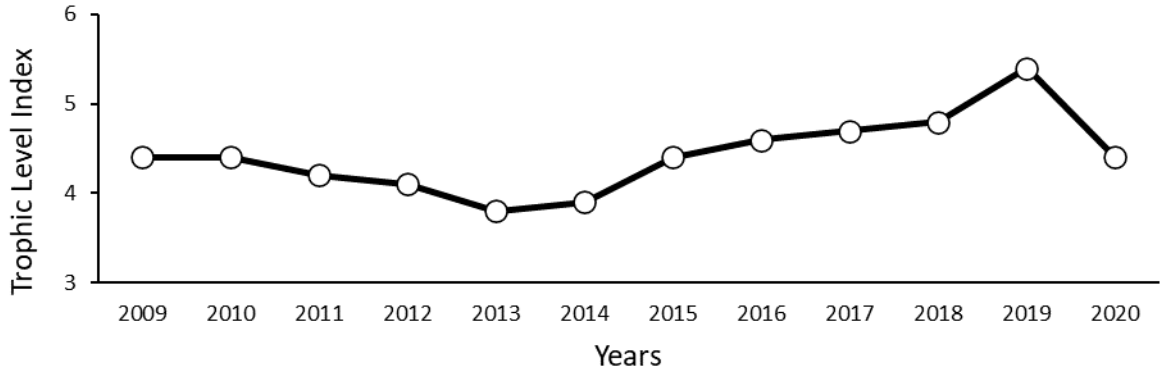

Figure 2.7. Trophic Level Index of Lake Rotoehu from 2009 – 2020. Data from Bay of Plenty Regional Council.

Input into the lake is via three main streams (Te Pohue, Te Maero and Rakaumakere streams) and numerous smaller surface streams and springs, including the warm, phosphorus-rich Waitangi Spring. There is no surface outlet, only a sinkhole in one of the lake's northern arms

(Jolly & Brown, 1975). The water residence time was observed to be short at between 1.4-1.7 years (Trolle *et al.*, 2011).

Cultural landmarks such as old pa sites are situated around the lake, making it a place of cultural significance to iwi, for which they play a role in the sustainable fishery of kakahi, tuna and koura present in the lake. The sheltered arms of the lake provide calmer waters for recreational fishing of the introduced rainbow trout. Lake Rotoehu has an extensive issue with aquatic pest plants, giving it the lowest submerged plant index score of all Te Arawa lakes with a 92% invasive impact (Burton & Clayton, 2015). Hornwort, oxygen weed and elodea can create large weed beds displacing native species; hornwort, the most problematic, was first detected in December 2004 and is now widespread throughout the lake, forming large surface mats, making it suitable for harvesting to remove phosphorus (Cronin *et al.*, 2007).

2.3 Spatial Study Sites

The Waikato Region lies in the central North Island of New Zealand and contains over 100 lakes varying in physical and biological characteristics. The lakes are grouped by geographical location and geomorphic formation and divided into riverine, peat, hydro, dune and geothermic lakes (Dean-Speirs *et al.*, 2014). The majority are shallow lakes, smaller than 10 ha in size, and make up 30 % of all lakes in New Zealand with poor water quality (Hamilton *et al.*, 2010). The major factors that were shown to cause a rapid decline in these lakes include declining water quality, invasive fish and plant species and the small size of the lakes, making them vulnerable to accelerated change (Edwards *et al.*, 2010). Many of these lakes have a predominantly pastoral catchment. With the intensification of farming in this region, increased use of phosphorus and nitrogen fertilisers has occurred, leading to increased nutrient inputs into water bodies via leaching and runoff, impacting water quality (Cichota & Snow, 2009). The increased nutrient load has led to many lakes suffering a unidirectional regime shift from high water quality dominated by submerged macrophytes to de-vegetated turbid phytoplankton dominated states (Dean-Speirs *et al.*, 2014). Very few lakes in this region are monitored or have any historical water quality data (Duggan, 2007). The Waikato Regional Council regularly monitors approximately 12 shallow lakes. The 2014 shallow lakes management plan outlined recommendations to improve stock and soil management and

improve drainage and waterways while improving lake margins to reduce nutrient and sediment loss from farmland (Özkundakci & Allan, 2019).

Five Lakes were selected (Table **2.3**), Peat Lakes Rotopiko and Mangakaware, and riverine Lakes Rotongaro, Rotongaroiti and Ohinewai. All five lakes are identified as significant wetlands in the Waikato Regional Plan. As with the seasonal sites, these aligned with concurrent and previous studies. Sampling sites were identified with GPS locations (Table **2.4**) and accessed by boat.

Table 2.3. Waikato lakes attributes. Secchi depth and Chlorophyll *a* result from 2020 sampling. TLI shown as the most recent recorded with Lakes Rotongaro and Rotongaroiti have no data available. Data from Environment Waikato.

Lake	Type	Maximum Depth (m)	Lake Area (ha)	Catchment (ha)	Secchi Disc (m^{-1})	Chlorophyll *a* ($ug\ L^{-1}$)	Trophic Level Index (year)
Rotopiko	Peat	4.0	5.3	163	2.54	5	4.7 (2019)
Mangakaware	Peat	4.8	12.9	238	1.05	27	5.8 (2019)
Rotongaro	Riverine	3.3	292	1950	0.18	18.3	N/A
Rotongaroiti	Riverine	0.5	53	2105	0.15	81	N/A
Ohinewai	Riverine	4.5	16	347	0.51	44	6.3 (2013)

Table 2.4. Waikato Lakes sampling locations.

Lake	Latitude	Longitude	Depth (m)
Rotopika	37.94°	175.32°E	3.8
Mangakaware	37.93	175.22	3.7
Rotongaro	37.48	175.11	3.2
Rotongaroiti	37.47	175.10	0.9
Ohinewai	37.49	175.17	3.6

2.3.1 Lake Rotopiko North

Rotopiko peat lakes, also known as Serpentine lakes, are located south of Hamilton City, formed during the last glaciation approximately 17,000 years ago (Lowe & Green, 1987). Prior to the drainage and development of the surrounding peatland, Lake Rotopiko was a single water body, and today Lake Rotopiko is comprised of three small water bodies (Figure **2.8**) Rotopiko North, East and South lakes (Barnes, 2001). The sampling for this project was

undertaken in Rotopiko North Lake (37.94°S, 175.32°E). The maximum depth of the north lake is 4.79 m, with a surface area of 5.29 ha.

The catchment area of 163 ha is entirely pastoral land. Immediately surrounding the lakes is a fenced 30 ha wildlife reserve with native riparian planting. Inflows are received from rainfall, groundwater, farm drains and surface runoff from the adjacent highway, surface inflow is weather dependent, and at times there would be no surface inflow entering the lakes (Wu *et al.*, 2013). After substantial rain, water levels rise to allow the North lake to flow into the South lake (Tempero & Hamilton, 2019), and during the winter months, an ephemeral wetland forms between North and South lake known as Winter Lake (Dean-Speirs *et al.*, 2014). The lake is currently described as eutrophic (TLI of 4.7), influenced by its pastoral catchment, improving from the 2017 TLI of 5.5 (Land Air Water Aotearoa, 2020). Water clarity is influenced by tannin input from peat soils surrounding the lake (Hamill, 1995).

North lake is considered to have the highest Lake SPI (90%) of all lakes in the Waikato Region, supporting only native submerged macrophyte communities (Edwards *et al.*, 2010). The lake houses native fish, including common bullies, black mudfish, longfin and shortfin eels (Wu *et al.*, 2013). Eradication of pest fish such as rudd (*Scardinius erythrophthalmus*), using netting techniques, and a downstream fish barrier is ongoing (Neilson *et al.*, 2004; Collier & Grainger, 2015).

In 2011 plans to restore the lakes and build a national wetland discovery centre commenced. To date, the restoration project has seen the installation of sediment traps on the main inlet drains, predator control, formation of new ponds for wading birds, and 3 km of walkways and viewing platforms.

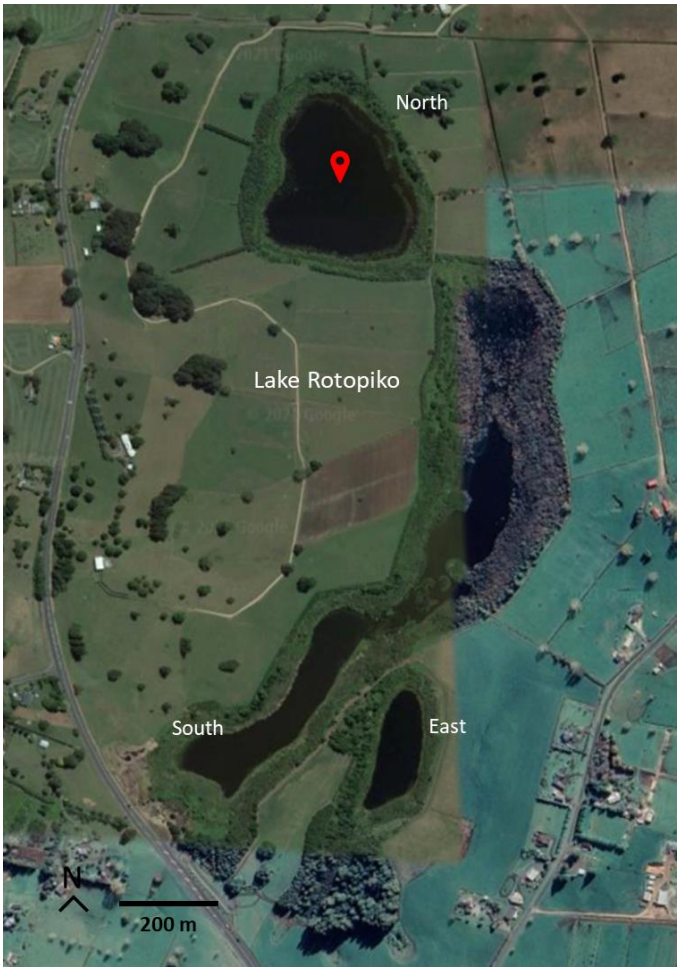

Figure 2.8. The three (North, South, and East) water bodies that makeup Lake Rotopiko. The North Lake indicating sampling site. Image from Google Earth.

2.3.2 Lake Mangakaware

Lake Mangakaware (Figure **2.9**) (37.55°S, 175.13°E) is a 13.3 ha hypertrophic polymictic Peat lake (maximum depth 4.8 m) stratifying during the summer months before mixing in winter, or when extensive windy conditions occur (Greenwood *et al.*, 1999).

The catchment covers 238 ha, it is predominantly pastoral dairy farming and grazing. The lake's perimeter is fenced, extending up to 240 m from the lake edge. It is currently a recreation reserve administered by the District Council until recently was leased for grazing (Waipa District Council, 2007). The lake has one major inflow in the north and several smaller ones coming from farm drains, which are heavily burdened with peat components, outflow is

situated at the lakes southern end, which supports a rock rubble weir, installed to maintain water levels (Dean-Speirs *et al.*, 2014).

The drying of the lakes peat margins and stock grazing has supported the growth of exotic species such as willow (*Salix* spp) and gorse (*Ulex europaeus*) and inhibited the survival of native vegetation. The lake houses small numbers of common bully and eels, along with diverse vegetation, giving it a Native Condition Index of 65 % (Edwards *et al.*, 2010).

Figure 2.9. Lake Mangakaware, indicating sampling site. Image taken from Google Earth.

2.3.3 Lake Rotongaro

A shallow riverine lake with a maximum depth of 3.3 m, it is the largest of the Waikato Lakes within this study with a surface area of 292 ha (Figure **2.10**) located in the lower Waikato District (37.29°S, 175.75°E) (Dean-Speirs *et al.*, 2014). Lake Rotongaro is not monitored for water quality. Toxic algal blooms have been reported, and in the summer of 2005, nine cattle died after drinking from the lake. Tests confirmed the presence of a *Microcystis* sp. producing microcystin 40 times higher than drinking water standards (Envirocare, 2005).

The catchment (1950 ha) is mainly pastoral, dairy, and dry stock with pockets of pine plantation. Pockets of damp hollows throughout the catchment support wetland vegetation, on the southwest corner, there is a wetland classified as significant, dominated by manuka (Wildland Consulting, 2011). Several surface inflows enter the lake with only one outflow, discharging through a channel into Lake Rotongaroiti, eventually reaching the Waikato River (de Winton & Champion, 1993).

Surrounding the lake edge, pockets of manuka and broadleaved species grow, along with the exotic willow and gorse. Records from 1986 report a Native Condition Index of 72 %, by 1991, this had declined to 28 %, and presently no submerged vegetation is recorded (Edwards *et al.*, 2010). Catfish and koi carp (*Cyprinus carpio*) have previously been recorded along with smelt, common bullies, and eels that were subjected to commercial eel fishing (Hayes, 1989).

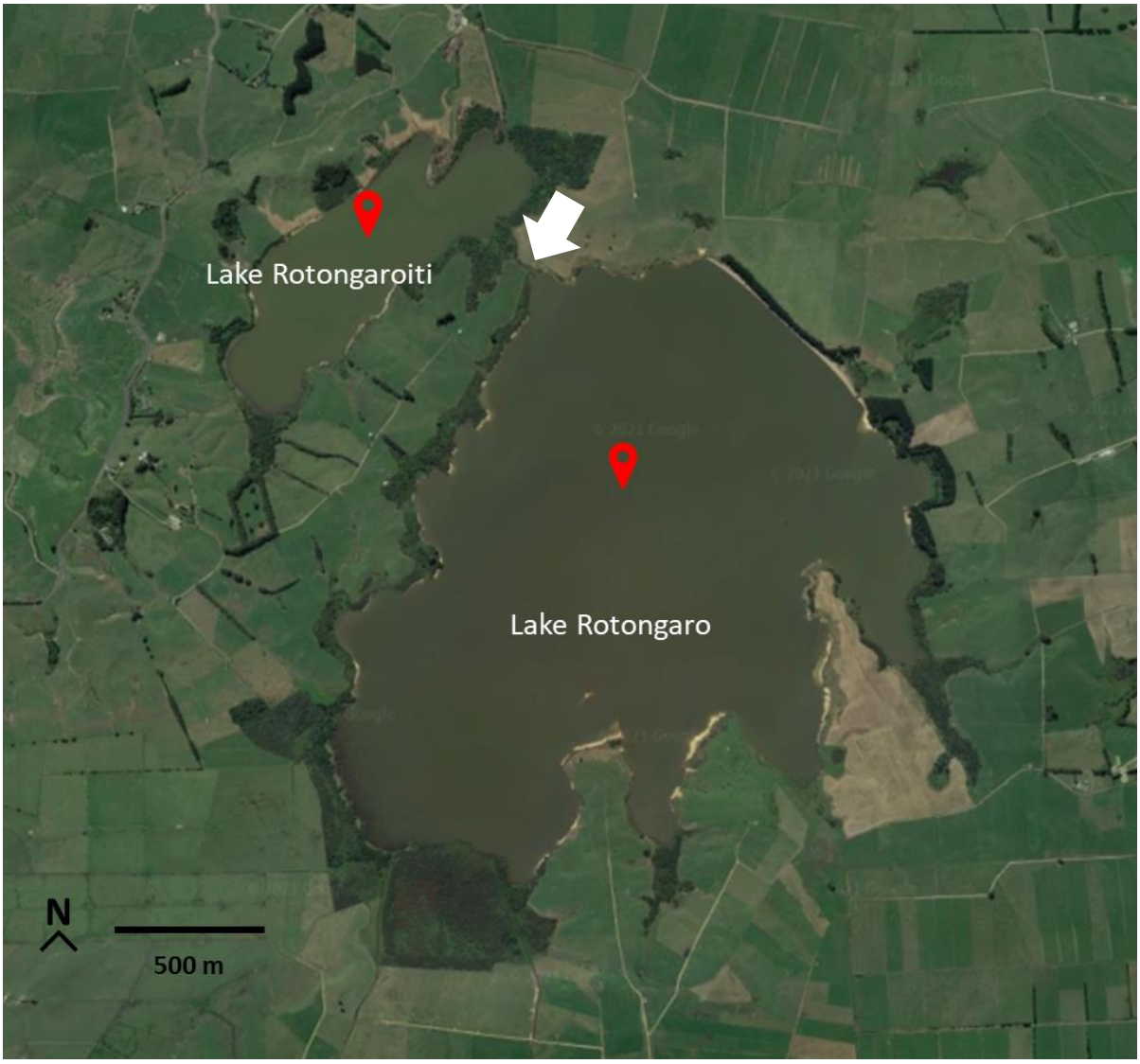

Figure 2.10. Lake Rotongaro and Rotongaroiti with sampling sites. Arrow indicates the channel joining the two lakes. Image from Google Earth.

2.3.4 Lake Rotongaroiti

A shallow (maximum depth 0.5 m) riverine lake located (37.47°S, 175.10°E) adjacent to Lake Rotongaro (Figure **2.10**), due to this connection, it is sometimes referred to as Lake Rotongaro's second basin (Boswell *et al.*, 1985). The 53 ha lake area is described as turbid, but no recent data on water quality is recorded.

The 2105 ha catchment is predominantly dairy farming with small standings of pine plantations. The lake falls within the same wildlife management reserve as Lake Rotongaro, which DOC manages. Inflow is from Lake Rotongaro via a small channel with an outflow into

the Rotongaro canal leading to Lake Whangape and then into the Waikato River (Dean-Speirs *et al.*, 2014). This outlet canal can dry up when water flow is restricted, especially when Waikato River levels drop (de Winton & Champion, 1993). The lake edge is fully fenced but not adequately to exclude stock (Dean-Speirs *et al.*, 2014).

Initially, Lake Rotongaroiti supported the same plant submerged plant species as Lake Rotongaro, and by 1992 only two species were recorded, and by 2005 the lake was recorded as de-vegetated (Edwards *et al.*, 2010). There is no current information on if the lake sustains any fish species.

2.3.5 Lake Ohinewai

A shallow (maximum depth 4.5 m) 16 ha riverine lake (Figure **2.11**) located on a floodplain close to the Ohinewai Peat Bog (Dean-Speirs *et al.*, 2014). Extensive development around the lake has resulted in much lower lake levels (Boswell *et al.*, 1985). The early 1990s saw a move from an oligotrophic state to a eutrophic state (Tempero *et al.*, 2015). In 2013 the recorded TLI was 6.3, classifying the lake as hypertrophic (Collier *et al.*, 2019).

The catchment is 331 ha of pastoral farming and is fully fencing to excluded stock, and little native vegetation can be seen within the lake's catchment (Dean-Speirs *et al.*, 2014). Input is from one drain located on the southwest side and outflow drains from the northeast to Lake Waikare via Lake Rotokawau (Tempero *et al.*, 2019).

The banks of the lake are steep, with the shallow littoral zone dropping to 2 m quickly, emergent vegetation grows around the lake margin (McLea, 1986). Reports in 1981 showed Egeria predominantly covering the lake bottom, and by the early 1990s, the lake was recorded to be in a de-vegetated state (Edwards *et al.*, 2010). Exotic pest fish such as *Gambusia*, goldfish and koi cap are present along with native common bully, shortfin, and longfin eel (Collier & Grainger, 2015). A study to reduce koi carp saw a one-way barrier installed in the outflow stream of Lake Ohinewai to stop koi carp recolonising the lake after removal but designed to allow migration of native species (Tempero *et al.*, 2019). This barrier saw 850 kg of koi carp biomass removed from the lake within six months (Collier & Grainger, 2015).

Figure 2.11. Lake Ohinewai indicating sampling site, inflow entering lake on southwest side and outflow can be seen to the north-eastern end of the lake. Image from Google Earth.

Chapter 3

Methods

3.1 Field collection and processing

Seasonal study sites were sampled monthly over two consecutive summer-autumn seasons. The first sequence was undertaken between November 2019 to May 2020. Due to the Covid 19 nationwide lockdown, *in situ* sampling was not undertaken in March and April 2020. The second sequence begun in October 2020 through March 2021. Due to time constraints, Lake Rotomā was not sampled in February 2020, and November 2020 sampling was postponed to the 2nd December due to adverse weather. All sampling was undertaken between 1000 and 1430 hours, and all three lakes were sampled on the same day, in the same order. Lake Rotomā was sampled first to reduce potential macrophyte contamination, followed by Lake Rotoehu. Lake Rotoiti was sampled last to avoid the possible translocation of the invasive catfish residing in the lake. Between lakes, equipment was checked for weed and catfish, and if necessary, the boat and trailer were sprayed with a diluted bleach solution.

The Waikato lakes underwent one-off sampling between the 27th and 28th of July 2020. Sampling was primarily designed to measure water colour, as the spectral reflectance of the lake water, and the main optically active substances in each lake that contribute to that colour.

3.2 Field procedures

Temperature profiles

Temperature profiles were recorded vertically through the water column at each station to a maximum depth of 25 m using an Aqua TROLL 600 multiparameter sonde (Figure **3.1**). Temperature measurements were recorded from 2 m downwards to remove any influence from diurnal stratification, and were terminated at 25 m depth when any thermal stratification was evident.

Figure 3.1. Aqua TROLL being lowered vertically into water column to obtain temperature readings.

Secchi Depth

Water clarity was measured using a 20 cm Secchi disc attached to a measuring tape (Figure **3.2**). The disc was lowered vertically through the water column until the black and white quadrants were just no longer visible, and the depth to the lake surface was recorded.

Figure 3.2. Secchi disc beginning its vertical descent into Lake Rotoiti.

Spectral Reflectance

A hyperspectral radiometer (Satlantic HyperOCR), with downwelling irradiance and upwelling radiance sensors, was used to obtain lake surface reflectance data. The sensors were mounted on a raft (Figure **3.3**), which was deployed at each station and manoeuvred to establish no less than ten meters from the boat to eliminate any shadowing before

commencing recordings. The radiance sensor was set to be just above the lake surface to avoid the need to make immersion corrections and was inside a Gershun Tube to eliminate glint. The device logged downwelling irradiance and upwelling radiance across 136 channels from 350 to 850 nm every second for approximately ten minutes before retrieval.

Figure 3.3. Satlantic HyperOCR with downwelling irradiance sensor (top right) and upwelling radiance sensor (bottom left) deployed in Lake Rotomā.

Reflectance was calculated as the upwelling radiance divided by downwelling irradiance. The recorded spectra were interpolated to 1 nm intervals, and any outliers due to skylight or glint were removed before calculating the final reflectance spectra as the mean of the remaining reflectance estimates.

Calculations were:

$$Rrs(\lambda) = L_u(\lambda) / E_d(\lambda)$$

Where:

Rrs = reflectance

L_u = upwelling radiance

E_d = downwelling irradiance

λ = wavelength

Water Sampling

Water samples were collected from just below the lake's surface for the analysis of phytoplankton composition, CDOM, total suspended solids, spectral absorption of algal and non-algal particles, chlorophyll *a* and phycocyanin. For phytoplankton composition, a 500 ml sample was immediately preserved with Lugol's iodine solution (20 g potassium iodide and 10 g crystalline iodine dissolved in 1 litre of water). For CDOM, 60 ml of surface water was filtered using a sterile 0.2 µm Minisart® syringe filter and a 60 ml sterile Terumo® syringe into clean PPE bottles. For the others, a bulk sample (5 L) of lake surface water was taken for filtration back in the laboratory. Samples were kept dark, on ice, for transport to the laboratory (up to 5 hours away) and then in a 4 - 8 ^{o}C refrigerator until processing.

3.3 Laboratory procedures

On return to the laboratory, filtration that could not be performed *in situ* was undertaken. All sub-samples were filtered under a vacuum of no more than 10 Hg, to prevent cell damage.

Total Suspended Solids

Pre dried and weighed 47 mm diameter GF/C Whatman filters (nominal 1.2 µm pore size) were used to filter known volumes of lake water for total suspended solids, then dried in a 60 °C drying oven for no less than 24 hours. Duplicate filters per site were processed.

Once dried, samples were re-weighed. The average for each site was taken and calculated as follows:

$$TSS\ (g\ m^{-3}) = (FW-PW)/V$$

where:

FW = final weight of filter once dried (g)

PW = weight of empty filter (g)

V = volume of lake water filtered (m^{-3})

Chlorophyll a and Phycocyanin

Sub-samples were filtered through 25 mm diameter Whatman GF/C filters. The filters were folded in half with tweezers, placed in cellophane pouches and stored at -65 °C. Duplicate filters per site were processed.

Extraction and analysis of chlorophyll *a* were processed in accordance with the protocol from Paul (2010) for fluorometric determination of chlorophyll *a* pigments. A Turner Designs model 10 fluorometer, calibrated using a chlorophyll *a* standard derived from *Anacystis nidulans* (Sigma Chemicals C6144-1MG). Thawed filters were ground with 5 ml of 90% (v/v) buffered acetone with a mortar and pestle. This slurry was transferred into a centrifuge tube, the mortar was rinsed with an additional 5 ml buffered acetone and added to the tube. The sample was then capped, shaken, wrapped in aluminium foil and steeped for 2 – 24 hrs at 4 ^{o}C in the dark. Samples were shaken at least once during this period. After the steeping period, samples were resuspended by vigorous shaking then centrifuged for 10 min at 3300 rpm. Tubes were left to stand in the dark for approximately 30 min before analysis. An analytical blank was measured in the fluorometer using 90% buffered acetone before duplicate 5 ml of sample extract were measured. If chlorophyll concentrations were above calibrated levels, buffered acetone was used to dilute the sample before re-measuring. To correct for background phaeopigments, acidification was undertaken by adding 150 ul of 0.1 N HCl mixed well within the sample before re-measuring.

Chlorophyll *a* concentration was calculated as follows:

$$Chl\ a\ (\mu g\ L^{-1}) = F_s\ [\ (R_1 - R_2)\ (r\ /\ r\text{-}1)]\ [(V_e\ x\ df)/V_f\ ]$$

where:

Chl a = Chlorophyll *a*

F_s = response factor for sensitivity setting (derived from recent fluorometer calibration)

R_1 = reading before acidification minus blank reading

R_2 = reading after acidification minus blank reading

r = acidification coefficient calculated by averaging the ratio of the unacidified and acidified readings of pure chlorophyll *a*

df = dilution factor

V_e = extraction volume

V_f = volume of water filtered

Phycocyanin

Samples for phycocyanin were only taken from October 2020 through to March 2021. Extraction and analysis of phycocyanin were undertaken following the standard operating procedure for spectrofluorometric determination of phycocyanin pigments from freshwater filtrate (Tempero & Ling, 2020). Sample filters were homogenised with 20 ml of 50 mM phosphate buffer (pH 7). Samples were covered in aluminium foil and refrigerated at 4-6 ^{o}C for 2 hours, then allowed to warm to 2 hrs at room temperature before centrifuging for 5 min at 3300 rpm. The spectrofluorometer (Shimadzu RF-5301 PC) was set to an excitation wavelength of 615 nm, an emission wavelength of 652 nm and high sensitivity. Extraction phosphate buffer was run as a blank. 2 ml of supernatant was transferred into a cuvette and left to sit for 30 s before reading.

Phycocyanin concentrations were calculated from fluorescence yield using a standard curve prepared from a dilution curve of pure phycocyanin (Sigma) in extraction buffer.

$$Phycocyanin\ (\mu g\ L^{-1}) = ((55.306 \cdot Sr) - 3.4514)) \cdot (Ev/Fv)$$

where:

Sr = Spectrofluorometer reading corrected for extractant blank

Ev = Sample extraction volume in ml

Fv = Sample filtration volume in ml

Spectral Absorption of Algal and Non-algal Particles

Sub-samples for each lake were filtered through 25 mm diameter Whatman GF/C (0.7 µm nominal pore size) glass fibre filters. Filters were placed in individual plastic containers and stored at -65 °C until analysis.

The absorption spectra of phytoplankton and non-algal particles was estimated using the Transmittance – Reflectance (T-R) method (Tassan & Ferrari, 2002). All measurements were

performed using a dual beam UV-VIS Spectrophotometer (UV-2600 series, Shimadzu) equipped with an integrating sphere, with sample and reference ports. The method essentially measures the transmission and reflection of light from the thawed sample filter against an open reference port and compares with those of a blank reference filter in the same configuration. All manipulations were exactly according to the established protocol (Tassan and Ferrari 2002). The reference filter was wetted with Milli-Q water to be directly comparable to the sample filter. Scans were repeated after bleaching the filters using 1 ml of 0.13% hypochlorite for 5-10 minutes and rinsing this off by mounting the filter in a filter tower and running 25 ml of Milli-Q water through it. Hypochlorite was used rather than an organic solvent to ensure that all phycobilin pigments (which are not soluble in organic solvents) were removed. If traces of pigments were evident in subsequent scans the bleaching procedure was repeated.

Values derived from the spectrophotometer, for both unbleached and bleached case, were:

PT_s = % transmission of the sample filter

PT_r = % transmission of the blank filter

PR_s = % reflectance of the sample filter

PR_r = % reflectance of the blank filter

Rf = reference spectrum of a fresh filter

Calculations were then as follows:

$$a_s = 1 - PT + Rf\,(PT\text{-}PF) / 1 + Rf\,PT\,T$$

$$OD_s = log\,(1 / 1 - a_s)$$

$$\alpha_p(\lambda) = 2.3\,OD_{sus}\,(\lambda) / X\,C$$

Where:

$PT = PTs / PTr$

$PR = PRs / PRr$

$T = 1.15 - 0.17\,OD_{tr}\,(\lambda)^*$

$OD_{tr}(\lambda)^* = OD(\lambda) - ½\,OD_{tr}\,(750)$

$OD = log_{10}(1\text{-}T)$ (dimensionless)

$OD_{sus} = (0.423 \pm 0.0125)\,OD_s + (0.479 \pm 0.06)\,OD_s^2$

a_s = absorption by the particles due to a normally incident unitary parallel light beam on a single through-way (dimensionless)

T = factor accounting for the fact that the radiation backscattered by the filter on particle deposit is diffuse radiation (dimensionless)

OD_s = optical density of particles on the filter

OD_{sus} = optical density of particle suspension

$OD_{tr}(\lambda)$ = optical density measured in the transmission mode

αp = Specific absorption coefficient of particulate (m^{-1} per unit mass concentration)

C = particle concentration (mass unit m^{-3})

X = ratio of the filtered volume to the filter clearance area (m)

Chromophoric Dissolved Organic Matter

The absorption spectrum of the filtrate was determined using a twin-beam UV-VIS Spectrophotometer (UV-2600 series, Shimadzu) with 10 cm quartz cuvettes. The spectrophotometer was baselined using Milli-Q water in both slots, then the absorption spectrum was determined by running lake water samples against Milli-Q water in the reference cell. The data underwent a null correction from $a(650)$ wavelength as discussed in (Loiselle *et al.*, 2009) and (Stedmon *et al.*, 2000).

Absorption (m^{-1}) was calculated from optical density as:

$$a_\lambda = 2.303 \cdot A_\lambda / l$$

Where:

a_λ = absorption at wavelength λ

A_λ = optical density at wavelength λ

l = cuvette pathlength (m)

λ = wavelength

To characterise CDOM, two values were determined, the absorption at 440 nm ($a_{CDOM}(440)$) and the exponent of the relationship between $a(\lambda)$ and λ.

Phytoplankton assemblages

Enumeration and identification of phytoplankton from the Lugol's fixed sample were undertaken using an inverted microscope (Olympus IM) at 400x magnification. Taxonomic guides from Prescott (1964), Moore (2000), Wood et al. (2009), Bellinger & Sigee (2015) and Nienaber & Steinitz-Kannan (2018) were used to identify phytoplankton down to genus level. A minimum cell count of 100 was completed for each sample, and cell numbers were estimated using the Utermöhl method (Utermöhl, 1958) as follows:

$$N = C \cdot f\,(A/b \cdot a \cdot V)$$

where:

N = number of algal cells per ml in the original water sample

C = total number of algal cells counted in all fields

A = total area of the bottom of the settling chamber (mm^2)

a = total area of the field of view (mm^2)

b = number of fields counted

f = dilution or concentration factor

V = volume of lake water settled (ml)

Biovolume was obtained by firstly determining cell volume for each species. Cell volume was calculated by taking the average measurement of 10 - 20 cells per species using an Olympus EP50 microscope digital camera. Cyanobacteria volumes were estimated following the guidelines from Wood *et al*. (2009) (Table **3.1**), while methods described by Hillebrand *et al*. (1999) and Sun (2003) were used for the remaining species. Measurements were taken of live vegetative cells only. For species where less than ten cells were observed, cell volumes from a national database maintained by the National Institute of Water and Atmosphere Research (NIWA) were used (NIWA pers. Com, 2021). Preservation in Lugol's iodine can cause cell shrinkage of up to 40 %, depending on Lugol's concentration and time before analysis (Hawkins *et al.*, 2005) which has not been accounted for here as this is not normal practice in NZ. The samples were typically stored for up to several months before counting.

Table 3.1. Shape and formula for cyanobacteria used to obtain cell volume (V) (µm^3).

Shape	Formula	Species
Ovoid (round)	V = ((4/3)·π·(diameter/2)^3)	*Aphanocapsa* sp.
		Microcystis sp.
Ovoid	V = (4/3) ·π· (width/2)^2 ·(length/2)	*Coelosphaerium* sp.
		Dolichospermum sp.

When identified, phytoplankton species were assigned to one of the following groups: Cyanobacteria, Green algae (chlorophyta and charophyta), Diatoms, Golden algae, Euglenoids, Dinoflagellates, and non-pigmented protozoa. The non-pigmented protozoa species were not enumerated.

Biovolume was calculated as:

$$BV\ (mm^3\ L^{-1}) = (n \cdot v_c) / 1 \cdot 10^6$$

Where:

BV = biovolume

n = number of cells in a sample (cells ml^{-1})

v_c = volume of each cell (um^3)

3.4 Data Analysis

Temperature profiles

Processing of temperature-depth profiles to detect the mixed layer depth involved the calculation of the rate of change of temperature with depth (ΔT - °C / m) as:

$$\Delta T = (T_1 - T_2) / (z_2 - z_1)$$

Where:

ΔT = change in temperature

T_n = temperature at depth n

z_n = depth n

ΔT for each profile was assessed to characterise stratification and classed as (1) distinct stratification, (2) a temperature gradient but no distinct thermocline, or (3) fully mixed. If distinct thermal stratification was observed, the thickness of the mixed layer and the depth of the thermocline were recorded as the depth at which ΔT began to increase and the depth of maximum ΔT respectively.

Statistical analysis

Main study lakes water quality variables

Prior to analysis, all variables were checked for normality, and where non-normality was evident (chlorophyll *a*, phycocyanin and biovolume) this was corrected using a log-transform. Differences for all variables between the two sites in each lake were then examined using paired t-tests and between lakes using ANOVA (Excel, Microsoft®). Linear and log regressions (Excel, Microsoft®) were used to determine if there were significant relationships between variables measured across the sampling dates. Relationships between variables were examined using a Pearson correlation matrix. Pearson correlations were undertaken in Statistica 14.0.0.15 (TIBCO Software Inc.).

Phytoplankton composition

Species diversity in the lakes was quantified using the Shannon-Wiener index (0 – 5). This index takes into account the richness and relative abundance of species, with high index indicating high heterogeneity. Sorenson's coefficient (0-1) was used to identify the degree of community similarity between sites in each lake based on the number of species that they had in common. The closer the result is to one, the more similarity exists.

Resemblance matrices based on the biovolume of the ten most abundant phytoplankton in each lake were calculated using Primer-7 (www.primer-e.com) and these were used to construct non- multidimensional scaling plots comparing the three Rotorua lakes. PERMANOVA, with *post-hoc* testing, was then undertaken using Lake as a factor to determine whether and where significant between-lake differences were evident.

Optical properties

Ternary plots were used to indicate the relative contributions of total absorption of CDOM, phytoplankton and non-algal particles at 440 nm wavelength across all lakes throughout the sampling dates.

Cluster analysis and PERMANOVA were used to group the reflectance spectra according to shape and to test the significance of lake and dominant phytoplankton in structuring the clustering pattern. For this, Primer-7 (www.primer-e.com) was used to construct a resemblance matrix based on Euclidean distance for all reflectance spectra from the Rotorua group of lakes, then hierarchical clustering was used to create a dendrogram. 2-way PERMANOVA, with *post-hoc* pairwise testing using as factors the dominant phytoplankton classes (by biovolume) and lake, were then undertaken to determine whether significant factor effects were evident.

Algorithms

Existing algorithms to estimate chlorophyll *a* and phycocyanin concentration from absolute reflectance spectra were selected from Zhu *et al.* (2014). Two algorithms for each pigment were assessed. The ability of each algorithm to predict the target pigment was assessed by linear regression of observed vs predicted, using Statistica.

Chlorophyll a

Algorithm 1: Four band multiple regression (O'Reilly *et al.*, 1998).

$$C = exp\ (a_0 + a_1 \cdot R_1 + a_2 \cdot R_2)$$

Where:

C = chlorophyll *a*

a_0 = intercept

a_1 = coefficient for R1

a_2 = coefficient for R2

R_1 =ln (Rrs 443/Rrs 555)

R_2 = ln (Rrs 412/Rrs 510)

Algorithm 2: Four band semi analytical model (Le *et al.*, 2009)

$$C = a\,[Rrs^{-1}(\lambda_1) - Rrs^{-1}(\lambda_2)] \cdot [Rrs^{-1}(\lambda_4) - Rrs^{-1}(\lambda_3)]^{-1}$$

Where:

a is a coefficient

λ_1 = 663 nm

λ_2 = 693 nm

λ_3 = 705 nm

λ_4 = 740 nm

Phycocyanin

Algorithm 1: An algorithm using a band ratio that was shown to have the maximum and minimum sensitivity to phycocyanin concentrations (Mishra *et al.*, 2009).

$$P = a\,[Rrs(700)/Rrs(600)]$$

Where:

P = phycocyanin

a is a coefficient

Algorithm 2: This algorithm uses three wavelength points on the absolute reflectance spectrum (Mishra *et al.*, 2019).

$$P = a\,[(Rrs(665)-Rrs(620))+(Rrs(620)-Rrs(681))\cdot(Rrs(665)-(Rrs(620))/(Rrs(681)-Rrs(620))]$$

Where:

P = phycocyanin

a = a coefficient

Chapter 4

Results

4.1 Seasonal Study

Stratification and mixing depth

The stratification regimes and mixing depths in the three study lakes were assessed based on temperature profiles. These were likely biased towards clear, relatively calm days as this was the requirement for the deployment of the optical equipment. Three basic types of profile were evident; a distinct mixed layer with an abrupt thermocline, fully mixed, and a temperature gradient (Figure **4.1**).

May 2020 saw all three lakes fully mixed (Figure **4.2**). Lakes Rotomā and Rotoiti followed similar stratification regimes, with gradients only seen during spring warming and a distinct stratification becoming evident during the summer at 14 – 22 m depth. Lake Rotoehu tended to show less stratification and, through the seasons, was often isothermal or showed a temperature gradient (Figure **4.2**).

Stratification patterns are illustrated in Figure **4.3** by comparing temperatures at 2 and 25 m depth (2 and 10 m for the shallow Lake Rotoehu). Lakes Rotomā and Rotoiti had distinct hypolimnia that remained at around 12 ^{o}C while surface waters warmed from November onwards, reaching maxima of ~22 ^{o}C in late summer (February to March). Lake Rotoehu's temperature profile showed a less distinct separation of an upper and lower water column, with both tracking upwards through summer and approaching 20 ^{o}C. During mixing in May 2020 all lakes approached 12 ^{o}C. A paired sample t-test showed temperatures between sites within each lake and at each depth were nonsignificant (p = >0.05), with no one site consistently higher or lower than the other.

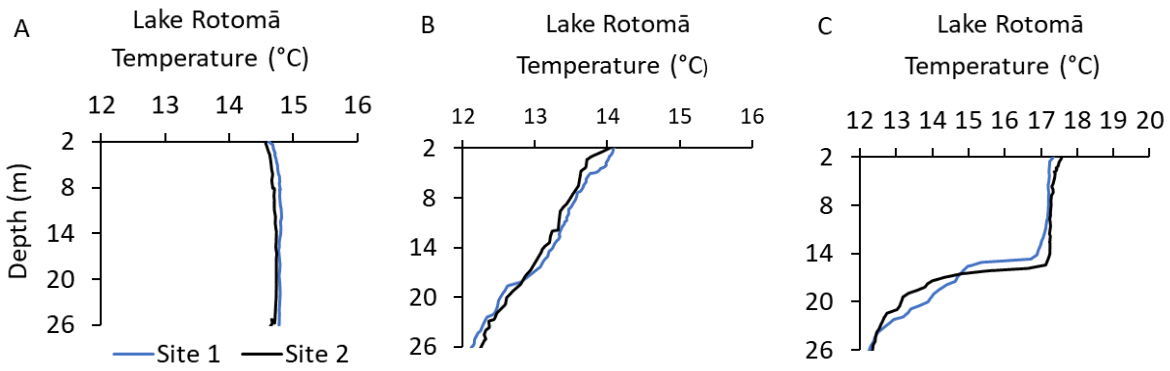

Figure 4.1. Examples of the three temperature profile gradients seen. A) May 2020 showing a thoroughly mixed water column B) October 2020 showing a temperature gradient with no clear thermocline, C) December 2nd 2020, indicating distinct stratification.

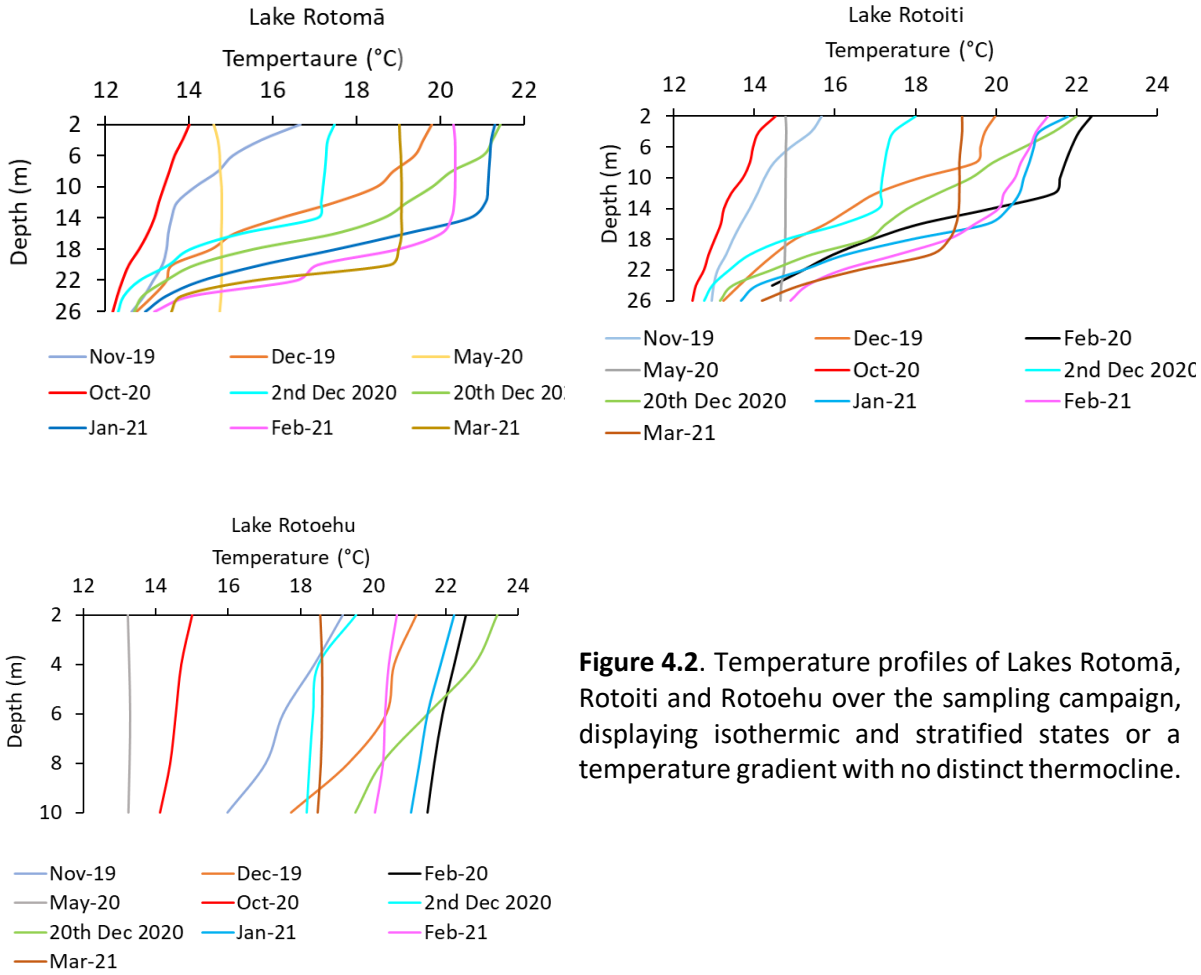

Figure 4.2. Temperature profiles of Lakes Rotomā, Rotoiti and Rotoehu over the sampling campaign, displaying isothermic and stratified states or a temperature gradient with no distinct thermocline.

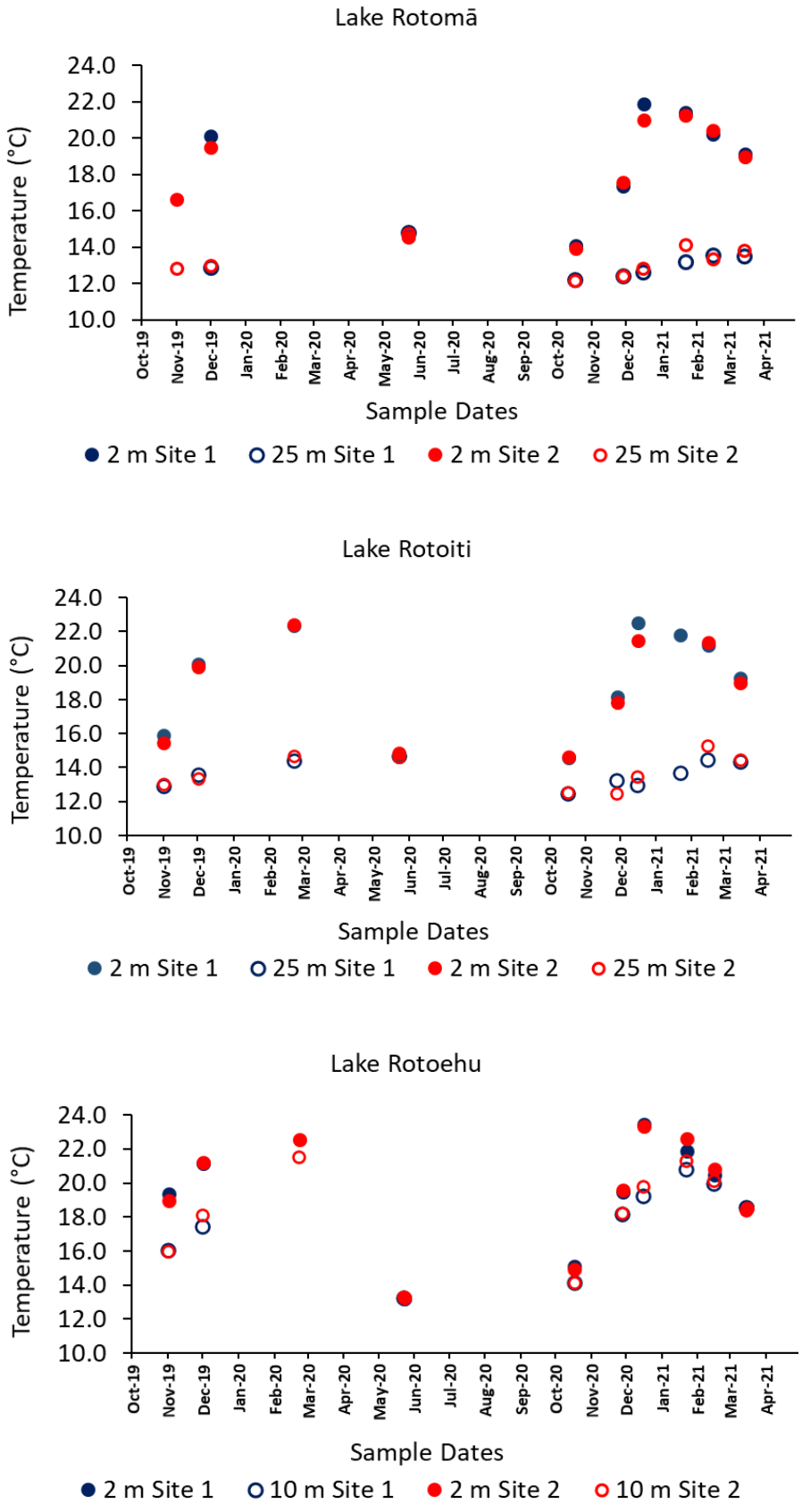

Figure 4.3. Temperatures were recorded at a depth of 2 m and 25 m across the sampling seasons for Lakes Rotomā and Rotoiti. Lake Rotoehu expressed at a depth of 2m and 10 m.

Secchi Depth

Secchi Depth was greatest in Lake Rotomā, with an average 11 m, compared to 5.6 m in Lake Rotoiti and 2.6 m in Lake Rotoehu (Figure **4.4**). Lake Rotomā was the only lake to show a significant difference between sites one and two (paired sample t-test, p = 0.02. There was a slight tendency for clarity to decline over the summer period in all lakes, but this was not strongly developed in any of the three lakes.

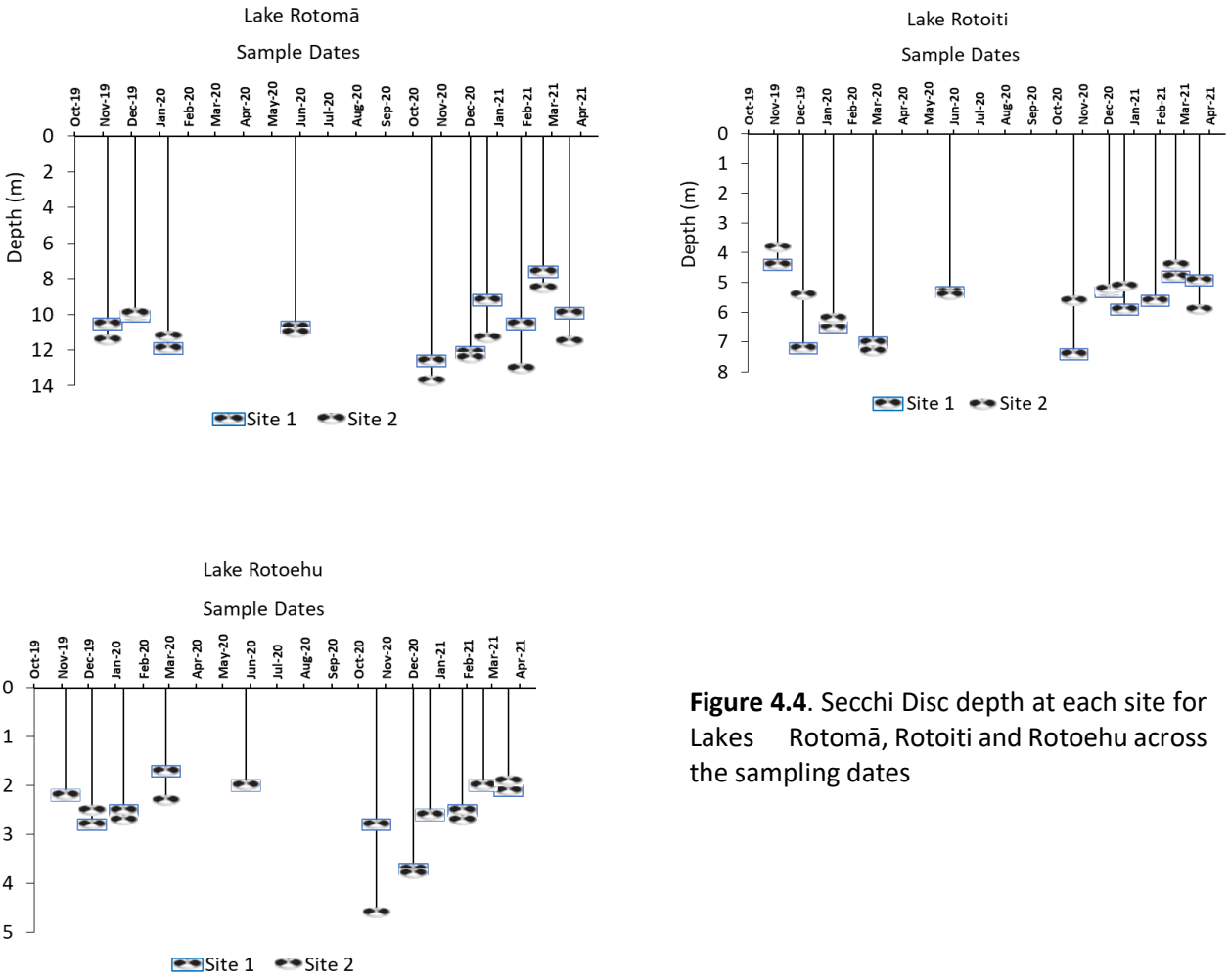

Figure 4.4. Secchi Disc depth at each site for Lakes Rotomā, Rotoiti and Rotoehu across the sampling dates

Total Suspended Solids

As with Secchi depth, TSS showed no pronounced temporal trend and no consistent difference between sites (paired t-test all p = >0.05). All lakes presented with relatively high concentrations in winter, when the lakes were fully mixed, but equally high values were observed at other times of the year. Variations were evident between lakes, with median TSS of 0.41 g m^{-3} within Lake Rotomā and 0.81 g m^{-3} in Lake Rotoiti, while Lake Rotoehu was substantially higher, with a median of 3.07 g m^{-3} (Figure **4.5)**. Lake Rotoehu was significantly higher than either of the others (ANOVA, p = > 0.05).

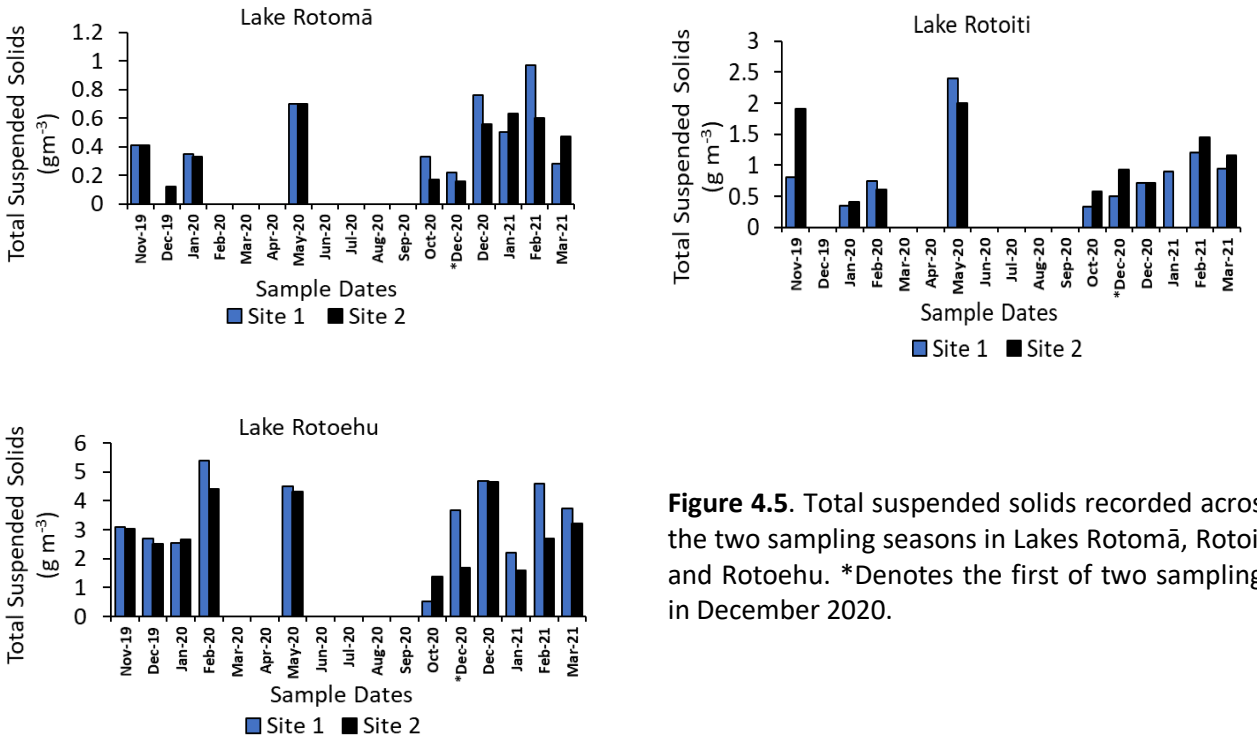

Figure 4.5. Total suspended solids recorded across the two sampling seasons in Lakes Rotomā, Rotoiti and Rotoehu. *Denotes the first of two samplings in December 2020.

Chromophoric Dissolved Organic Matter

CDOM, ($a_{CDOM}(440)$) varied between lakes, in the order Lake Rotomā (average 0.07 m^{-1} range 0.05 – 0.09 m^{-1}), Lake Rotoiti (average 0.176 m^{-1}, range 0.067 – 0.369 m^{-1}) and Lake Rotoehu (average 0.318 m^{-1}, range 0.185 - 0.513 m^{-1}) (Figure **4.6**). At 440 nm, many Lake Rotomā samples were below the detection limits of the spectrophotometer (<0.046 m^{-1}). There was variability between sites in all lakes (paired sample t-test p = > 0.05), and no distinct seasonality was evident. Variability between sampling dates was highest in Lake Rotoehu.

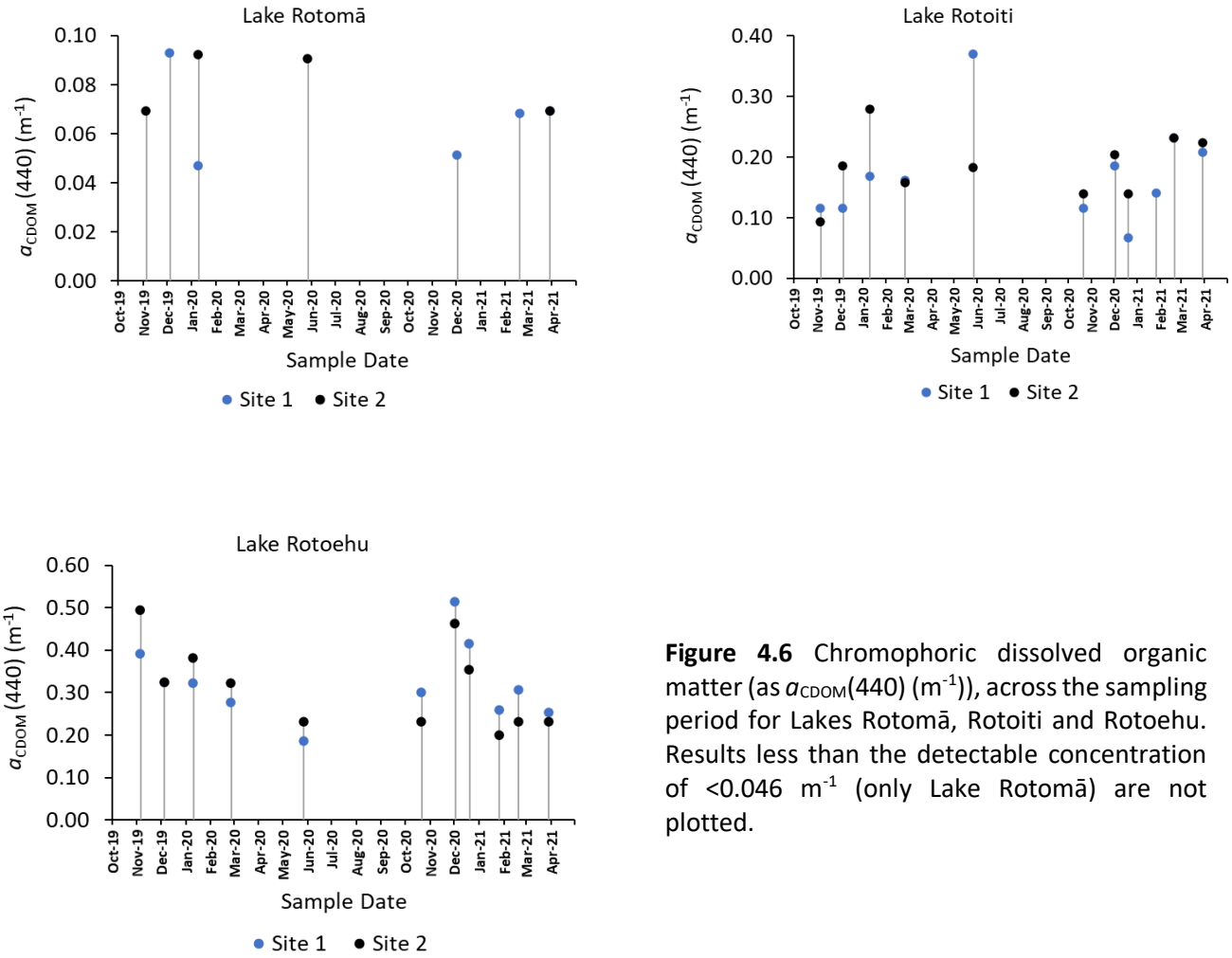

Figure 4.6 Chromophoric dissolved organic matter (as $a_{CDOM}(440)$ (m^{-1})), across the sampling period for Lakes Rotomā, Rotoiti and Rotoehu. Results less than the detectable concentration of <0.046 m^{-1} (only Lake Rotomā) are not plotted.

Chlorophyll a and phycocyanin

Phycocyanin samples were taken only during the second summer-autumn season 2020 – 2021. Changes in chlorophyll *a* and phycocyanin were similar throughout the year for the two deep, stratified lakes with low concentrations in mid-summer, increasing as the mixing broke down in March to May (Figure **4.7**). No seasonal pattern was evident in polymictic Lake Rotoehu.

Chlorophyll *a* and phycocyanin were nonsignificant between sites within all lakes (paired t-test p = > 0.05) with site two in Lake Rotoiti and site one in Lake Rotoehu tending to record higher concentrations.

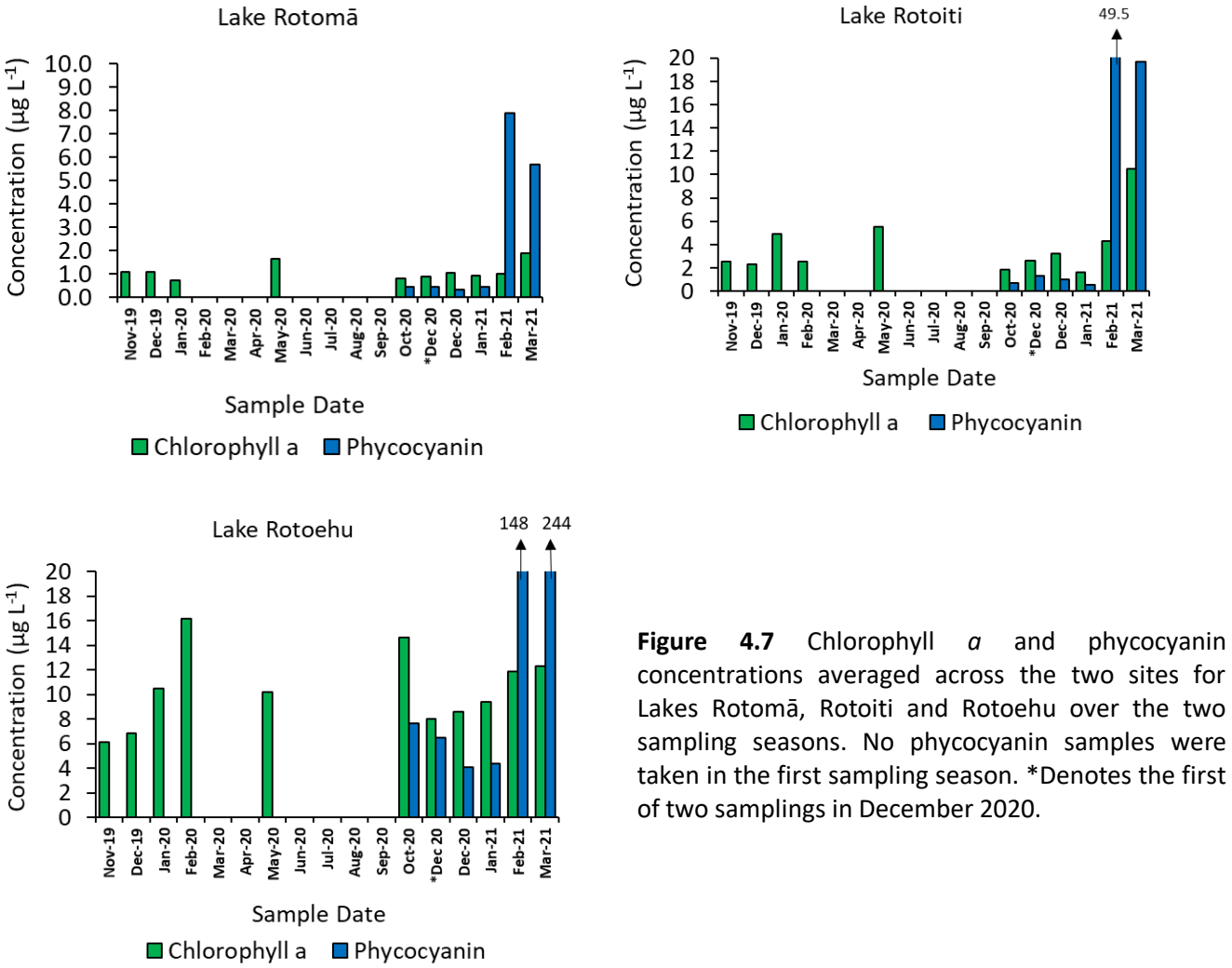

Figure 4.7 Chlorophyll *a* and phycocyanin concentrations averaged across the two sites for Lakes Rotomā, Rotoiti and Rotoehu over the two sampling seasons. No phycocyanin samples were taken in the first sampling season. *Denotes the first of two samplings in December 2020.

Phytoplankton assemblages and biovolume

Thirty-five phytoplankton species were counted within Lake Rotomā, and 46 in Lakes Rotoiti and Rotoehu. Average Shannon-Wiener index was 2.4 for Lake Rotomā, 3.6 for Lake Rotoehu, and 3.9 in Lake Rotoiti. Total phytoplankton biovolume varied between lakes (ANOVA = >0.05) and between sites (Paired t-test p = > 0.05), with site two tending to record higher biovolume in each lake.

Lake Rotomā's highest recorded total phytoplankton biovolume of 0.470 $mm^3 L^{-1}$ occurred under stratified conditions in March 2021, and a minimum of 0.08 $mm^3 L^{-1}$ was seen in November 2019 (Figure **4.8**). Lake Rotoiti recorded its highest biovolume in May 2020 under

a fully mixed water column, reaching 1.90 mm^3 L^{-1}, while October 2020 saw the lowest biovolume at 0.27 mm^3 L^{-1}. Biovolume in Lake Rotoehu reached a maximum of 9.54 mm^3 L^{-1} during February 2020 under the warmest isothermal conditions recorded, this was followed by a decrease in May 2020 with the lowest biovolume recorded in January 2021 of 0.72 mm^3 L^{-1}.

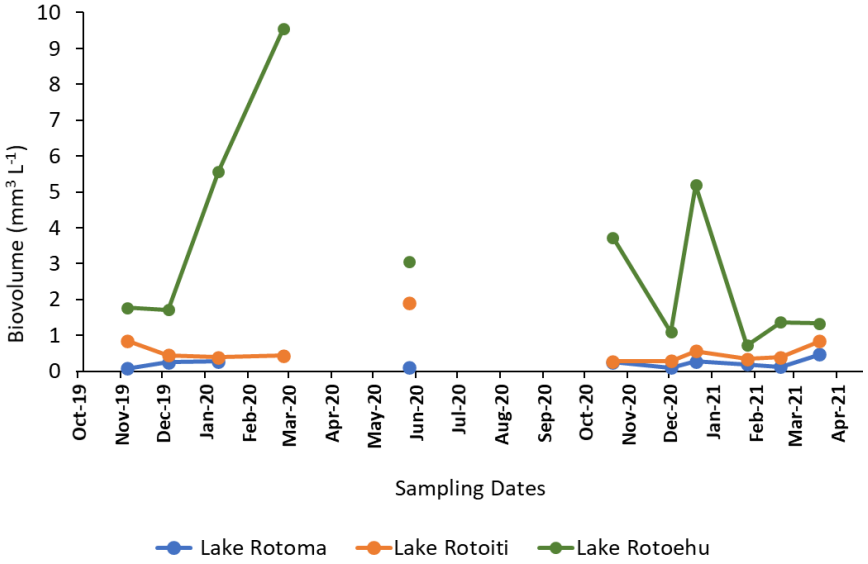

Figure 4.8. Total phytoplankton biovolume obtained from microscope counts over the two sampling seasons for Lakes Rotomā, Rotoiti and Rotoehu. Each point is the average counts from two sites in each lake.

Sorenson coefficient analysis confirmed communities between sites in each lake showed strong similarity, with the coefficient always exceeding 0.89. The top 10 phytoplankton taxa by biovolume varied between lakes (Figure **4.9**). Where definitive allocations to genus or species level could not be made, but cells could be allocated to specific, repeatable morphospecies, pseudonyms were allocated. For example, green sp #1, that formed part of Lake Rotomā's top 10, was a spherical, unflagellated chlorophyte with a diameter of ~7.6 µm, but could not be identified further at 400 x magnification. *Botryococcus*, a colonial green, was seen in Lake Rotoehu's top 10 but could not be enumerated to cells ml^{-1}, therefore evaluated as the average biovolume of the colony (15,150 μm^3). The armoured dinoflagellate *Peridinium* (Figure **4.11.H**) was present across all lakes, with an average diameter of 45 µm and had the largest cellular biovolume of all species counted at 56,506 μm^3.

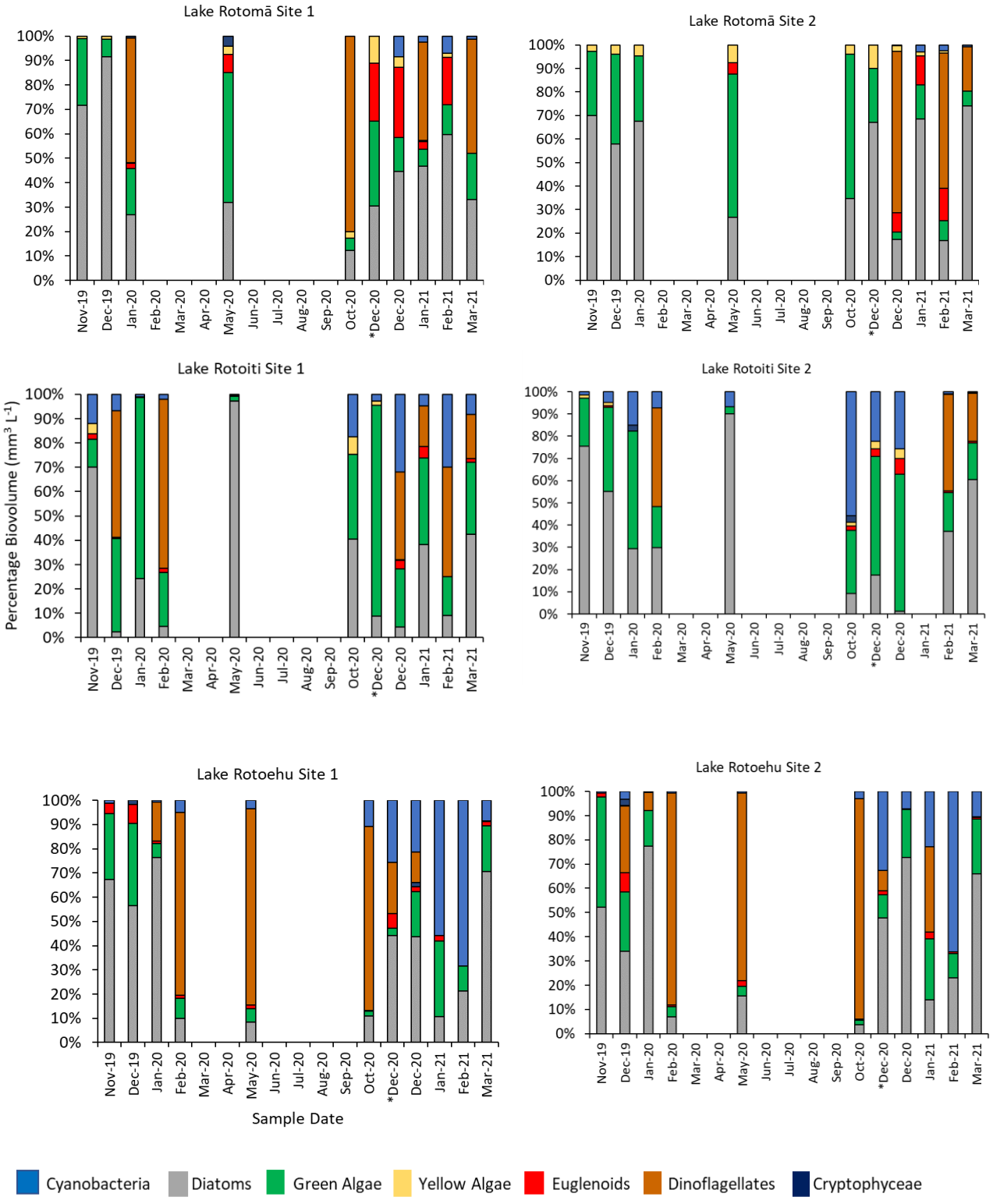

Figure 4.9. Percentage composition, as biovolume of major phytoplankton groups recorded at each site over the sampling seasons in Lakes Rotomā, Rotoiti and Rotoehu. *Denotes the first sampling in December 2020.

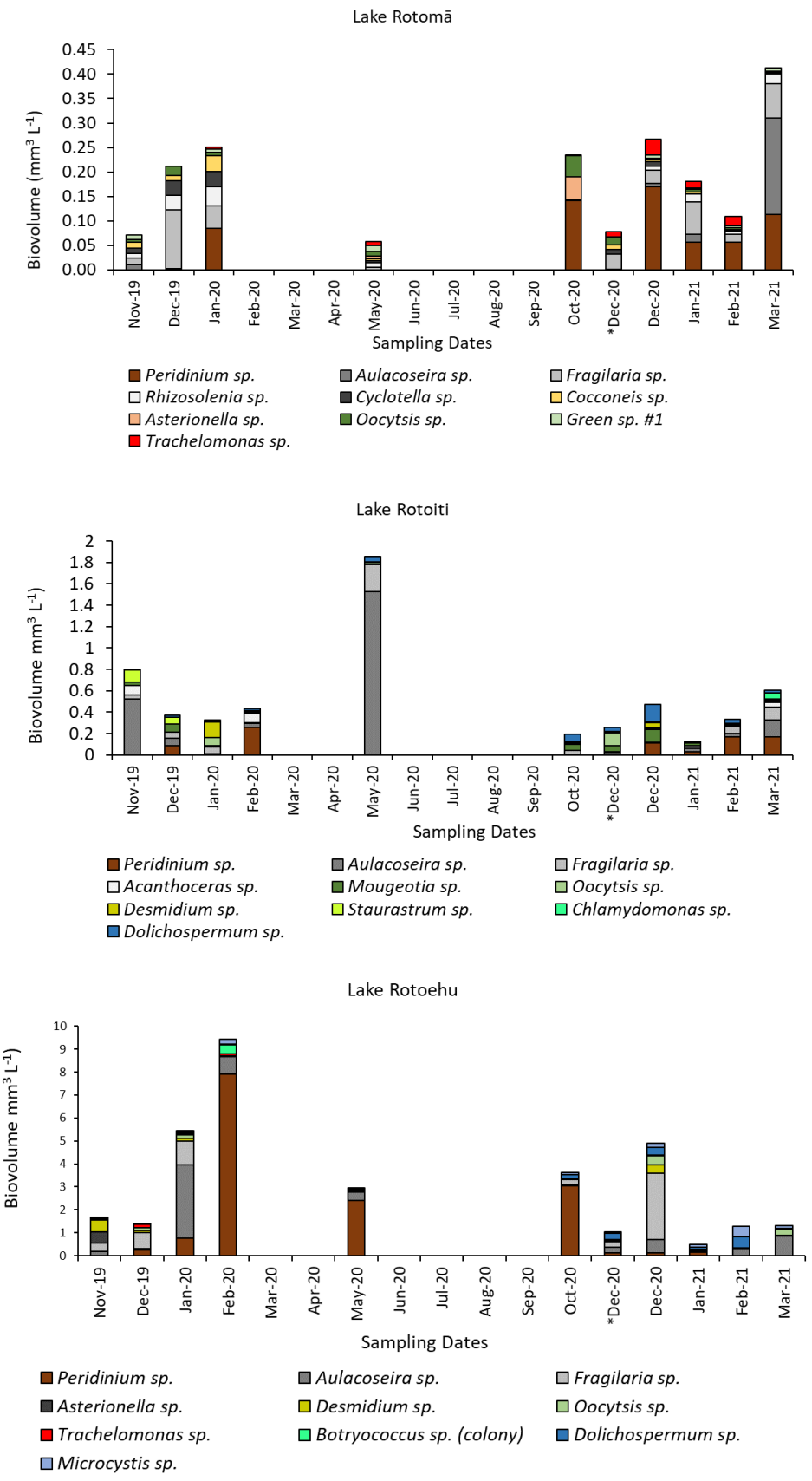

Figure 4.10. Top 10 taxa by biovolume in Lakes Rotomā, Rotoiti and Rotoehu. Each bar represents the average of two sites at each lake.

In the first summer, Lake Rotomā biovolume was dominated by a mix of diatom genera together contributing up to 90%, with a small contribution from two chlorophytes, *Oocytsis* and Green sp #1. Filamentous diatoms from the genera *Aulacoseira* and *Fragilaria* (Figure **4.11.E & F**), were the dominant diatoms. The dinoflagellate *Peridinium* appeared briefly at the end of the summer before disappearing in winter, when dominance switched to green algae, with smaller oblate and elliptic species accounting for the majority of the 61% of chlorophyte biovolume, and diatoms 30% biovolume. In the second summer, diatom dominance was reduced by the frequent presence of large numbers of *Peridinium* and the euglenoid *Trachelomonas,* though diatom dominance increased again as the thermocline deepened at the end of summer*. Peridinium* has a large cell volume, and an increase of relatively few cells in a sample allowed it to assume dominance by biovolume. No desmids or cyanobacteria were in the top ten taxa.

As with Lake Rotomā, the start of Lake Rotoiti's first summer was dominated by diatoms, accounting for 77% by biovolume, again with *Aulacoseira* spp. making up the vast majority. As the summer progressed and the filamentous green algae *Mougeotia* and *Desmidium,* along with the colonial, *Oocytsis,* became dominant, before a brief peak in the dinoflagellate *Peridinium* was seen at the end of summer. During water column turnover in May 2020 *Aulacoseira* made up 80% of the total biovolume. Green algae resumed dominance at the start of the second summer, *Mougeotia* and *Oocytsis* again accounting for most chlorophytes. By late in the second summer, these greens gave way to *Peridinium* and *Aulacoseira,* recording their highest biovolume in March 2021 at 0.167 and 0.156 mm^3 $L^{-1,}$ respectively. The filamentous diazotrophic cyanobacterium *Dolichospermum* was present at low to moderate concentrations throughout, reaching its maximum biovolume in December 2020.

In Lake Rotoehu, the filamentous *Fragilaria, Aulacoseira* (Figure **4.11**) and the star-shaped *Asterionella* dominated the start of the first summer season, while as in the other lakes towards the end of summer, *Peridinium* and in addition the colonial green *Botryococcus* recorded its greatest biovolume of 0.409 mm^3 L^{-1}, representing 72% of green algal biovolume. *Peridinium* continued to dominate through winter until early December 2020, when a diatom peak was seen, this time with *Fragilaria* accounted for 83% of the diatom biovolume. Two cyanobacteria, *Dolichospermum* and *Microcystis* were frequently part of the phytoplankton,

but only dominated biovolume in February 2021. The desmid *Desmidium* was present, but not abundant, and *Dinobryon* (Figure **4.11G**) a golden-brown alga which was seen at low biovolume throughout the year in lakes Rotomā and Rotoiti was not seen in Lake Rotoehu.

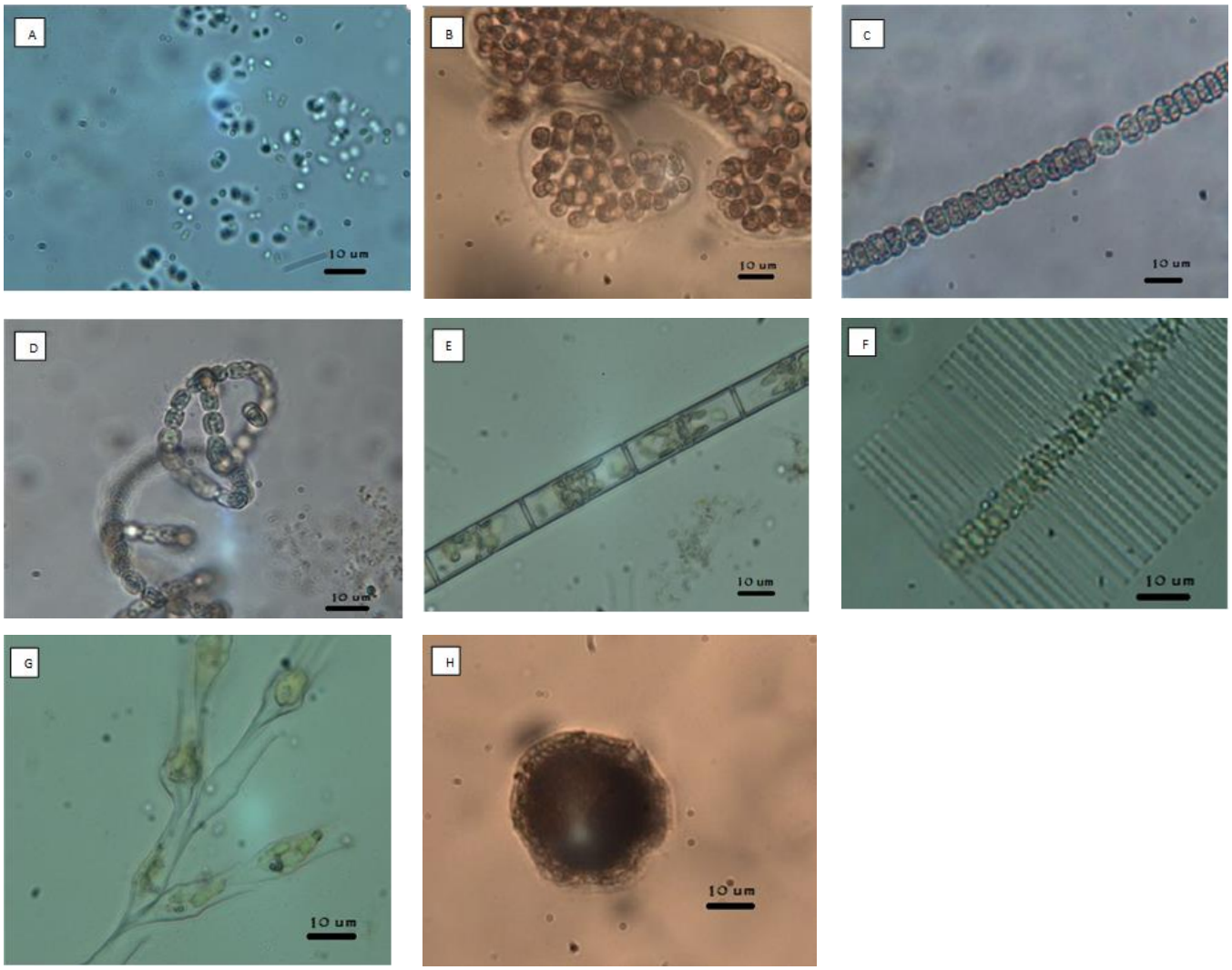

Figure 4.11. Phytoplankton species at 400x magnification identified in Seasonal study sites. (A) *Aphanocapsa* sp. (Lake Rotomā), (B) *Microcystis wesenbergeii* (Lake Rotoehu), (C)&(D) *Dolichospermum* sp. (Lake Rotoiti), (E) *Aulacoserira granulata* (Lake Rotoiti), (F) *Fragilaria* sp. (Lake Rotoehu), (G) *Dinobryon* sp. (Lake Rotomā) and (H) *Peridinium* sp. (Lake Rotomā). All samples fixed in Lugols solution.

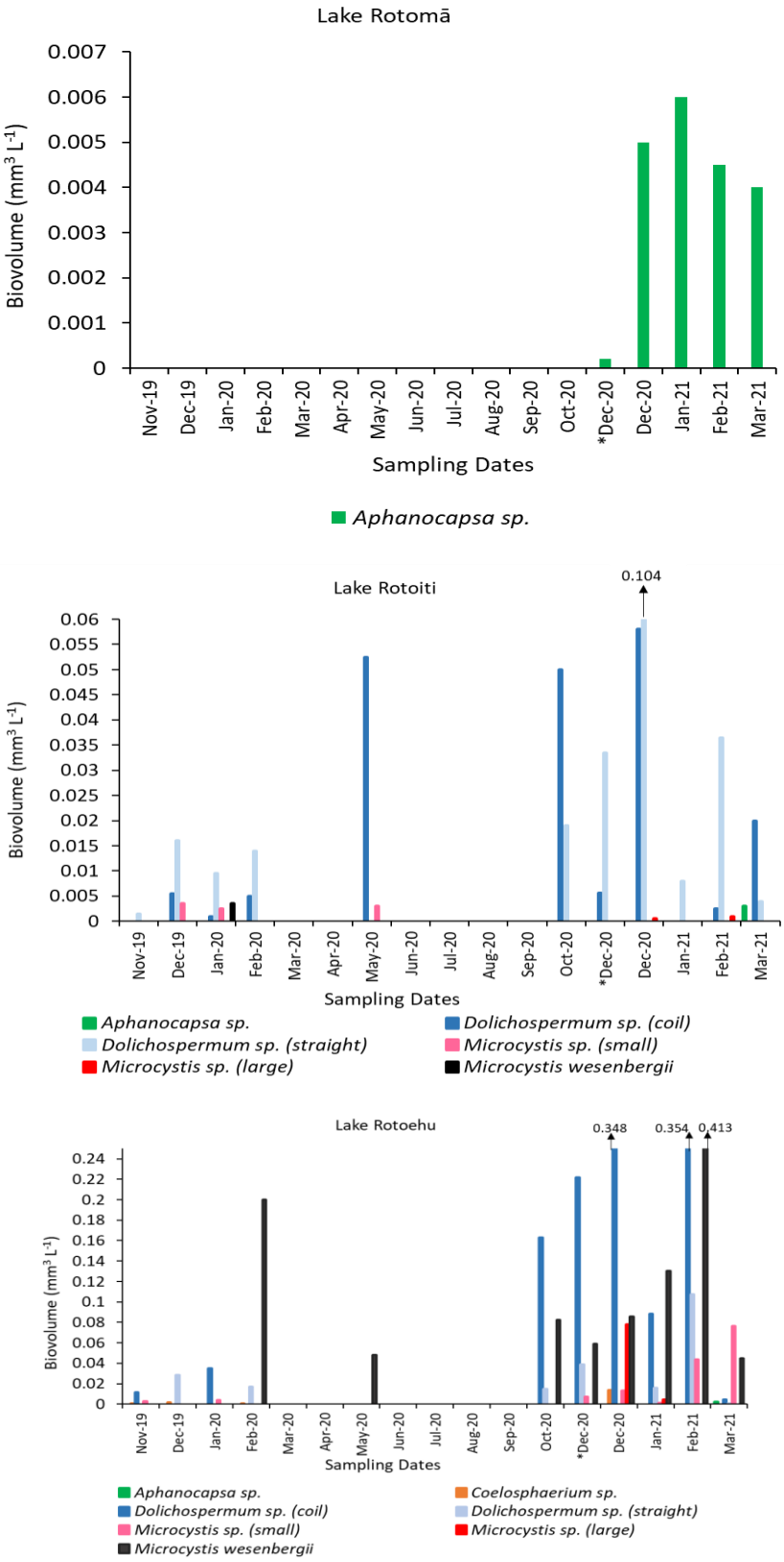

Figure 4.12. Biovolume of cyanobacteria over the sampling period for Lakes Rotomā, Rotoiti and Rotoehu. *Denotes the first of two sampling in December 2020. Each bar represents the average of two sites at each lake. Note that the scale of the vertical axis is different for each lake.

Cyanobacterial biovolume was higher in all lakes in the second sampling season than the first (Figure **4.12**). *Aphanocapsa* sp., a potentially toxic small sphere-shaped cell with a diameter of just 1.5 µm, forming globular gelatinous colonies, was recorded in Lake Rotomā at low concentrations (Figure **4.11.A**). Another potentially toxic species, *Dolichospermum* (Figure **4.11**.**C & D**) dominated the cyanobacterial flora of Lake Rotoiti, at much higher concentrations, while Lake Rotoehu supported the highest cyanobacterial biovolumes, predominately *Dolichospermum* and *Microcystis*. February 2021 saw a cyanobacterial bloom in Lake Rotoehu **(**Figure **4.13**), the predominant taxa were *Microcystis wesenbergii* (Figure **4.11.B**), closely followed by *Dolichospermum* (coiled) sp. (Figure **4.11**.**D**).

Figure 4.13. Cyanobacterial bloom in Lake Rotoehu in February 2021 produced by *Microcystis sp*.

Valid statistical comparison of the phytoplankton populations was difficult as sufficient replication of samples was too time consuming. Non-metric multidimensional scaling and PERMANOVA of biovolume data in Figure **4.20** was used to provide information on the extent of seasonal compositional differences, using the monthly data as samples. The assumption that the samples were independent is likely, not valid, and this analysis should be viewed as indicative. Using raw biovolume data, good separation of the three lakes was evident (Figure **4.14A**), and PERMANOVA suggested that the three lakes were significantly different (PERMANOVA $p = 0.001$). However, when biovolume was standardised as relative biovolume (Figure **4.14B**), Lake Rotomā remained separate from the other two lakes (PERMANOVA p =

0.001) but lakes Rotoiti and Rotoehu were insufficiently distinct to be statistically significant (PERMANOVA $p = 0.068$), suggesting that the difference seen in raw data reflected biovolume differences between the lakes as well as differences in the overall species composition.

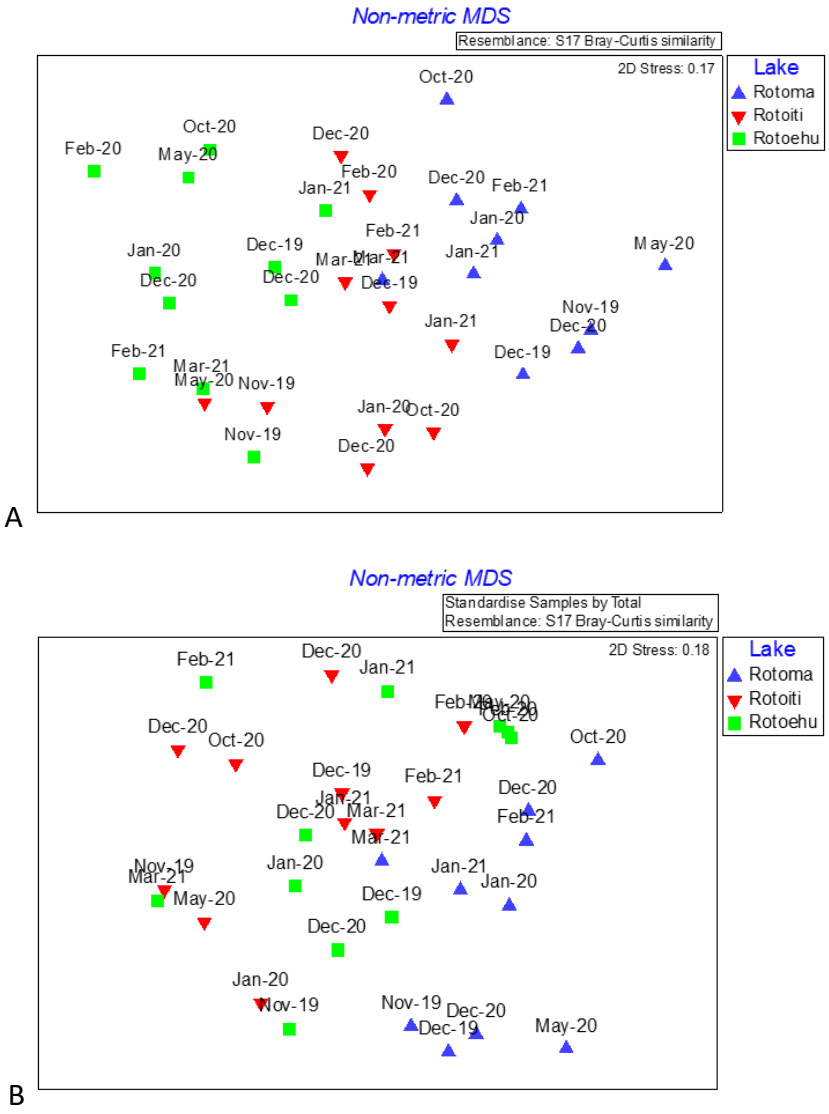

Figure 4.14 Non-metric multidimensional scaling plots using the data in figure 4.20; A) raw biovolume and B) relative biovolume. Collection dates are indicated.

Spectral absorption of algal particles

As discussed in section 1.2, phytoplankton contain a range of photosynthetic and photo-protective pigments, some of which are confined to specific taxonomic groups. These pigments have characteristic absorption spectra (Figure **4.15**), and thus overall absorption

spectra of phytoplankton can potentially provide insights into the population's taxonomic composition. Phytoplankton absorption spectra (a_p) from each lake were analysed to assess magnitude (absolute spectra) and shape (spectra normalised to absorption maxima) (Figure **4.16**).

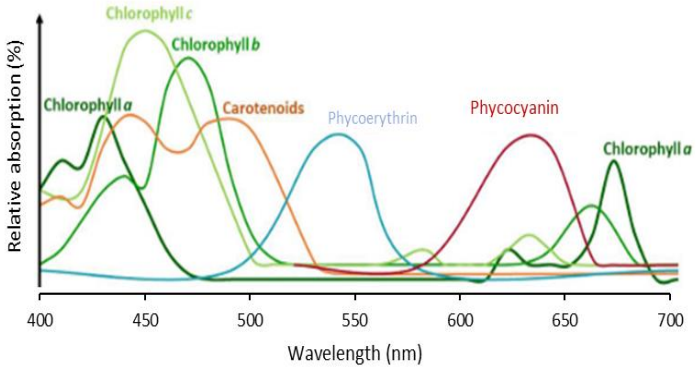

Figure 4.15. Spectral absorption of photosynthetic pigment from phytoplankton. Adapted from (Roy *et al.*, 2011; Taiz *et al.*, 2015)

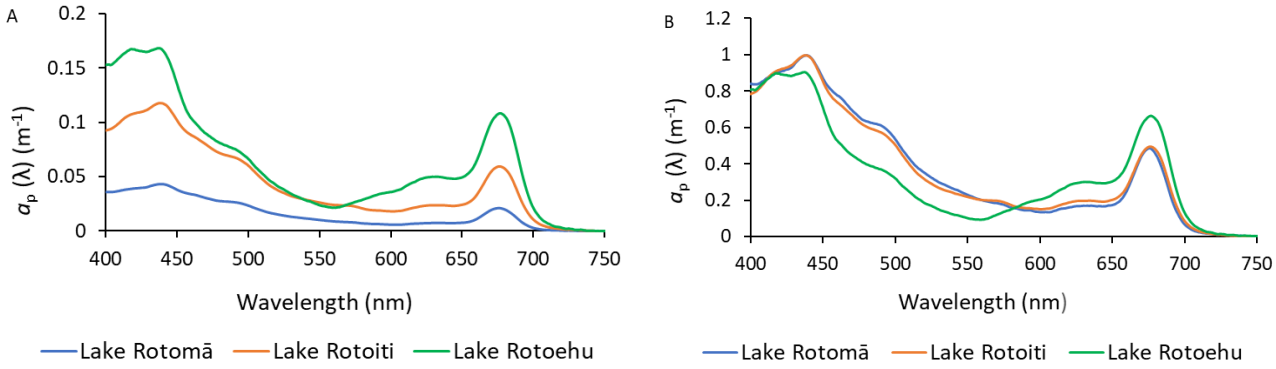

Figure 4.16. Phytoplankton absorption spectra, showing. A) averaged absolute absorption, and B) averaged absorption normalised to absorption maxima. For each spectrum for Lakes Rotomā, Rotoiti and Rotoehu throughout the sampling campaign

Lake Rotoehu recorded the highest values for a_p, followed by Lake Rotoiti, with Lake Rotomā displaying the lowest (Figure **4.16**). Spectra from all lakes showed two main absorption peaks, in the blue (437 nm – 440 nm) and the red (672 nm – 679 nm), though the relative sizes of these were more similar in Lake Rotoehu than in the other lakes. These two peaks coincide with the blue and red absorption peaks of chlorophyll *a*. Shoulders to the 440 nm peak were seen between 460 nm and 500 nm in all lakes, coinciding with the absorption of carotenoids.

A peak in a_p coincident with phycocyanin at around 630 nm was less well defined but may have been present in both Lakes Rotoiti and Rotoehu, showing a broader peak in the latter lake. Normalised spectra show Lakes Rotomā and Rotoiti had more similar absorption spectra to each other than to Lake Rotoehu (Figure **4.16).**

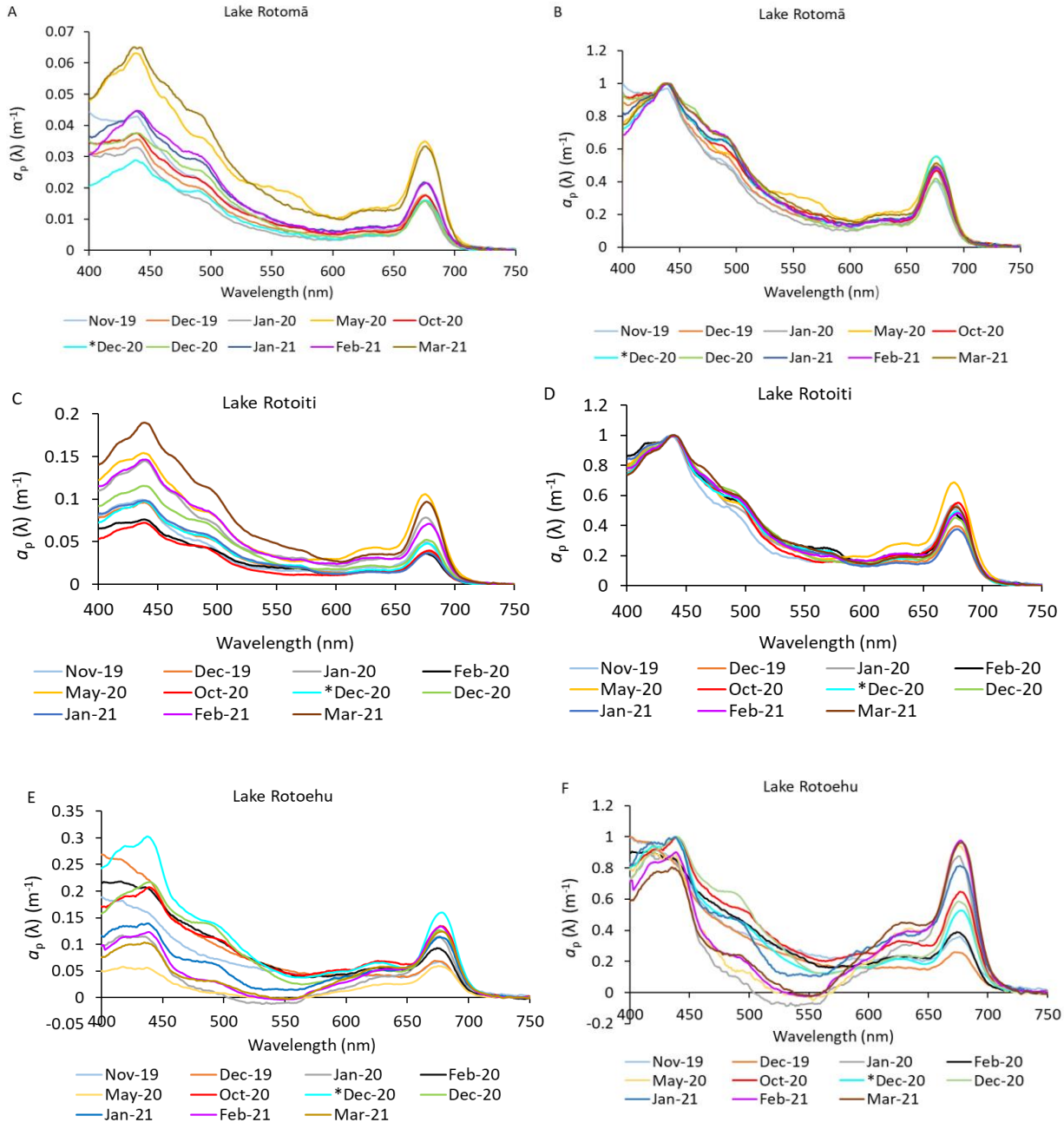

Figure 4.17. Phytoplankton absorption spectra for Lakes Rotomā, Rotoiti and Rotoehu across the sampling campaign. A, C, F) absolute spectra, B, D, F) normalised to absorption maxima. *Denotes first of two samplings in December 2020.

When viewed across sampling dates (Figure **4.17**), the absorption peak at ~440 nm was always very distinct in lakes Rotomā and Rotoiti. In Lake Rotoehu, the ~440 nm peaks were more variable and less sharply defined than the other lakes, with more of a shoulder between 400 – 440 nm that was not seen in the other two lakes. On a few dates, Lake Rotoehu showed no distinct ~440 nm peak at all.

Samples from Lake Rotoehu showed the greatest variability in a_p between months, with $a_p(440)$ ranging over more than an order of magnitude from 0.02 – 0.38 m^{-1} (average 0.17 m^{-1}). This was followed by Lake Rotoiti (range 0.06 – 0.21 m^{-1}, average 0.11), with Lake Rotomā displaying little variation ranging little more than 2-fold from 0.03 – 0.07 m^{-1} (average 0.04 m^{-1}). The months of May 2020 and March 2021 showed the highest a_p in the two deeper lakes, with 2nd December 2020 being the highest for Lake Rotoehu (Figure **4.17**). Normalised absorption spectra from Lakes Rotomā and Rotoiti were similar, with peaks and shoulders at the same wavelengths and relative magnitude (Figure **4.17.B.&D.**). Both showed absorption declining quasi-linearly from the 440 nm maximum to minima at around 600 nm, with little variability between samplings. Normalised spectra from Lake Rotoehu showed much more variability between samplings than the other lakes, and 440 nm was often not the maximum absorption wavelength. Absorption was maximal at 675 nm on several occasions. In addition, in samples from Lake Rotoehu, the size of the 480 nm shoulder was variable, with steep drops into the green and absorption minima of 550 nm.

Three samples fell to or below zero in Lake Rotoehu's absolute absorption spectra (Figure **4.17.E.**), these dates corresponded with very large colonies of Microcystis forming a bloom, which caused uneven sample dispersal on the filter. This was exacerbated in the normalised spectra (Figure **4.17.F**) due to the wide variations between the blooming sites. This negative reading has been seen elsewhere (Sathyendranath *et al.*, 1987), particularly when high carotenoid pigment was present.

Spectral absorption of non-algal particles

The absorption of non-algal particles at 440 nm ($a_{NAP}(440)$) was used as a reference point for non-algal particles. Lake Rotoehu showed the highest $a_{NAP}(440)$ across the three lakes with an average of 0.39 m^{-1} , Lake Rotoiti with average 0.09 m^{-1} and Lake Rotomā at 0.04 m^{-1} were considerably lower and similar to each other (Figure **4.18**). Lake Rotoehu showed similar variability between sampling dates (0.27 – 0.59 m^{-1}) to the other two deeper lakes, Lake Rotoiti (0.06 – 0.13 m^{-1}), Lake Rotomā (0.024 – 0.051 m^{-1}) but displayed increasing absorption as the summer progressed (Figure **4.19**). This trend was not seen in Lakes Rotoiti and Rotomā, which tended to decrease through the summer months. Several filters were overloaded with particles, and complete bleaching was not possible, resulting in a small residual peak at $a(675)$.

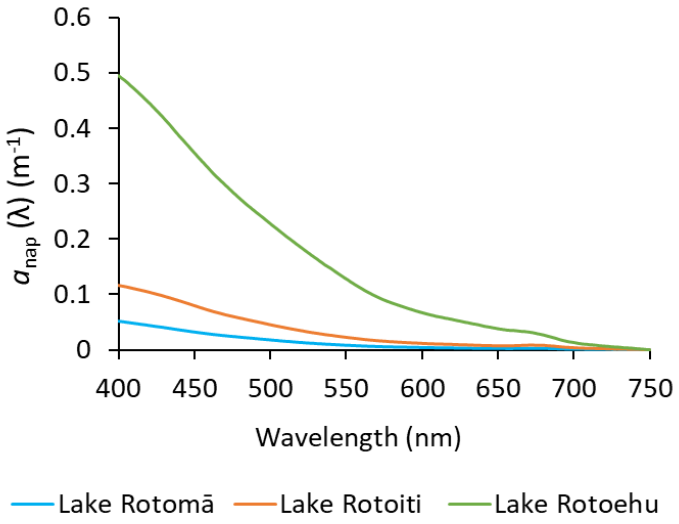

Figure 4.18. Absorption spectra showing averaged absolute concentrations of non-algal particles in Lakes Rotomā, Rotoiti and Rotoehu throughout the sampling campaign.

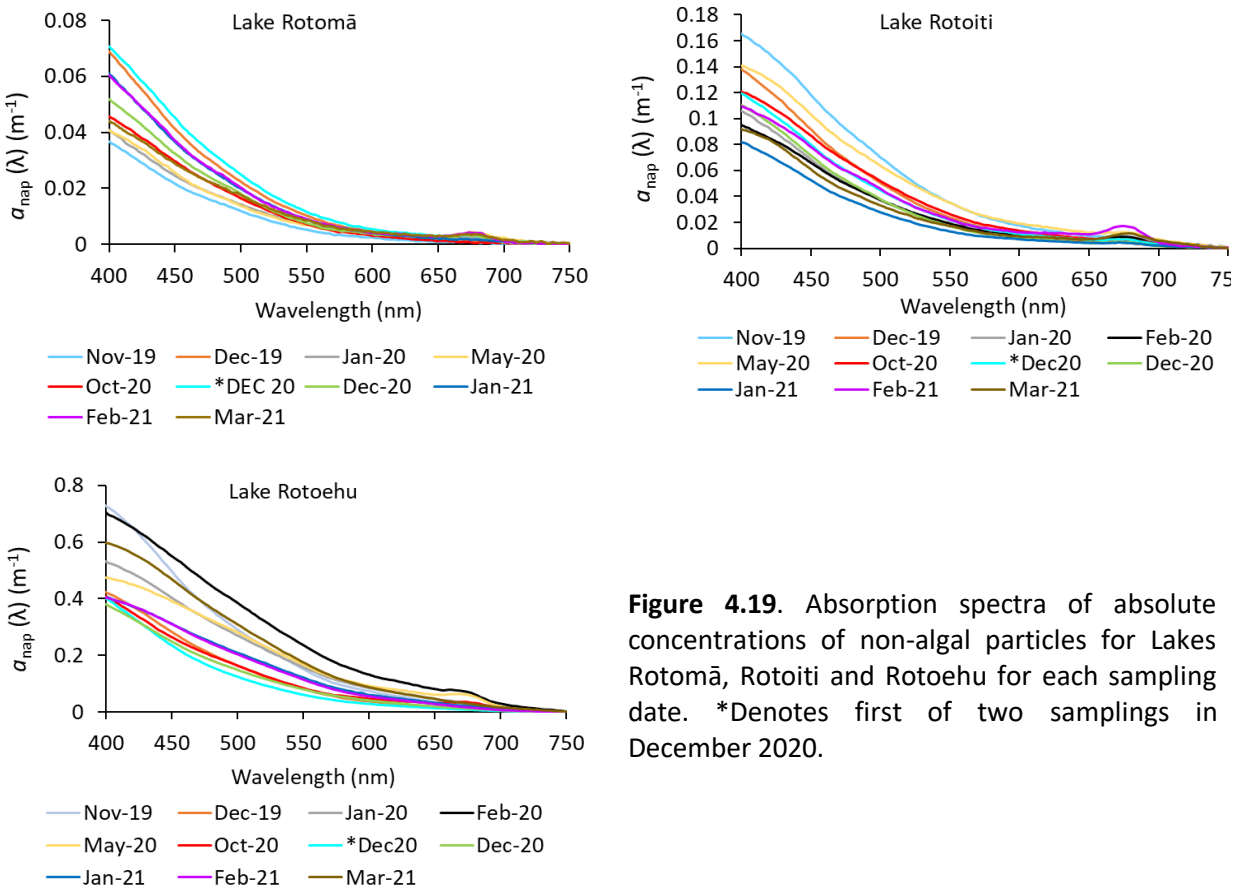

Figure 4.19. Absorption spectra of absolute concentrations of non-algal particles for Lakes Rotomā, Rotoiti and Rotoehu for each sampling date. *Denotes first of two samplings in December 2020.

Contribution to overall absorption of optically active constituents

To compare the relative contributions to overall spectral absorption, that of key optically active constituents; CDOM, non-algal particles and phytoplankton were assembled in stacked plots (Figure **4.20**), using the average values of each site and month. To this absorption by water, was added. Water played the greatest role in absorption in Lake Rotomā, with overall maximum absorption in the red part of the spectrum, indicating maximum transmission in the blue and green. In Lake Rotoiti, the sum of other optically active substances, with CDOM being the highest amongst these, was equivalent to that of water resulting in a near symmetrical absorption spectrum centred on 550 nm, in the green. The high concentrations of CDOM, algal and non-algal particles in Lake Rotoehu meant that overall absorption spectrum in this lake was at the blue end of the spectrum (Figure **4.20**).

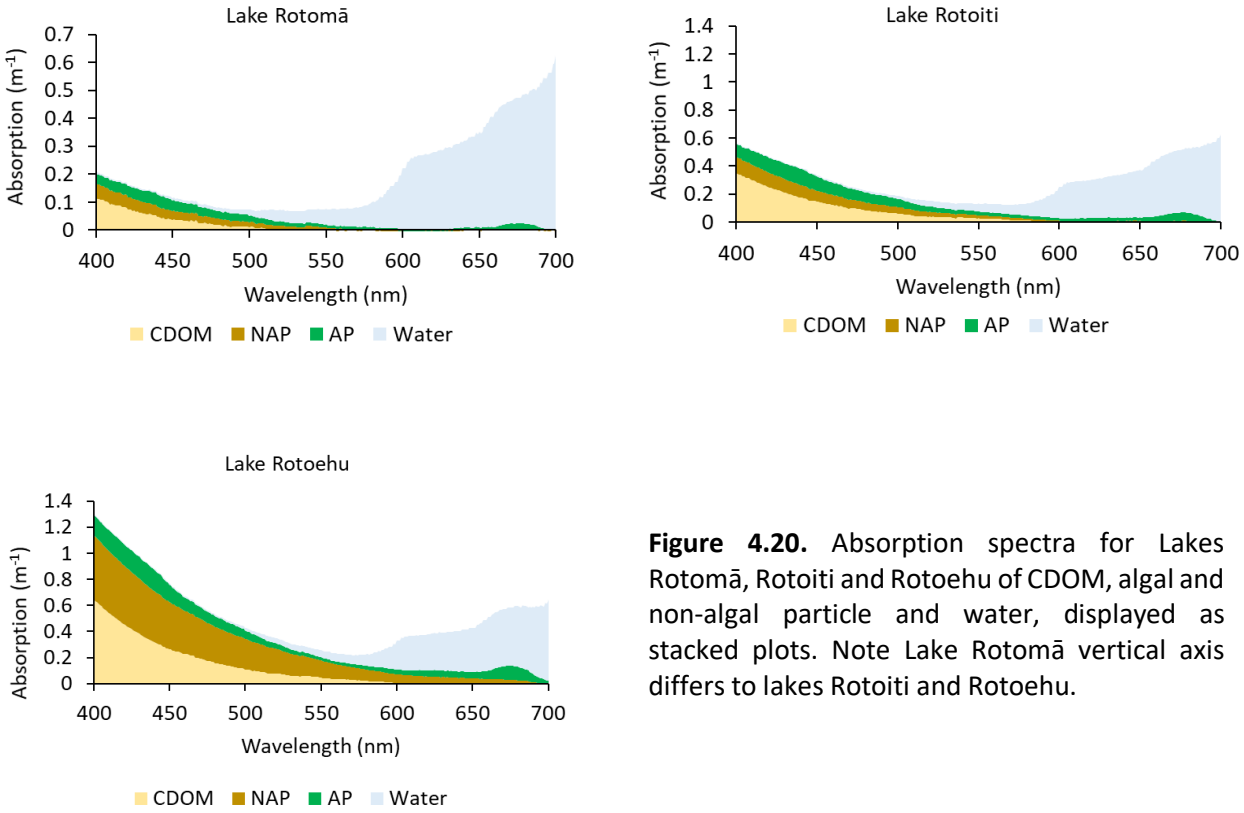

Figure 4.20. Absorption spectra for Lakes Rotomā, Rotoiti and Rotoehu of CDOM, algal and non-algal particle and water, displayed as stacked plots. Note Lake Rotomā vertical axis differs to lakes Rotoiti and Rotoehu.

A ternary plot was created to further visualise the *relative* contributions to total absorption for each sampling from CDOM, algal and non-algal particles at 440 nm wavelength. 440 nm has been used extensively in previous studies for comparison between optical active constituents (Lee & Carder, 2004; Brezonik *et al.*, 2015; Xi *et al.*, 2015). No points when CDOM was below detectable concentration were plotted. When visualised in this way, Lake Rotoehu separated from the other two Rotorua lakes largely due to the high contribution from non-algal particles (Figure **4.21**). Waikato lakes are also plotted here and, while it only indicates single samples, it illustrates how these lakes are optically different to the Rotorua group. Absorption at 440 nm in Lake Rotopiko is dominated by CDOM, as, to lesser extents are lakes Mangakaware and Ohinewai. In contrast, Lake Rotongaro saw similar absorption from CDOM and algal particles with less than 20% of non-algal particle absorption. Lake Rotongaroiti was not plotted here as no absorption data at 440 nm wavelength was obtained.

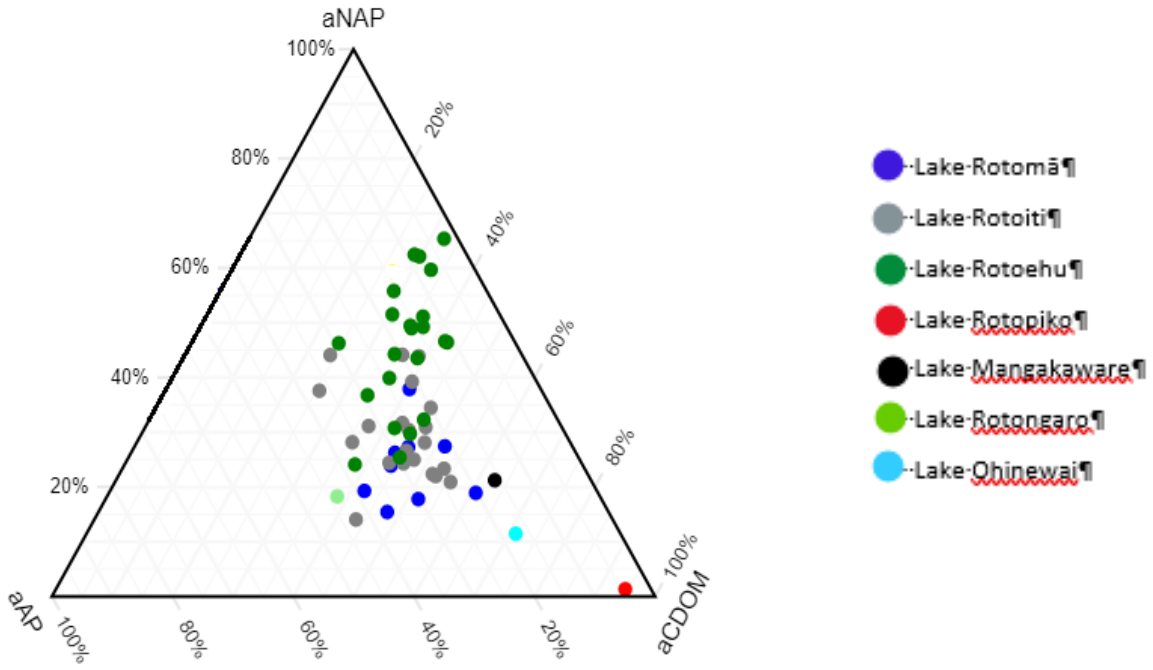

Figure 4.21. Ternary plot showing relative absorption of CDOM, algal and non-algal particles at 440 nm wavelength in all lakes sampled in this study.

Reflectance

Reflectance spectra from each lake were analysed to assess magnitude (absolute spectra) and shape (spectra normalised to reflectance maxima) (Figure **4.22**). Average absolute reflectance at their maximum wavelengths were similar for lakes Rotomā (0.0025 sr^{-1}) and Rotoiti (0.003 sr^{-1}) and were lower than Lake Rotoehu (0.005 sr^{-1}). This difference persisted at wavelengths longer than 600 nm (orange to red), making Rotoehu the brightest of the three lakes. When normalised, it was evident that Lake Rotomā reflectance comprised two peaks (~490 and ~530 nm - Figure **4.22**). In contrast, reflectance maxima of lakes Rotoehu and Rotoiti were consistently positioned at 575 and 550 nm respectively. Overall, the average reflectance spectra of the three lakes indicated a shift from a broad blue-green colour in Lake Rotomā, to a narrow green reflectance peak in Lake Rotoiti to a green-orange reflectance in Lake Rotoehu.

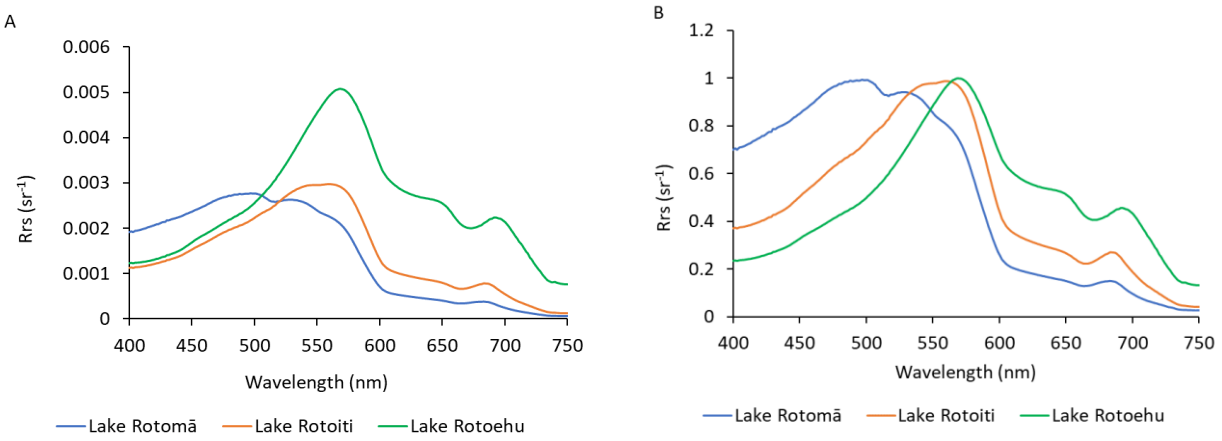

Figure 4.22. Reflectance spectra averaged showing A) absolute reflectance B) reflectance normalised to reflectance maxima for each spectrum for Lakes Rotomā, Rotoiti and Rotoehu

Seasonal variability

Reflectance spectra from Lake Rotomā displayed relatively little seasonal variation, with the cooler months, May 2020 and October 2020, recording lower reflectance, most easily seen in the blue and green wavelengths (Figure **4.23.A**), whereas slightly higher reflectance was seen through mid-summer, December 2020 and January 2021. Normalised plots (Figure **4.23.B**) showed very little variation in shape between months, though the small peak at 675 nm varied somewhat in size.

For Lake Rotoiti, as in Lake Rotomā, May and October 2020 had the lowest absolute reflectance, however, the difference to samples for November to January was more pronounced, particularly at the longer wavelengths and particularly the 675 nm peak (Figure **4.23.C**). When normalised, however, with the exception of May 2020 the reflectance spectra tended to be very similar, with most of the variability in the blue and red parts of the spectrum (Figure **4.23.D).**

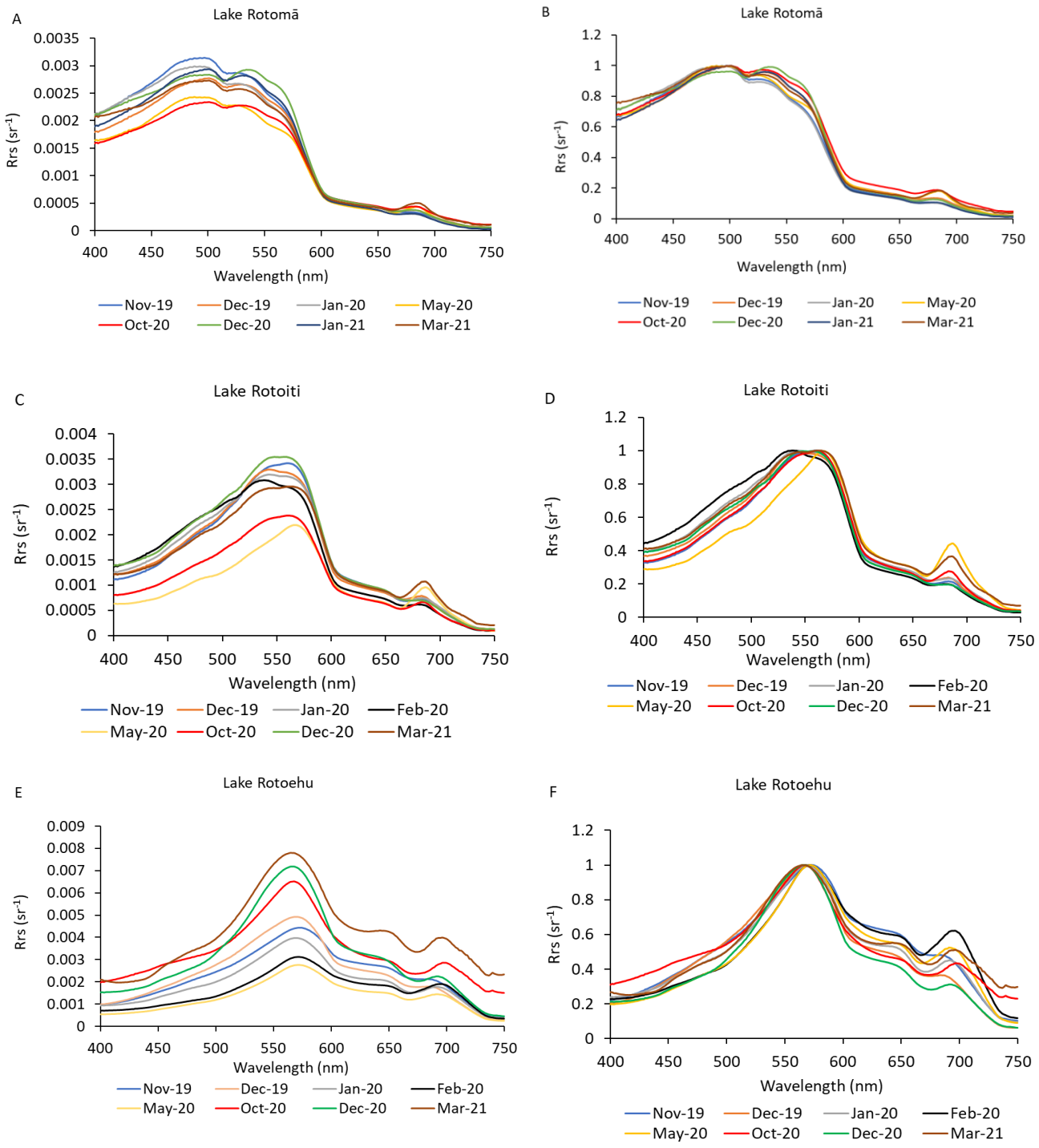

Figure 4.23. Reflectance spectra in Lakes Rotomā, Rotoiti and Rotoehu using the mean of sites one and two. Graphs A, C and E are absolute spectra and B, E, and F are normalised.

Reflectance spectra of Lake Rotoehu were much more varied than for the other two lakes and could be allocated to three distinct groupings. Absolute spectra from the first summer season (November 2019 to January 2020) tended to be distinguishable from those from the second summer season (October 2020 to March 2021) an those from February and May 2020 (Figure

4.23.**E**), primarily in terms of the overall magnitude of reflectance. Normalised spectra (Figure **4.23**.**F**) showed more consistency in shape throughout the dates, particularly at shorter wavelengths, however, variation was much more evident towards red wavelengths across all seasons.

Cardinal points within reflectance spectra

A synthetic "typical" eutrophic lake reflectance spectrum, developed from Schalles and Yacobi (2000) and Lehmann et al. (2017) (Figure **4.24**), was used to identify the key features of the reflectance spectrum. Within the spectrum, a series of cardinal points are identified as points A to E. Points A (440 nm) and E (665 nm) indicate absorption maxima for chlorophyll *a*, point B (450 – 530 nm), the "carotenoid shoulder", and point D (630 nm) phycocyanin. Peak C (reflectance maximum˜560 nm) indicates the wavelength of minimal absorption.

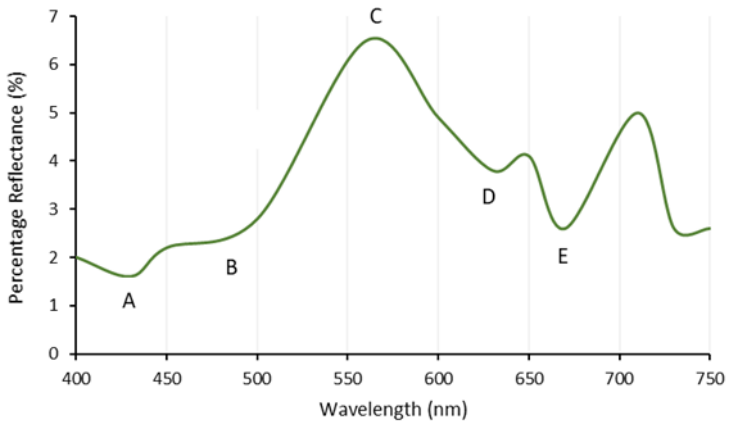

Figure 4.24. A "typical" eutrophic lake reflectance spectrum, indicating the features of reflectance and absorption. Points A and E are absorption maxima for chlorophyll *a*, B indicates carotenoids, and D indicates phycocyanin. C peak indicating reflectance maxima. Adapted from (Schalles & Yacobi, 2000; Lehmann *et al.*, 2017).

As would be expected, Lake Rotomā, the most oligotrophic of the three lakes, corresponded poorly to the eutrophic spectrum in Figure **4.24**, with only points A and E weakly discernible, at 429 nm and between 663 - 677 nm. The deepest troughs at Point E corresponded with March 2021 (9.2 x10^{-5} sr^{-1}), May 2020 (7.4 x 10^{-5} sr^{-1}) and October 2020 (4.0 x 10^{-5} sr^{-1}). The phycocyanin trough (point D) was only weakly seen in one sample (March 2021), and a distinct reflectance maximum (point C) was not evident.

The reflectance spectra of Lake Rotoiti were more concurrent with the eutrophic model with, in addition to points A and E, hints of troughs at points B between 490 – 500 nm, with May 2020 and March 2021 displaying the deepest troughs. There was little evidence of phycocyanin (point D), with March 2021 and May 2020 the only months showing a weak trough at 629 nm. The chlorophyll *a* trough (point E) varied between 663 and 673 nm with May 2020 showing the most depth at 2.5 x 10^{-4} sr^{-1}, followed by October 2020 1.7 x 10^{-4} sr^{-1} and March 2021 at 1.2 x10^{-4} sr^{-1}. Point C, the reflectance maxima, was better developed than in Lake Rotomā, peaking between 538 nm (February 2020) to 568 nm (May 2020).

In contrast, Lake Rotoehu showed a characteristic eutrophic reflectance spectrum, with all of the cardinal points evident in some or all of the samples. The reflectance peak (point C) is clearly defined at 570 nm and it was the only lake to show a distinct phycocyanin trough (point D) at 629 nm, albeit only well developed in March 2021. The carotenoid shoulder (point B) and chlorophyll troughs (point A and E) were seen in all samples. The deepest chlorophyll *a* trough (point E) was seen in March 2021 (8.1 x 10^{-4} sr^{-1}), October 2020 (5.5 x10^{-4} sr^{-1}) followed by December 2020 (5.2 x 10^{-4} sr^{-1}). For subsequent analysis, the size of the chlorophyll *a* and phycocyanin toughs was estimated by joining the top left and right edge of the trough and measuring down to the deepest point.

4.1 Waikato Lakes

The two shallowest lakes, Rotongaroiti and Rotongaro, recorded the highest TSS and phycocyanin concentrations within the Waikato lakes and the shallowest Secchi depths (Table **4.1**). In contrast, Lake, Rotopiko, showed the deepest Secchi depth at 5.54 m together with the lowest suspended solids and chlorophyll *a* concentration.

Table 4.1. Results for Secchi Depth, Total Suspended Solids, CDOM, chlorophyll *a* and Phycocyanin for Waikato Lakes.

Lake	Secchi Depth (m^{-1})	Total suspended solids (g m^{-3})	*a*440 (m^{-1})	Chlorophyll *a* (µg L^{-1})	Phycocyanin (µg L^{-1})
Rotopiko (peat lake)	5.54	1.38	4.68	5.37	57.34
Mangakaware (peat lake)	1.05	10.4	2.62	27.18	142.59
Rotongaro (riverine)	0.18	51.5	3.73	18.3	654.82
Rotongaroiti (riverine)	0.15	134.94	2.51	81.03	1901.34
Ohinewai (riverine)	0.51	20	5.76	44.06	563.07

Absorption of algal and non-algal particles

The two peat lakes, Rotopiko and Mangakaware, had the lowest $a_p(\lambda)$ values across the spectrum (Figure **4.25**). This was closely followed by Lake Ohinewai, while Lake Rotongaro, had the highest absorption through the blue and into the green by a considerable amount, which then fell away into a smooth concave curve through to a small peak at $a_p(674)$. Lake Rotongaroiti was not analysed for a_p due to the extreme amount of non-algal particles of the filter which made it difficult to bleach.

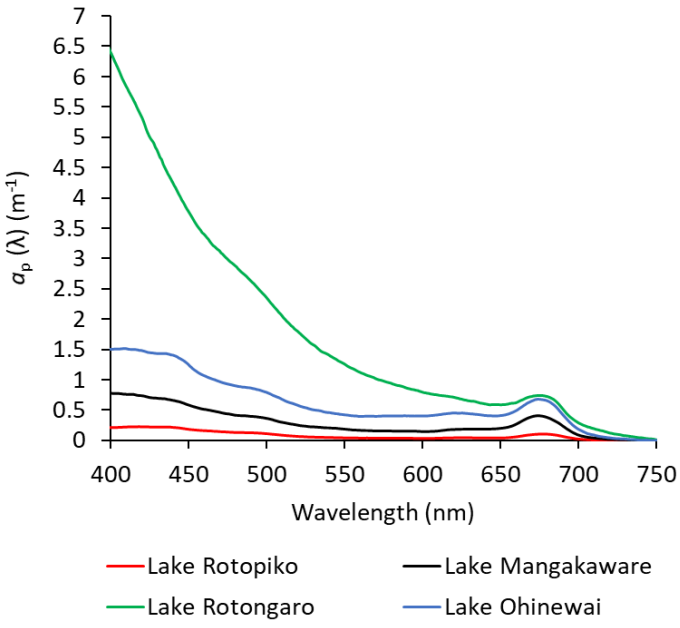

Figure 4.25. Phytoplankton absorption spectra showing absolute values for Waikato lakes (excluding Lake Rotongaroiti) taken in July 2020.

The riverine lakes contained higher a_{NAP} (λ) with Lake Rotongaroiti, the shallowest of all lakes with the high suspended solids also displayed the highest concentration $a_{nap}(440)$ at 5.5 m^{-1} (Figure **4.26**). At $a_{nap}(440)$, Lake Rotongaro recorded the next highest concentrations at 1.79 m^{-1}, lakes Ohinewai (0.93 m^{-1})and Mangakaware (0.92 m^{-1}) recorded very similar results. The less turbid Lake Rotopiko showed minimal $a_{nap}(440)$ with 0.07 m^{-1}.

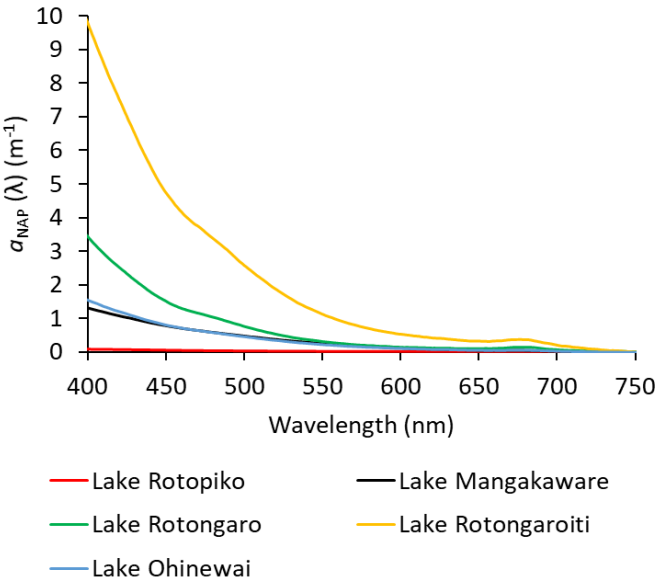

Figure 4.26. Absorption of concentrations of non-algal particles in Waikato lakes taken in July 2020.

Absorption ratios of optically active constituents

The two peat Lakes Rotopiko and Mangakaware recorded high CDOM values relative to algal and non-algal particles, which was also seen in the riverine Lake Ohinewai (Figure **4.27**) (see also ternary plot Figure **4.21**). Lake Rotongaro saw phytoplankton dominate through most of the wavelengths in contrast to Lake Rotongaroiti, which saw non-algal particles dominate up to 553 nm before alternating to phytoplankton.

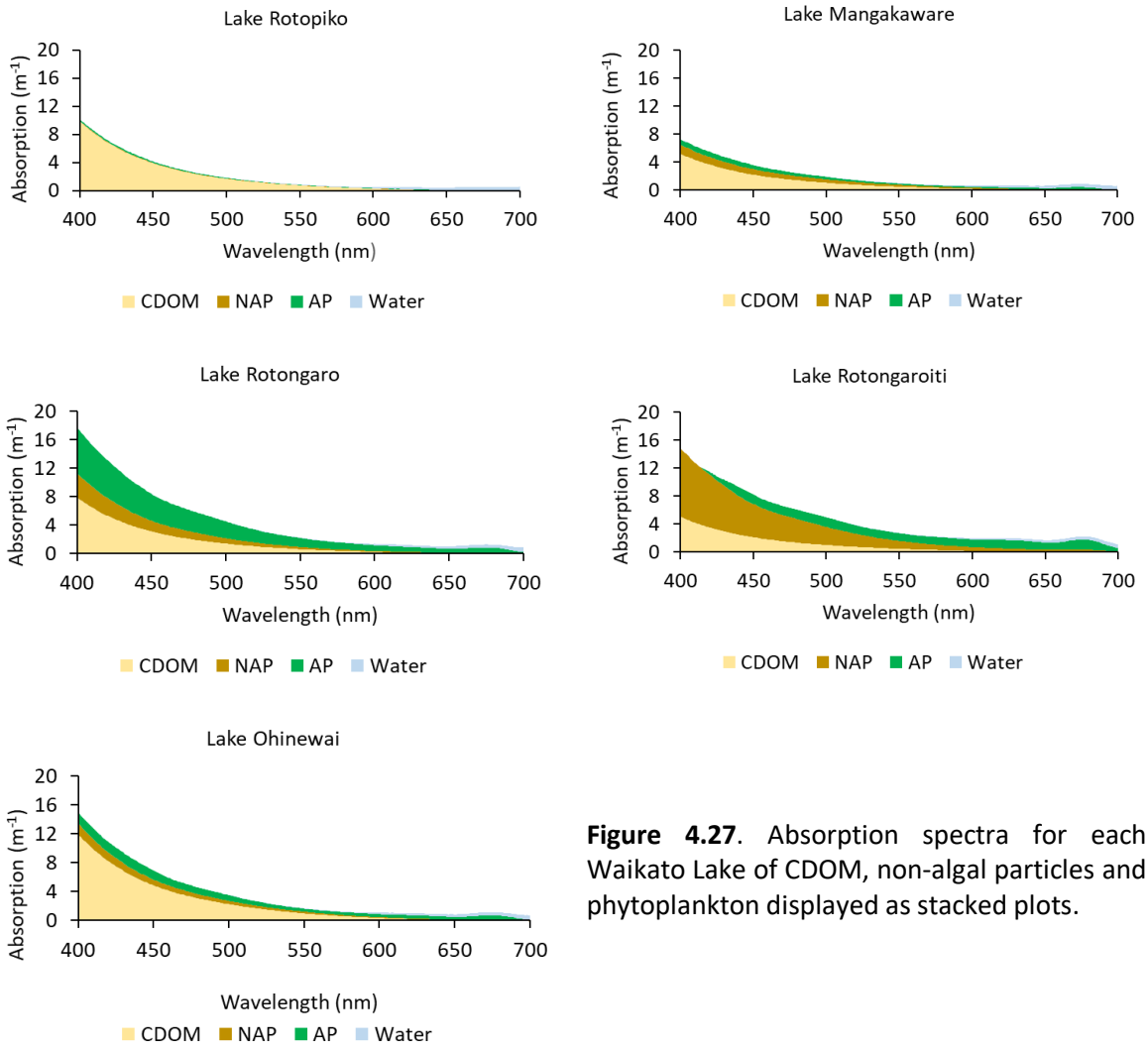

Figure 4.27. Absorption spectra for each Waikato Lake of CDOM, non-algal particles and phytoplankton displayed as stacked plots.

Reflectance

The highest reflectance throughout the wavelengths was from the milky brown water of Lake Rotongaro, followed by Lake Rotongaroiti. Reflectance spectra were similar for lakes Mangakaware and Ohinewai, with the lowest reflectance from Lake Rotopiko (Figure **4.28**). Reflectance maxima from the three riverine lakes were recorded at 700 nm, Lake Rotongaro 0.028 sr^{-1}, Lake Rotongaroiti 0.020 sr^{-1} and Ohinewai 0.006 sr^{-1}, and reflectance was very low in the blue. The two peat lakes had reflectance maxima at ~580 nm in the green, Lake Mangakaware at 0.005 sr^{-1} and Lake Rotopiko at 0.0008 sr^{-1}.

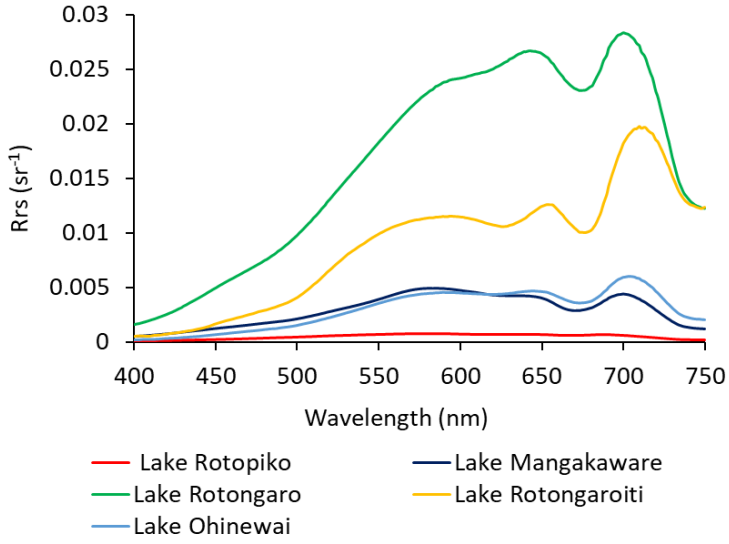

Figure 4.28. Reflection spectra for Lakes Rotopiko, Mangakaware, Rotongaro, Rotongaroiti and Ohinewai, showing absolute values, taken July 2020.

When the lake reflectance spectra were normalised, the peat lakes were separable from the riverine lakes by higher reflectance in the blue and distinct maxima in the green (Figure **4.29**).

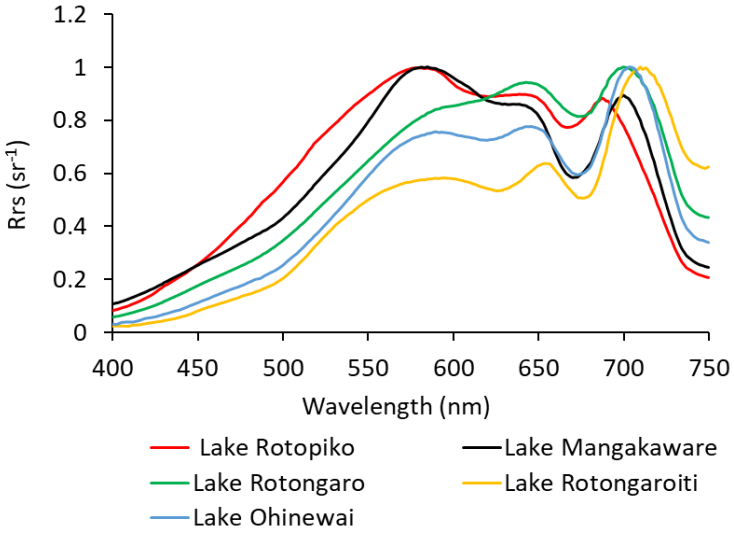

Figure 4.29. Reflectance spectra, normalised, for Lakes Rotopiko, Mangakaware, Rotongaro, Rotongaroiti and Ohinewai taken July 2020.

Phytoplankton assemblages

Twenty different phytoplankton species were counted in Lake Rotongaroiti, 17 in Lake Mangakaware, 16 in Lakes Rotongaro and Ohinewai and only 9 in Lake Rotopiko. The Shannon-Wiener index of diversity showed all Waikato lakes (Table **4.2**) were found to have lower diversity than two of the Rotorua Lakes, Rotoiti (3.9) and Rotoehu (3.6).

Table 4.2. Diversity using Shannon-Wiener Index and Biovolume from Waikato Lakes.

Lake	Diversity Shannon-Wiener Index	Biovolume ($mm^3 L^{-1}$)
Rotopiko	2.2	0.61
Mangakaware	2.8	22.06
Rotongaro	3.0	4.56
Rotongaroiti	2.7	33.75
Ohinewai	2.5	22.28

Dinoflagellates, green algae and euglenoids were the most abundant algal groups across all of the lakes. Although all lakes also contained diatoms, they accounted for less than 1 % of biovolume in Lake Rotopiko (Figure **4.30),** which was entirely of *Aulacoseira* sp. Lake Rotongaroiti contained the most diatoms at 23% biovolume, spread across five species. Green algae were dominant by biovolume in Lake Rotongaro (72%), predominantly made up of a small spherical species that was too small to identify under 400 x magnification. Of the Euglenoids, *Euglena* and *Trachelomonas* were found in all lakes, while *Phacus* was only seen in Lake Rotongaro. The two peat lakes biovolume was dominated by the dinoflagellate *Peridinium*, (Lake Rotopiko 51% and Lake Mangakaware 79%), which was absent from two of the riverine Lakes, Rotongaro and Ohinewai. The Cryptophyceae group was made up of a single species of *Cryptomonas* and recorded in all lakes except Lake Rotopiko.

Cyanobacteria were seen only in the three riverine lakes. Lakes Rotongaro and Rotongaroiti contained a single cyanobacteria species *Aphanocapsa*. Although the cell count was high (2,679 and 47,398 cells ml^{-1} respectively), this species is extremely small, with a diameter of 1.5 µm, and it contributed only 0.11 % and 0.27 % of the total biovolume. The water sample from Lake Rotongaroiti was very gelatinous; this may have been due to the high number of *Aphanocapsa* present as they are known to form colourless mucilaginous colonies. Lake Ohinewai was the only lake to have a substantial cyanobacterial component (39% biovolume), and contained two potentially toxic species, *Dolichospermum* (straight) and *Microcystis* (small).

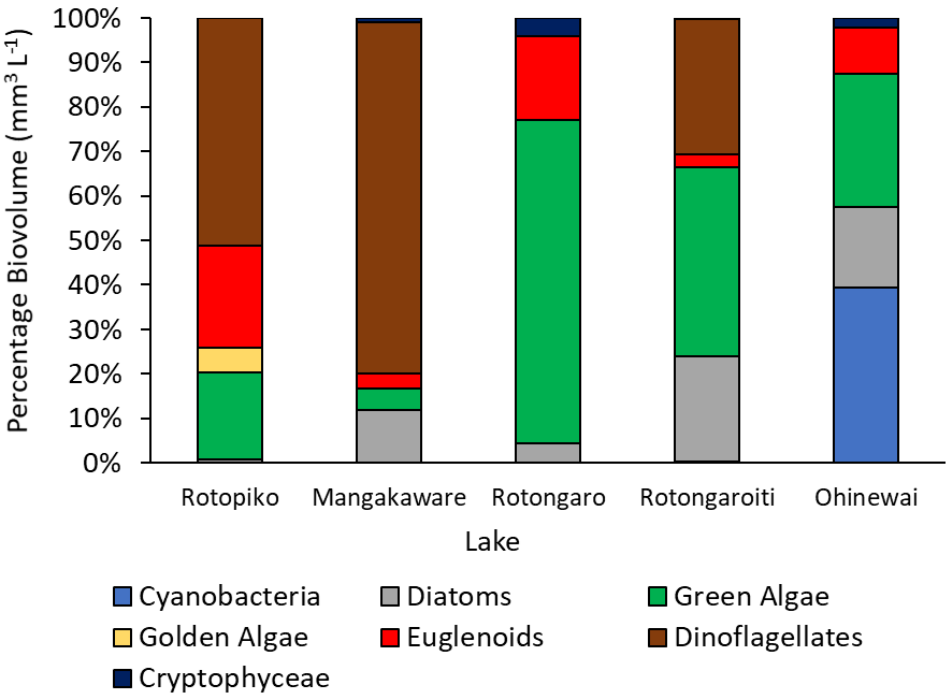

Figure 4.30. Proportion biovolume of phytoplankton groups within each Waikato Lake.

Chapter 5

Data Analysis

5.1 Rotorua Lakes

Relationships amongst optically active variables

Correlation was used to identify statistical connections between measured variables. As described in the statistical analysis section 3.4, the variables (Secchi, CDOM, TSS, chlorophyll *a*, phycocyanin and biovolume) were checked for normality, with departure from normality evident in chlorophyll *a*, phycocyanin and biovolume values. These variables were normalised using a log-transform, and these log values were used for all tests. Averages of site one and two were used. A Pearson correlation matrix was constructed to examine relationships among optically active variables in the Rotorua lakes (Table **5.1**).

Table 5.1. Pearson correlation matrix showing the relationship between optical variables for Lakes Rotomā, Rotoiti and Rotoehu displaying *P* (lower left corner) and R^2 values (upper right corner). Statistically significant correlations are indicated by dark green shading (p = <0.05) and near-significant correlations (0.05<p<0.01) by pale green shading. *Indicates insufficient data for analysis.

Lake Rotomā

	Secchi	CDOM	TSS	Chl *a*	PC	BV
Secchi		R^2=0.19	R^2=0.25	R^2=0.05	R^2=0.49	R^2=0.03
CDOM	P=0.20		R^2=0.02	R^2=0.20	*	R^2=0.03
TSS	P=0.15	P=0.68		R^2=0.04	R^2=0.10	R^2=0.01
Chl *a*	P=0.52	P=0.20	P=0.60		R^2=0.24	R^2=0.23
PC	P=0.12	*	P=0.55	P=0.32		R^2=0.01
BV	P=0.63	P=0.66	P=0.76	P=0.13	P=0.85	

Lake Rotoiti

	Secchi	CDOM	TSS	Chl *a*	PC	BV
Secchi		R^2=1.x10^{-5}	R^2=0.32	R^2=0.04	R^2=0.51	R^2=0.12
CDOM	P=0.99		R^2=0.23	R^2=0.47	R^2=0.72	R^2=0.14
TSS	P=0.09	P=0.17		R^2=0.13	R^2=0.73	R^2=0.70
Chl *a*	P=0.59	P=0.03	P=0.30		R^2=0.64	R^2=0.34
PC	P=0.11	P=0.03	P=0.04	P=0.06		R^2=0.23
BV	P=0.33	P=0.28	P=0.003	P=0.08	P=0.34	

Lake Rotoehu

	Secchi	CDOM	TSS	Chl *a*	PC	BV
Secchi		R^2=0.17	R^2=0.45	R^2=0.03	R^2=0.48	R^2=0.02
CDOM	P=0.20		R^2=0.0003	R^2=0.34	R^2=0.17	R^2=1.x10^{-5}
TSS	P=0.02	P=0.96		R^2=0.02	R^2=0.10	R^2=0.16
Chl *a*	P=0.62	P=0.06	P=0.67		R^2=0.34	R^2=0.22
PC	P=0.12	P=0.42	P=0.54	P=0.23		R^2=0.05
BV	P=0.70	P=0.99	P=0.22	P=0.14	P=0.67	

No significant correlations were observed in Lake Rotomā. In Lake Rotoiti, chlorophyll *a* and phycocyanin concentrations correlated positively with CDOM (Figure **5.1**) and phycocyanin and TSS also saw a positive relationship (Figure **5.1**). TSS concentration also showed a significant relationship with phytoplankton biovolume, not seen in any other lake (Figure **5.1**).

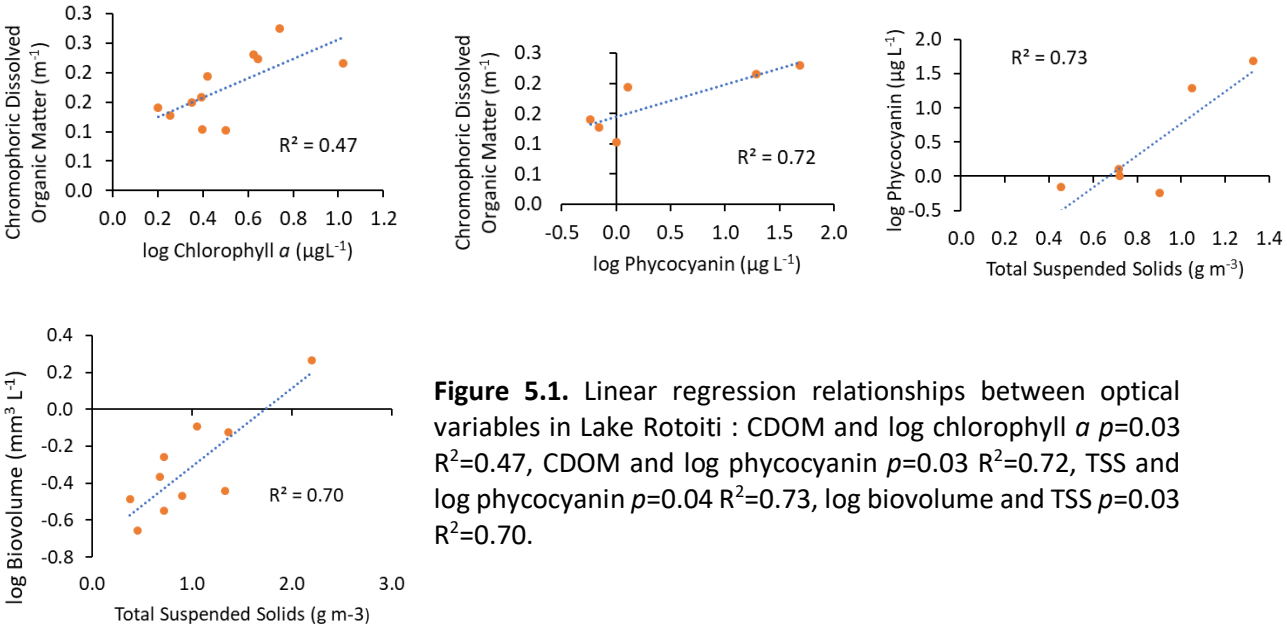

Figure 5.1. Linear regression relationships between optical variables in Lake Rotoiti : CDOM and log chlorophyll *a* p=0.03 R^2=0.47, CDOM and log phycocyanin p=0.03 R^2=0.72, TSS and log phycocyanin p=0.04 R^2=0.73, log biovolume and TSS p=0.03 R^2=0.70.

Chlorophyll *a* and phycocyanin were not significantly correlated in any of the three lakes. A closer relationship between the two was seen in Lake Rotoiti at p = 0.06, albeit not statistically significant. Secchi depth and TSS was the only significant relationship between variables in Lake Rotoehu (Table **5.1**, Figure **5.2**).

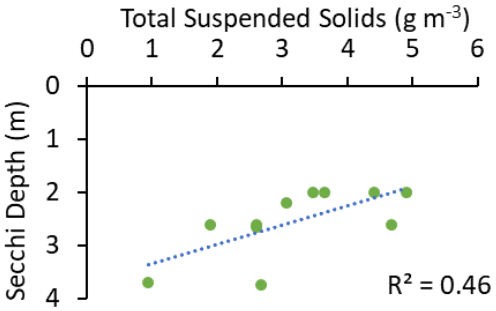

Figure 5.2. Relationship between total suspended solids and Secchi depth for Lake Rotoehu, p = 0.02 and R^2=0.46.

Grouping of reflectance spectra

In order to assess whether measured variables were able to predict the reflectance spectra characteristics clustering of normalised reflectance spectra from the three seasonal study lakes was used to group those with the most similar shapes. This showed strong and consistent differences between lakes (Figure **5.3**). Lake Rotomā showed the tightest grouping of the three, and while Lakes Rotoiti and Rotoehu showed more similarity to each other than to Lake Rotomā, each formed a discreet cluster. Pair-wise testing in PERMANOVA showed that there was a significant separation of the three lakes (p = 0.001).

For the most part, replicate sites within Lake Rotomā clustered together, but there was variation between the two sites in both January 2021 and October 2020. On both occasions, there were different dominant phytoplankton taxa in each site, with one dominated by *Peridinium* and the other by greens and diatoms, respectively, suggesting some effect of phytoplankton composition. However, this was not consistent in Lake Rotomā with other *Peridinium*-dominated samples not clustering together, and no significant effect of dominant species evident in 2-way PERMANOVA tests.

Lake Rotoiti showed more variation between sites, which also occurred when dominant taxa differed between sites. May 2020 stood apart from the other seasons creating its own cluster that coincided with the highest biovolume recorded, dominated by diatoms, but again no statistically significant effect of composition was evident with PERMANOVA.

Lake Rotoehu showed the most variation over sampling events, but with less variation between sites. The greatest variation in reflectance spectra between sites was seen in February 2020 when the dominant *Peridinium* was seen at twice the biovolume in site two than site one and may have been responsible for decreasing the reflectance at site two through the red wavelength. *Peridinium*-dominant months tended to show the reflectance spectra grouped apart from diatom-dominant spectra. However, PERMANOVA again showed that there was no significant effect of composition, though the closest to significant effect was for diatoms vs *Peridinium* in both Rotoehu (p = 0.076) and Rotoiti (p = 0.082). Relatively small sample sizes for this analysis limit the confidence that can be placed in statistical inferences.

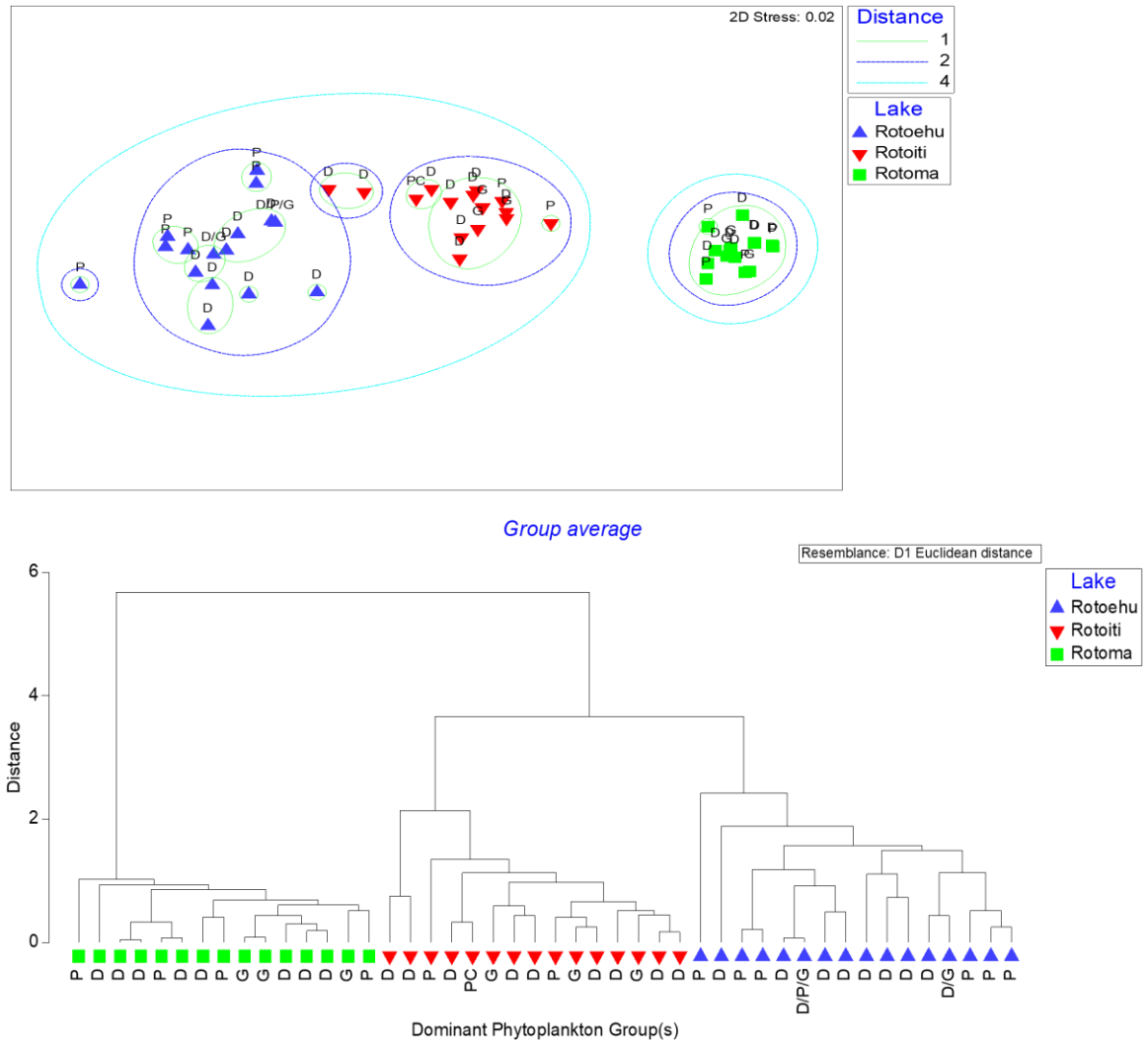

Figure 5.3. Non-metric multidimensional scaling (top) and clustering plots analysis showing the relationship between normalised reflectance spectra and dominant phytoplankton taxa across sites and sampling months in the Rotorua lakes.

5.2 Combined lakes

Phytoplankton absorption spectra and pigment concentrations

If reflectance spectra are to prove useful measures of different classes of phytoplankton biomass, relationships between biomass indicators and spectral features should be present. Regression analyses were therefore performed between chlorophyll *a* and phycocyanin concentrations and wavebands within the measured absolute absorption spectra here these pigments are expected to contribute most to absorption. This equated to comparing all measurements of chlorophyll *a* and phycocyanin concentrations against appropriate $a_p(675)$ and $a_p(629)$, respectively. In some a_p spectra, the peaks were slightly off these target wavelengths, and under these conditions, the actual peak wavelength was used, while for consistency they are referred to as a_p(chla) and a_p(pc).

Of these, a_p(chla) showed a strong relationship with chlorophyll *a* concentration ($p << 0.001$, $R^2 = 0.90$) (Figure **5.4A**). The relationship between a_p(pc) and log phycocyanin concentration was also significant ($p << 0.001$, $R^2 = 0.63$) (Figure **5.4B**).

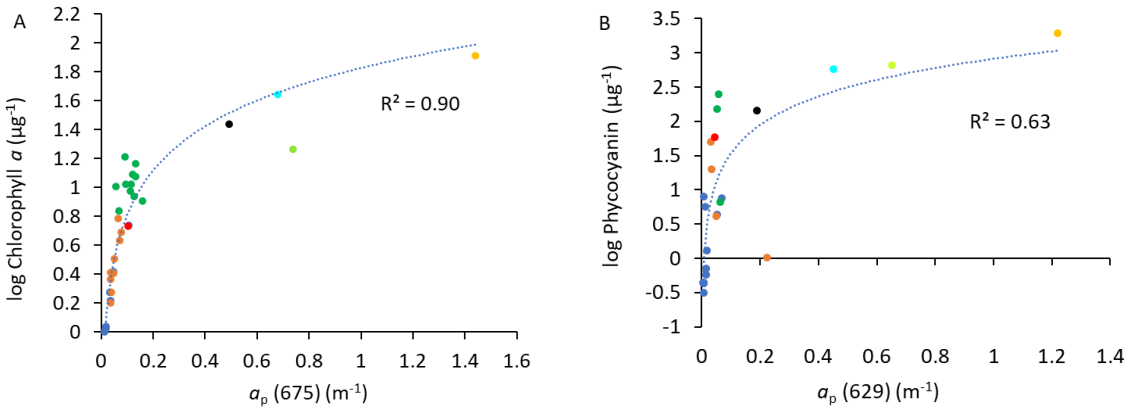

Figure 5.4. A) relationship between chlorophyll *a* concentrations and $a_p(675)$ in all Rotorua and Waikato Lakes (p=<<0.001, R^2=0.90). B) relationship between log phycocyanin concentrations and $a_p(629)$ (p=<<0.001 and R^2=0.63).

Regression analysis for all phytoplankton and cyanobacteria biovolume was also performed at the same wavelengths and fitted with an exponential trend line which resulted in phytoplankton biovolume *vs* $a_p(675)$ recording p = <<0.001, R^2 = 0.73. No significant relationship was seen between cyanobacterial biovolume at $a_p(629)$ with p = 0.58, R^2 = 0.02.

Absorption of non-algal particles and total suspended solids

Log regression analysis was also used to examine if there was a correlation between TSS and $a_{NAP}(440)$ across all lakes. The analysis found a significant relationship with p = <<0.001 and a strong R^2 of 0.84 (Figure **5.5**).

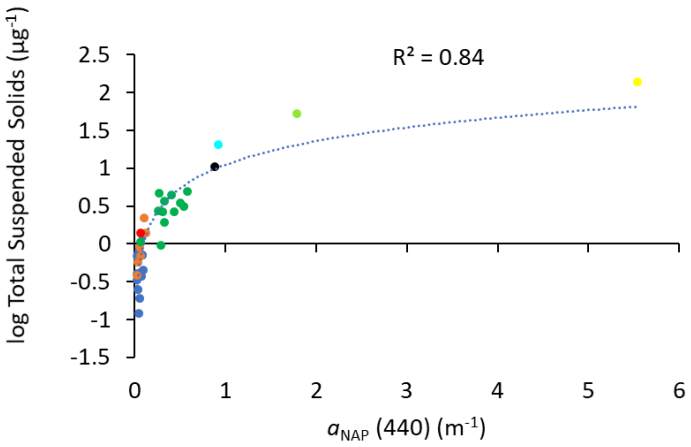

Figure 5.5. Relationship between log total suspended solids and absorption of non-algal particles at 440 nm across all lakes, p=<<0.001, R^2=0.84

Reflectance and phytoplankton pigments chlorophyll a and phycocyanin

Having established that some metrics of algal biomass were predictable from relevant features of the $a_p(\lambda)$ spectra, the next stage of the analysis sought to determine if these features contributed to the form of the reflectance spectra. Regression analysis was performed to assess if the chlorophyll *a* and phycocyanin concentrations also correlated with the depths of troughs at the relevant wavelengths of the reflectance spectra. As with algal absorption spectra, the exact wavelength at which the reflectance troughs minima occurred varied slightly about Rrs(675) and Rrs(629) and a similar approach for deriving Rrs(chla) and Rrs(pc) from the maximum tough depth were used. When all Waikato and Rotorua Lakes were plotted together, a significant relationship between log chlorophyll *a* and Rrs(chla) was obtained (p = 0.006), R^2 (0.74) (Figure **5.6**).

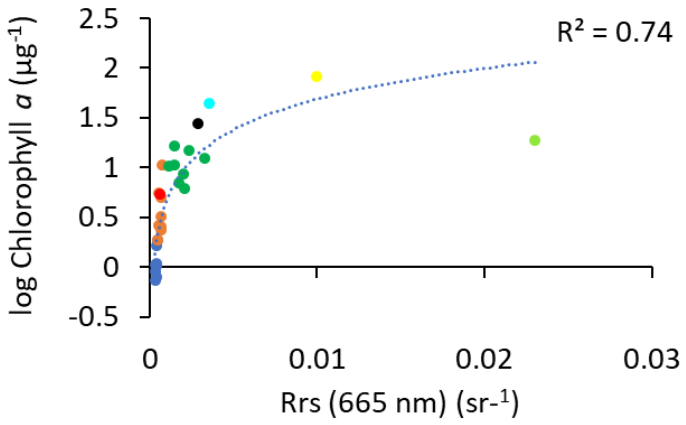

Figure 5.6. Relationship between log chlorophyll *a* log and troughs from all lakes averaged across site and sampling dates at approximately 665 nm seen on absolute reflectance spectra and Waikato Lakes p= 0.006 R^2=0.74

When all lakes were combined, again a significant relationship between Rrs(pc) and phycocyanin was evident (p = 0.01 R^2=0.67) (Figure **5.7**) though this was strongly affected by a single outlier.

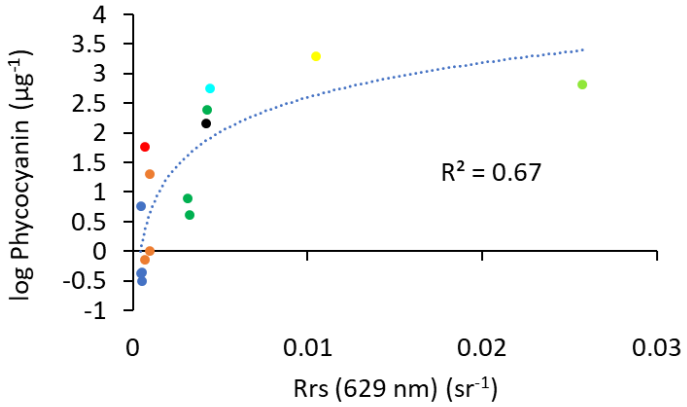

Figure 5.7. Relationship between log phycocyanin and trough in all lakes averaged between sites and sampling dates at approximately 629 nm seen on absolute reflectance spectra p = 0.01 R^2=0.67.

Linear regression of log phytoplankton biovolume *vs* Rrs(chla) showed a significant relationship (p = 0.01 R^2, = 0.21), but no similar relationship for cyanobacterial biovolume and Rrs(pc) was found (p = 0.84, R^2 = 0.05).

Existing algorithms

Use of reflectance spectra features to estimate pigment concentrations has been widely addressed in the remote sensing literature, and many of the algorithms that have been produced were reviewed by Zhu *et al*. (2014). To determine how well the data presented in this thesis fit these existing algorithms, two good-performing examples for each of chlorophyll *a* and phycocyanin were selected and applied to the complete dataset, as described in section 3.4.

Chlorophyll *a* (O'Reilly *et al.*, 1998).

The first algorithm tested (Figure **5.8**) was a multiple regression equation (O'Reilly *et al.*, 1998), of the form (a0 + a1 · R1 + a2 ·R2), where R1 and R2 are reflectance ratios at specific wavelengths (R1 = Rrs(433/555) and R2 = Rrs(412/510)). Once the multiple regression was performed, it showed that the R1 portion of the algorithm was significantly related to chlorophyll *a*, but that the second regression component (R2) added very little to the overall prediction accuracy and was not significant. Therefore, R2 was eliminated, resulting in a linear relationship between R1 and log chlorophyll *a* concentration which showed p <<0.001 and R^2= 0.83.

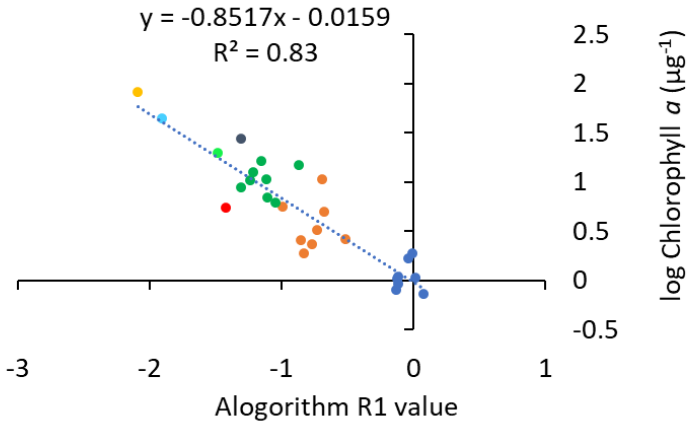

Figure 5.8. Relationship between the log chlorophyll *a* concentration and algorithm value for all Rotorua and Waikato lakes, P=<<0.001 and R^2 =0.83.

Chlorophyll *a* (Le *et al.,* 2009)

The second algorithm (Figure **5.9**) was a four-band semi-analytical model (Le *et al.*, 2009) of the form $[Rrs^{-1}(663) - Rrs^{-1}(693)]\cdot[Rrs^{-1}(740) - Rrs^{-1}(705)]^{-1}$. The authors selected these reflectance wavelengths as 663 nm indicated maximum phytoplankton absorption, from which Rrs(693) was subtracted to minimise the impact of TSS, CDOM and water absorption. The 740 nm and 705 nm were used to minimise the effect of the increased water absorption occurring in the NIR red region while removing backscattering from constituents within the water body. The authors found this improved the signal to noise ratio to benefit lakes with lower chlorophyll *a* concentration. Using Waikato and Rotorua Lake data, this algorithm achieved p << 0.001 and R^2 = 0.54.

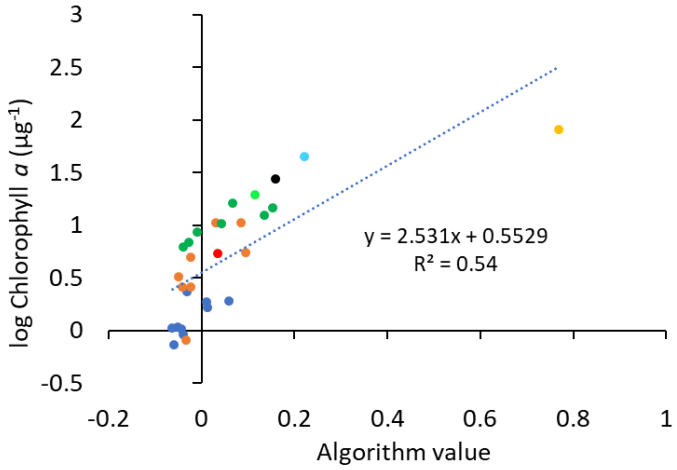

Figure 5.9 Relationship between log chlorophyll *a* concentration for all Rotorua and Waikato lakes and algorithm value P=<<0.001 and R^2 = 0.54

Phycocyanin (Mishra *et al.*, 2009)

This algorithm was designed to exclude chlorophyll *a* influence, it relates a simple band ratio of Rrs(700)/Rrs(600) to phycocyanin concentrations. The authors Mishra *et al.*, (2009) argue that at 700 nm phycocyanin and other pigments have little effect on reflectance, at 600 nm, phycocyanin absorption is high with little influence from chlorophyll *a*. When all lakes were plotted together, the relationship between observed phycocyanin concentrations and algorithm was significant (p << 0.001, R^2=0.92) (Figure **5.10**) with strong correlations across all lake types.

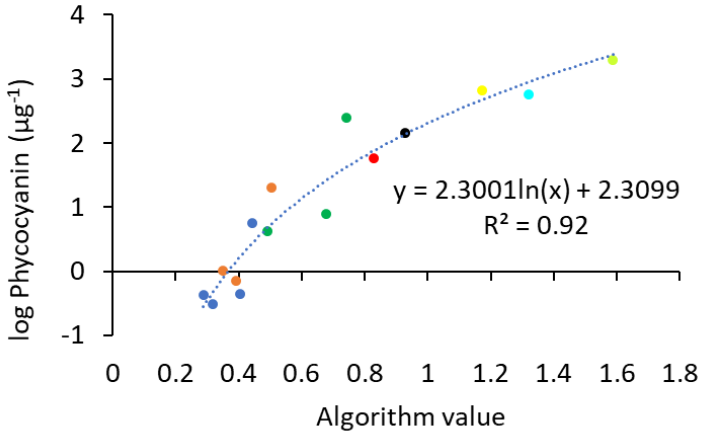

Figure 5.10. Relationship between log phycocyanin concentrations for all Rotorua and Waikato Lakes averaged between sites and sampling months and algorithm value p=<<0.001 R^2=0.92.

Phycocyanin (Mishra *et al.* (2019)

The second algorithm (Figure **5.11**) required the use of reflectance at three wavelengths (681, 665 and 620 nm). This algorithm produced no significant relationship with observed phycocyanin concentrations.

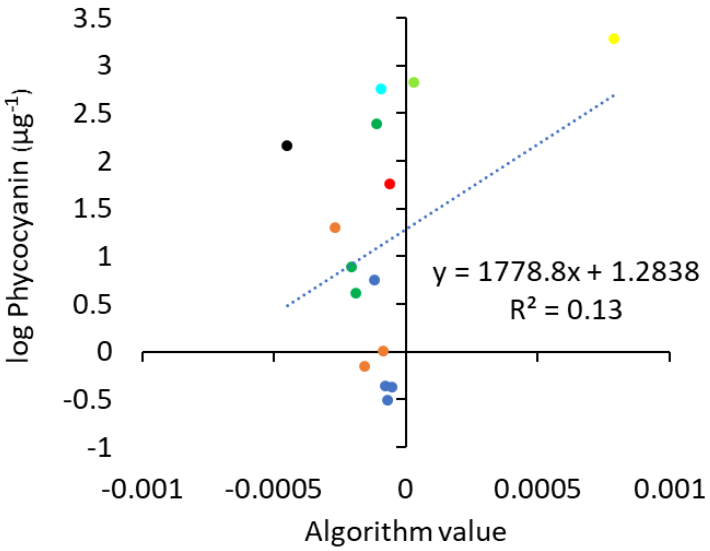

Figure 5.11. Relationship between log phycocyanin for all Rotorua and Waikato Lakes averaged between sites and sampling months and algorithm value p=0.19 R^2=0.13.

Chapter 6

Discussion

6.1 Overview

The results described in this thesis were designed to address the extent to which phytoplankton composition, particularly the presence and biomass of cyanobacteria, is reflected in the optical properties of lakes in the central North Island of New Zealand. Three Rotorua lakes that vary in trophic state from oligotrophic to eutrophic were sampled repeatedly over two summer seasons to address changes in optical properties as the phytoplankton populations underwent seasonal succession. In addition, single samples from five Waikato lakes provide a more extensive range of optical water types. In each case the overall optical characteristics of each lake was measured as the reflectance spectrum at the lake surface and, to interpret this, information was collected on the variables that most contribute to absorption and scattering of light in-water, and hence the quantity and quality of light that is backscattered through the water-air interface. To achieve this, concentrations of chlorophyll *a* and phycocyanin near the lake surface were measured, phytoplankton composition, biovolume and absorption spectra are described, together with absorption spectra of CDOM and non-algal particles, and these were variously analysed to determine how they contributed to general and specific features of reflectance spectra.

Reflectance spectra from all lakes showed characteristic differences based on proportional concentrations of optically active constituents such as CDOM, non-algal particles, TSS, and phytoplankton resulting in different perceived water colour. The shape of reflectance spectra have been used in a number of studies to classify lakes by optical type (Eleveld *et al.*, 2017; Lehmann *et al.*, 2018). In the case of the Rotorua lakes investigated here, Lake Rotomā falls onto the blue class of lakes, class 1 of Eleveld *et al.,* (2017), Lake Rotoiti into class 3 and Rotoehu into class 4 or 5, the higher numbers representing more eutrophic conditions. In general, there was an inverse relationship between the absorption and reflectance spectra, with the shapes of reflectance spectra showing the relative importance of the various absorbing materials. Lake Rotomā, for example, has the best water quality of all lakes in this

study with low turbidity and is considered a blue lake with maximum reflectance seen in the blue wavelength. This is consistent with low concentrations of a_{CDOM}, a_{NAP} and $a_{p,}$ which all contribute to blue absorption (Scholes & Hamill, 2016), while low reflectance at red wavelengths showed the strong proportional influence of water absorption, which increases rapidly at approximately 550 nm and continues into the longer wavelengths. In this lake there were minimal impacts from phycocyanin and chlorophyll *a* to form reflectance troughs at 629 and 675 nm.

Reflectance maxima averaged 554 nm in Lake Rotoiti, giving the lake a dominant green appearance, and absorption and reflectance again showed inverse correspondence. An increase in a_{CDOM}, a_{NAP}, a_p relative to that seen in Lake Rotomā lead to higher absorption in the blue wavelength, balancing the absorption from water and TSS occurring in the red. This led to a more "symmetrical" reflectance spectrum (and absorption spectrum) on either side of the green maxima peak. In this mesotrophic lake, with its moderate concentration of chlorophyll, a distinct reflectance trough could be seen at 675nm, consistent with the published chlorophyll *a* and measured a_p absorption spectra.

The shallow, polymictic Lake Rotoehu, with the constant suspension of particulate matter and phytoplankton mixing throughout the water column and high concentrations of the blue-absorbing CDOM, pushed the maximum reflectance peak into the green-orange wavelengths. Unlike the two deep lakes, Lake Rotoehu's reflectance did not decrease nearly as much in the orange to red wavelength due to higher TSS and phytoplankton biovolume. This sustained higher reflectance at the red end ensured Lake Rotoehu was the brightest of the three Rotorua lakes.

The Waikato lakes, with higher concentrations of CDOM, non-algal particles, and phytoplankton than that recorded in the Rotorua lakes, showed high absorption in the blue – green wavelengths. This was most evident in the riverine lakes pushing the reflectance maxima into the red wavelengths. Higher concentrations of TSS and pigment absorption influenced the scattering in these shallow, highly turbid lakes, making the absorption from water insignificant.

Seasonal variation

Each of the three Rotorua lakes that formed the bulk of the data presented here contained similar phytoplankton taxa throughout the study, though the most oligotrophic had the most distinct flora. By biovolume, diatoms were the most dominant phytoplankton across the three lakes, confirming previous observations (Wilding, 2001; Paul *et al.*, 2012), though occasional dinoflagellate pulses were seen in all three lakes. The very large size of *Peridinium* means that relatively few cells contribute a large biovolume, so this shift can occur quickly. Phytoplankton population dynamics are often attributed to resource availability and physical environmental changes such as stratification (Carpenter *et al.*, 1998; Reynolds, 1998). Diatoms tend to have a high sinking rate, and dominance is common under well mixed, low light winter conditions (Reynolds & Wiseman, 1982). Sedimentation rates of diatoms can alter throughout the development of the population, with a decrease in the active growing stage and increasing with the presence of stable stratification (Smayda, 1974; Reynolds & Wiseman, 1982; Peperzak *et al.*, 2003), the latter suggested as a response to increasing nutrient limitation (Zhou *et al.*, 2017). CDOM concentrations, while showing high variations between lakes, remained largely stable within each lake year-round. Non-algal particles absorption decreased in the two deeper lakes as summer progressed, consistent with sedimentation out of the epilimnion through the stratified phase, in contrast to the increase of a_{NAP} through summer in polymictic Lake Rotoehu. Winter saw increases in TSS as did other dates in late summer, so no temporal trend could be recognised. The relatively small changes in concentrations of optically active substances is consistent with the reflectance spectra of these lakes being largely lake-specific, with limited overlap between lakes.

The general picture of phytoplankton succession observed in Lake Rotomā showed increased absorption during winter but did not see the spike in biovolume. In this lake chlorophyta were dominating in winter, which were small in cell size, while chlorophyll *a* concentration was high, as seen in the extracted chlorophyll *a* values and the more evident 675 nm trough. An increase in lake temperature in conjunction with the onset of stratification in the second summer season was a precursor to developing a cyanobacterial population in Lake Rotomā. The thermal precursor of stratification for cyanobacterial bloom formation has been recognised in many studies (Sverdrup *et al.*, 1942; Reynolds, 1998; Diehl, 2002). The concentrations of cyanobacteria in any month did not produce enough phycocyanin to be detected as a clear

trough in the reflectance spectra. Overall, reflectance spectra from Lake Rotomā gave little indication of what was present but more indication of what was not – specifically, there was no optical evidence of cyanobacteria in this oligotrophic lake.

Lake Rotoiti followed a similar pattern with a winter peak, with an increase in phytoplankton biomass, with diatoms dominant, followed by a shift under summer stratification that included an increased cyanobacterial growth, following that seen by Vincent *et al.* (1984). In addition to the spike in biovolume, winter also saw concentrations of TSS and non-algal particles increase in this lake. This increase in a_{NAP} and a_p was seen in the reduced reflectance at blue wavelengths and, along with higher levels of carotenoids absorption around 500 nm, pushed the reflectance maxima into the longer wavelengths, increased the depth of the chlorophyll *a* trough at 675 nm and resulting in greater backscattering in the red. November 2019 also saw high diatom biovolume, but average concentrations of non-algal particles, which once again pushed the reflectance maxima further right, indicating carotenoids influence the position of the green reflectance peak, also suggested by Schalles and Yacobi (2000). The remaining months showed higher variation in the blue wavelength and less so in the red, indicative of the changing concentrations of non-algal particles with minimal impact from relatively stable algal concentrations

No dramatic fluctuation of phytoplankton species was seen in the shallow isothermic Lake Rotoehu, rather a gradual succession. In this lake, the absence of stratification and relatively high concentrations of nutrients (Scholes & Hamill, 2016) suggests that other physical conditions may play an important role in driving this gradual change. More vigorous wind and wave action in winter, increasing mixing, appeared to favour dinoflagellates, with some species able to migrate vertically through the water column using flagella (Harris *et al.*, 1979) allowed for optimum positioning for maximum growth. Diatoms increased in early summer, and with the rise in surface temperature and reduced wind stress in late summer cyanobacteria populations dominated. The carotenoid absorption was clearly seen in the absorption spectrum for December 2020, January and March 2021 but failed to make an impact on the respective reflectance spectrum, with limited movement of the green maxima peak. Although recording the highest cyanobacteria across the Rotorua lakes, only March

2021 showed a distinct trough at 629 nm. All other months tended to reflect the concentrations of optically active rather than differentiating between taxa.

Detection of cyanobacteria

All lakes supported cyanobacteria, and biovolume and species composition correlated with trophic levels. *Dolichospermum* and *Microcystis* were the dominant blue-green species in the mesotrophic and eutrophic Rotorua lakes. This aligned with previous reports by Wood *et al.* (2006) (2001 – 2004) and Paul *et al.* (2012) from 2003 – 2007. *Dolichopsermum* favoured the less eutrophic conditions of Lake Rotoiti, where it dominated over *Microcystis,* which prefers a lake with a higher nutrient load (Vincent, 1989; Garcia & De Emiliani, 1993). This advantage could perhaps be attributed to nitrogen fixation, which is not present in *Microcystis* (Paerl & Otten, 2013). *Dolichospermum* were noted to have produced heterocysts, which allow the reduction of N_2 to $NH_4^{+,}$ providing a competitive advantage when the lake water becomes limited in nitrogen sources (Wood *et al.*, 2010b). This adaptation is particularly well suited to Lake Rotoiti, which may become nitrogen-limited during summer (Scholes & Hamill, 2016), particularly as nitrogen limitation can reduce buoyancy which would also disadvantage *Microcystis* (Carey *et al.*, 2012).

Phycocyanin troughs

One of the major aims of this study was to detect cyanobacteria in lake waters. There is only a very small waveband (centred approximately on 629 nm) within the reflectance spectrum that indicates phycocyanin, and other pigment absorption can also occur in the region making it difficult to distinguish. This study confirmed that phycocyanin was less sensitive to detection using hyperspectral data than chlorophyll. Stumpf *et al.* (2016) suggest phycocyanin concentrations must be double that of chlorophyll *a* for an equivalent response from satellite data. This occurred in the Waikato lakes, where well-defined troughs were seen but was only evident in one sample across the Rotorua Lakes (March 2021, Lake Rotoehu). We must also keep in mind there was no hyperspectral data available for January – February 2021, during cyanobacterial dominance in Lake Rotoehu, due to instrument failure.

Despite the apparent absence of phycocyanin signals in the reflectance spectra, they were present when specific wavebands were examined using targeted algorithms. Two algorithms

for each pigment (chlorophyll *a* and phycocyanin) were assessed to determine the best relationship for the estimation of these specific pigments. The strongest correlation for chlorophyll *a* was seen in the single regression algorithm adapted from O'Reilly *et al.*, (1998) using the blue-green wavebands ($p << 0.001$ and $R^2 = 0.83$) compared to the four-band semi-analytical model (Le *et al*., 2009) using red and NIR wavebands ($p << 0.001$ and $R^2 = 0.54$). This may be due to more variation seen between lakes in the red and NIR wavelengths on the reflectance spectra, particularly seen in Lake Rotongaroiti, displaying the impact of high TSS and chlorophyll *a* concentration by becoming an outlier. The results indicate using the blue – green wavelengths were a better fit for lakes with large differences in TSS and biovolume concentrations due to potential interference.

The results for phycocyanin showed the simple band ratio phycocyanin algorithm Rrs(700)/Rrs(600) from Mishra *et al.*, (2009), was the only one to show a significant relationship ($p << 0.001$, $R^2=0.92$). At 600 nm Emerson & Lewis, (1942) found 89% of light absorption was from phycocyanin compared to 11% from chlorophylls, 700 nm indicates minimal phycocyanin absorption, therefore this algorithm took into account the variable ratio of phycocyanin:chlorophyll *a* pigment ratio which showed a wide range within the studies lakes. Mishra *et al*., (2009) also indicated this algorithm was well suited to waterbodies with varying chlorophyll *a* concentrations and different cyanobacterial species, which were also recorded in this study. The two algorithms deemed best fit for the lakes in this study with variable concentrations of optically active constituents provide a tool to estimate both chlorophyll *a* and phycocyanin concentrations from hyperspectral imagery to a significantly high degree.

Overall, the seasonal reflectance changes suggested Rotorua lakes were influenced more by CDOM and changes in the concentrations of non-algal particles and TSS than that of changes in the phytoplankton community. Ternary plot confirming the influence of these constituents over phytoplankton absorption and cluster analysis illustrating the minimal impact phytoplankton succession had on the reflectance spectrum.

6.2 Conclusions

The aim of this study was to examine the extent to which information on within-and between-lake variations in phytoplankton composition and biovolume could be derived from the reflectance spectra in selected Rotorua and Waikato lakes. It formed part of a larger project that seeks to monitor the development of cyanobacterial blooms in lakes of Aotearoa New Zealand using remote sensing tools.

Results showed a general inverse relationship between absorption and reflectance spectra. Each lake studied had a characteristic reflectance spectrum that corresponded well to the relative contributions of absorbing constituents in the water body. The effects of phytoplankton were evident, particularly in the more eutrophic water bodies, but contributed too little to the overall absorption spectrum for any taxonomic differences between lakes or over the annual cycle to be detected from reflectance spectra.

In most cases, the biovolume of cyanobacteria in lakes was not large enough to present enough phycocyanin to display a distinct phycocyanin reflectance signal. Where present in significant amounts, phycocyanin was evident in both particulate absorption and water reflectance spectra. A phycocyanin-specific algorithm was able to quantify the pigment, but the biovolume of cyanobacteria could not be predicted.

Chlorophyll *a* was more easily detected in absorption and reflectance spectra than phycocyanin. Applying specifically selected algorithms suggest a potential to predict chlorophyll *a* concentration from reflectance spectra.

This work will ultimately contribute to the ongoing development of a biovolume risk assessment tool undertaken by the Eye on Lakes project. Further research of water types and catchments not seen in this study is needed to develop even more robust algorithms.

References

Abell, J., Özkundakci, D., & Hamilton, D. (2010). Nitrogen and Phosphorus Limitation of Phytoplankton Growth in New Zealand Lakes: Implications for Eutrophication Control. *Ecosystems (New York), 13*(7), 966-977.

Aguirre-Gomez, R., Weeks, A. R., & Boxall, S. R. (2001). The identification of phytoplankton pigments from absorption spectra. *International journal of remote sensing, 22*(2-3), 315-338.

Allan, M. G., Hamilton, D. P., Hicks, B. J., & Brabyn, L. (2011). Landsat remote sensing of chlorophyll a concentrations in central North Island lakes of New Zealand. *International Journal of Remote Sensing, 32*(7), 2037-2055.

Barnes, G. (2001). *Aquatic & Marginal Vegetation of Lake Serpentine North*. Environment Waikato.

Bay of Plenty Regional Council. (2020). *Recreational waters surveillance report 2019/2020 bathing season*.

Becker, R. H., Sultan, M. I., Boyer, G. L., Twiss, M. R., & Konopko, E. (2009). Mapping Cyanobacterial Blooms in the Great Lakes Using MODIS. *Journal of Great Lakes Research, 35*(3), 447-453.

Bellinger, E. G., & Sigee, D. C. (2015). *Freshwater algae: identification, enumeration and use as bioindicators*. John Wiley & Sons.

Beyá, J., Hamilton, D., & Burger, D. (2005). *Analysis of catchment hydrology and nutrient loads for Lakes Rotorua and Rotoiti*. Centre for Biodiversity of Ecology Research, University of Waikato, Hamilton.

Boswell, J., Russ, M., & Simons, M. (1985). *Waikato small lakes : resource statement*. Technical report ; 1985/7. Hamilton, N.Z: Waikato Valley Authority.

Brezonik, P. L., Olmanson, L. G., Finlay, J. C., & Bauer, M. E. (2015). Factors affecting the measurement of CDOM by remote sensing of optically complex inland waters. *Remote sensing of environment, 157*, 199-215.

Bryant, D. A. (1981). The Photoregulated Expression of Multiple Phycocyanin Species: A General Mechanism for the Control of Phycocyanin Synthesis is Chromatically Adapting Cyanobacteria. *European Journal of Biochemistry, 119*(2), 425-429.

Burns, N., McIntosh, J., & Scholes, P. (2005). Strategies for Managing the Lakes of the Rotorua District, New Zealand. *Lake and reservoir management, 21*(1), 61-72.

Burns, N., McIntosh, J., & Scholes, P. (2009). Managing the lakes of the Rotorua District, New Zealand. *Lake and reservoir management, 25*(3), 284-296.

Burns, N. M., Rutherford, J. C., & Clayton, J. S. (1999). A Monitoring and Classification System for New Zealand Lakes and Reservoirs. *Lake and Reservoir Management, 15*(4), 255-271.

Burstall, P. (1880). The introduction of freshwater fish into the Rotorua Lakes. *Rotorua, 1980*, 115-121.

Burton, T., & Clayton, J. (2015). *Assessment of the Rotorua Te Arawa lakes using Lake SPI - 2015.*, Report HAM2015-091 for Bay of Plenty Regional Council.

Carey, C. C., Ibelings, B. W., Hoffmann, E. P., Hamilton, D. P., & Brookes, J. D. (2012). Eco-physiological adaptations that favour freshwater cyanobacteria in a changing climate. *Water research (Oxford), 46*(5), 1394-1407.

Carey, C. C., Weathers, K. C., Ewing, H. A., Greer, M. L., & Cottingham, K. L. (2014). Spatial and temporal variability in recruitment of the cyanobacterium Gloeotrichia echinulata in an oligotrophic lake. *Freshwater Science, 33*(2), 577-592.

Carmichael, W. W. (1994). The toxins of cyanobacteria. *Scientific American, 270*(1), 78-86.

Carmichael, W. W. (2001). Health Effects of Toxin-Producing Cyanobacteria: "The CyanoHABs". *Human and ecological risk assessment, 7*(5), 1393-1407.

Carpenter, S. R., Caraco, N. F., Correll, D. L., Howarth, R. W., Sharpley, A. N., & Smith, V. H. (1998). Nonpoint pollution of surface waters with phosphorus and nitrogen. *Ecological applications, 8*(3), 559-568.

Chang, D.-W., Hobson, P., Burch, M., & Lin, T.-F. (2012). Measurement of cyanobacteria using in-vivo fluoroscopy–Effect of cyanobacterial species, pigments, and colonies. *Water research, 46*(16), 5037-5048.

Cichota, R., & Snow, V. O. (2009). Estimating nutrient loss to waterways-an overview of models of relevance to New Zealand pastoral farms. *New Zealand journal of agricultural research, 52*(3), 239-260.

Clayton, J., & Edwards, T. (2006). LakeSPI. *User Manual Version, 2.*

Clayton, J. S., Chapman, V. J., & Brown, J. M. A. (1981). Submerged vegetation of the Rotorua and Waikato lakes 4. Lake Rotoma. *New Zealand journal of marine and freshwater research, 15*(4), 447-457.

Collier, K. J., Garrett-Walker, J., Özkundakci, D., & Pingram, M. A. (2019). Characteristics of consumer trophic resources for Waikato shallow lake food webs. *New Zealand journal of marine and freshwater research, 53*(4), 588-602.

Collier, K. J., & Grainger, N. (2015). *New Zealand invasive fish management handbook*. Hamilton: LERNZ The University of Waikato.

Cronin, J., Winters, K., & Curtis, T. (2007). *Lake Rotoehu Action Plan-Hearing panel decisions.* Environment Bay of Plenty. Environmental Publication 19.

de Winton, M., & Champion, P. (1993). *The vegetation of the lower Waikato Lakes.* NIWA Ecosystems publication No. 8., Hamilton.

Dean-Speirs, T., Neilson, K., Reeves, P., & Kelly, J. (2014). *Waikato region shallow lakes management plan*. Waikato Regional Council technical report, 2014/58, 2014/59. Hamilton [New Zealand: Waikato Regional Council.

Deely, J. M., McIntosh, J. J., & Gibbons-Davies, J. (1995). *Water Quality Regional Monitoring Network Lakes Report, 1990-1995*. Environment BOP.

Devcich, A. A. (1979). *An ecological study of Paranephrops planifrons white (Decapoda: Parastacidae) in Lake Rotoiti, North Island.* thesis, University of Waikato.

Diehl, S. (2002). Phytoplankton, Light, and Nutrients in a Gradient of Mixing Depths: Theory. *Ecology (Durham), 83*(2), 386.

Dörnhöfer, K., & Oppelt, N. (2016). Remote sensing for lake research and monitoring – Recent advances. *Ecological indicators, 64*, 105-122.

Duggan, I. C. (2007). *An assessment of the water quality of ten Waikato lakes based on zooplankton community composition*. Environment Waikato Regional Council.

Edwards, T., de Winton, M., & Clayton, J. (Compiler) (2010). *Assessment of the ecological condition of lakes in the Waikato region using LakeSPI*: NIWA Client Report: HAM2005-125, Hamilton: National Institute of Water and Atmospheric Research.

Eleveld, M. A., Ruescas, A. B., Hommersom, A., Moore, T. S., Peters, S. W. M., & Brockmann, C. (2017). An optical classification tool for global lake waters. *Remote sensing (Basel, Switzerland), 9*(5), 420.

Envirocare. (2005). *Retrived from*. Issue 43. from https://www.waikatoregion.govt.nz/assets/PageFiles/13635/2005/Envirocareautumn2005.pdf.

Environment Bay of Plenty. (2009). *Lake Rotoma background information*. Whakatane, N.Z. : Environment Bay of Plenty.

Foley, J. A., DeFries, R., Asner, G. P., Barford, C., Bonan, G., Carpenter, S. R., Chapin, F. S., Coe, M. T., Daily, G. C., & Gibbs, H. K. (2005). Global consequences of land use. *science, 309*(5734), 570-574.

Garcia, M. O., & De Emiliani, G. (1993). Seasonal succession of phytoplankton in a lake of the Paraná River floodplain, Argentina. *Hydrobiologia, 264*(2), 101-114.

Giardino, C., Bresciani, M., Valentini, E., Gasperini, L., Bolpagni, R., & Brando, V. E. (2015). Airborne hyperspectral data to assess suspended particulate matter and aquatic vegetation in a shallow and turbid lake. *Remote Sensing of Environment, 157*, 48-57.

Gibbs, M. M., Hawes, I., & Stephens, S. A. (2003). *Lake Rotoiti-Ohau Channel: Assessment of Effects of Engineering Options on Water Quality*. National Institute of Water & Atmospheric Research.

Gillies, R., Bycroft, C., Shaw, W., & Bawden, R. (2010). *Bird monitoring in the vicinity of the Ohau channel diversion structure at Lake Rotoiti - 2020 progress report.*

Greenwood, T. L., Green, J. D., Hicks, B. J., & Chapman, M. A. (1999). Seasonal abundance of small cladocerans in Lake Mangakaware, Waikato, New Zealand. *New Zealand journal of marine and freshwater research, 33*(3), 399-415.

Hamill, K. D. (1995). *Nutrient Transformations in the Lacustrine Groundwater of a Waipa Peat Lake: Lake Serpentine.* thesis, University of Waikato.

Hamill, K. D. (2001). Toxicity in benthic freshwater cyanobacteria (blue-green algae): First observations in New Zealand. *New Zealand journal of marine and freshwater research, 35*(5), 1057-1059.

Hamilton, D., Vant, W., & Neilson, K. (2010). Lowland lakes. *The Waters of the Waikato: Ecology of New Zealand's Longest River'.(Eds KJ Collier, DP Hamilton, WN Vant and C. Howard-Williams.) pp*, 245-264.

Hamilton, D. P. (2003). *An historical and contemporary review of water quality in the Rotorua lakes.* Presented at the Proceedings Rotorua Lakes 2003, Practical Management for Good Lake Water Quality conference. p 3-15.

Hamilton, D. P. (2005). *Lake Rotoiti fieldwork and modelling to support considerations of Ohau Channel diversion from Lake Rotoiti*. Hamilton N.Z. : University of Waikato, Centre for Biodiversity and Ecology Research.

Hamilton, D. P., Alexander, W., & Burger, D. F. (2004). Nutrient Budget for Lakes Rotoiti and Rotorua. Part I: Internal Nutrient Loads.

Hamilton, D. P., Collier, K. J., Quinn, J. M., & Howard-Williams, C. (2019). *Lake Restoration Handbook: A New Zealand Perspective*. Cham: Springer International Publishing AG.

Harper, D. (1992). *Eutrophication of Freshwaters Principles, problems and restoration*. Dordrecht: Springer Netherlands.

Harris, G., Heaney, S., & Talling, J. (1979). Physiological and environmental constraints in the ecology of the planktonic dinoflagellate Ceratium hirundinella. *Freshwater Biology, 9*(5), 413-428.

Hawes, I., Jungblut, A. D., Obryk, M. K., & Doran, P. T. (2016). Growth dynamics of a laminated microbial mat in response to variable irradiance in an Antarctic lake. *Freshwater biology, 61*(4), 396-410.

Hawkins, P. R., Holliday, J., Kathuria, A., & Bowling, L. (2005). Change in cyanobacterial biovolume due to preservation by Lugol's Iodine. *Harmful Algae, 4*(6), 1033-1043.

Hayes, J. W. (1989). Comparison between a fine mesh trap net and five other fishing gears for sampling shallow-lake fish communities in New Zealand (Note). *New Zealand journal of marine and freshwater research, 23*(3), 321-324.

Healy, J. (1975). Volcanic lakes. *New Zealand lakes*, 70-83.

Hillebrand, H., Dürselen, C. D., Kirschtel, D., Pollingher, U., & Zohary, T. (1999). Biovolume calculation for pelagic and benthic microalgae. *Journal of Phycology, 35*(2), 403-424.

Hoepffner, N., & Sathyendranath, S. (1993). Determination of the major groups of phytoplankton pigments from the absorption spectra of total particulate matter. *Journal of Geophysical Research: Oceans, 98*(C12), 22789-22803.

Huisman, J., Codd, G., Paerl, H., Ibelings, B., Verspagen, J., & Visser, P. (2018). Cyanobacterial blooms. *Nature Reviews. Microbiology, 16*(8), 471-483.

Jolly, V. H. (1968). The comparative limnology of some New Zealand lakes: 1. Physical and chemical. *New Zealand journal of marine and freshwater research, 2*(2), 214-259.

Jolly, V. H., & Brown, J. M. A. (1975). *New Zealand lakes*. Auckland University Press.

Jones, R. I. (1998). Phytoplankton, primary production and nutrient cycling. In *Aquatic humic substances* (pp. 145-175). Springer.

Kusabs, I. A., Hicks, B. J., Quinn, J. M., & Hamilton, D. P. (2015). Sustainable management of freshwater crayfish (kōura, Paranephrops planifrons) in Te Arawa (Rotorua) lakes, North Island, New Zealand. *Fisheries research, 168*, 35-46.

Kusabs, I. A., & Quinn, J. M. (2009). Use of a traditional Maori harvesting method, the tau kōura, for monitoring kōura (freshwater crayfish, Paranephrops planifions) in Lake Rotoiti, North Island, New Zealand. *New Zealand journal of marine and freshwater research, 43*(3), 713-722.

Kutser, T. (2009). Passive optical remote sensing of cyanobacteria and other intense phytoplankton blooms in coastal and inland waters. *International Journal of Remote Sensing, 30*(17), 4401-4425.

Kutser, T., Pierson, D. C., Kallio, K. Y., Reinart, A., & Sobek, S. (2005). Mapping lake CDOM by satellite remote sensing. *Remote sensing of environment, 94*(4), 535-540.

Kutser, T., Verpoorter, C., Paavel, B., & Tranvik, L. J. (2015). Estimating lake carbon fractions from remote sensing data. *Remote sensing of Environment, 157*, 138-146.

Land Air Water Aotearoa. (2020). *Retrieved August 2021* from https://www.lawa.org.nz/explore-data/lakes/.

Lass, H. (2012). Rotorua lakes weed cordons–a freshwater biosecurity tool. In *Proceedings of the 18th Australasian Weeds Conference, ed. V. Eldershaw* (pp. 25-29).

Le, C., Li, Y., Zha, Y., Sun, D., Huang, C., & Lu, H. (2009). A four-band semi-analytical model for estimating chlorophyll a in highly turbid lakes: The case of Taihu Lake, China. *Remote Sensing of Environment, 113*(6), 1175-1182.

Lee, Z., & Carder, K. L. (2004). Absorption spectrum of phytoplankton pigments derived from hyperspectral remote-sensing reflectance. *Remote sensing of environment, 89*(3), 361-368.

Lehmann, M., Nguyen, U., Allan, M., & van der Woerd, H. (2018). Colour Classification of 1486 Lakes across a Wide Range of Optical Water Types. *Remote sensing (Basel, Switzerland), 10*(8), 1273.

Lehmann, M. K., Schallenberg, L. A., & Allan, M. G. (2017). *Feasibility of water quality monitoring by remote sensing in the Waikato Region.* . Prepared for Waikato Regional Council. Reoprt No. 87.

Loiselle, S. A., Bracchini, L., Dattilo, A. M., Ricci, M., Tognazzi, A., Cózar, A., & Rossi, C. (2009). The optical characterization of chromophoric dissolved organic matter using wavelength distribution of absorption spectral slopes. *Limnology and Oceanography, 54*(2), 590-597.

Lowe, D. J., & Green, J. D. (1987). Origins and development of the lakes. In A. B. Viner (Ed.), *Inland Waters of New Zealand* (pp. 1-64). Wellington: New Zealand Department of Scientific and Industrial Research.

Malthus, T. J., Grieve, L., & Harwar, M. D. (1997). *Spectral modeling for the identification and quantification of algal blooms: A test of approach.* Environmental Research Institute of Michigan, Ann Arbor, MI (United States).

Matson, P. A., Parton, W. J., Power, A. G., & Swift, M. J. (1997). Agricultural intensification and ecosystem properties. *Science, 277*(5325), 504-509.

McBride, C. G., Tempero, G. W., Hamilton, D. P., Cutting, C. T., Muraoka, K., Duggan, C., & Gibbs, M. M. (Compiler) (2019). *Ecological effects of artificial mixing in Lake Rotoehu*: Environmental Research Institute, Faculty of Science and Engineering, The University of Waikato.

McDowall, R. M. (2011). *Ikawai : Freshwater fishes in Māori culture and economy*. Christchurch, N.Z. : University of Canterbury.

McLea, M. C. (1986). *Ohinewai regional resource study : biology and water quality*. Technical publication / Waikato Valley Authority, no. 37. Hamilton [N.Z: Waikato Valley Authority.

Mille, K. (2020). *Rotorua Te Arawa Lakes: Aquatic Plant Management Plan.* Report prepared for Bay of Plenty Regional Council.

Ministry for the Environment and Ministry of Health. (2009). *New Zealand guidelines for managing cyanobacteria in recreational fresh waters-Interim Guidelines. Prepared for the Ministry for the Environment and the Ministry of Health by SA Wood, DP Hamilton, WJ Paul, KA Safi and WM Williamson.* . Wellington, Ministry for the Environment and Ministry of Health Wellington.

Mishra, S., Mishra, D., & Schluchter, W. (2009). A Novel Algorithm for Predicting Phycocyanin Concentrations in Cyanobacteria: A Proximal Hyperspectral Remote Sensing Approach. *Remote sensing (Basel, Switzerland), 1*(4), 758-775.

Mishra, S., Stumpf, R. P., Schaeffer, B. A., Werdell, P. J., Loftin, K. A., & Meredith, A. (2019). Measurement of Cyanobacterial Bloom Magnitude using Satellite Remote Sensing. *Scientific reports, 9*(1), 18310-17.

Moore, S. C. (2000). *Photographic guide to the freshwater algae of New Zealand*. Otago Regional Council.

Mouw, C. B., Greb, S., Aurin, D., DiGiacomo, P. M., Lee, Z., Twardowski, M., Binding, C., Hu, C., Ma, R., & Moore, T. (2015). Aquatic color radiometry remote sensing of coastal and inland waters: Challenges and recommendations for future satellite missions. *Remote sensing of environment, 160*, 15-30.

Muraoka, K., Paul, W., Hamilton, D., & Von Westernhagen, N. (2010). *Effect of different operational regimes of Okere gates on the effectiveness of the Ohau channel diversion wall in Lake Rotoiti.* CBER Report 107.

Neilson, K., Kelleher, R., Barnes, G., Speirs, D., & Kelly, J. (2004). Use of fine-mesh monofilament gill nets for the removal of rudd (Scardinius erythrophthalmus) from a small lake complex in Waikato, New Zealand. *New Zealand journal of marine and freshwater research, 38*(3), 525-539.

Nelson, C. S. (1983). Bottom sediments of Lake Rotoma. *New Zealand journal of marine and freshwater research, 17*(2), 185-204.

Nienaber, M. A., & Steinitz-Kannan, M. (2018). *A guide to cyanobacteria: identification and impact*. University Press of Kentucky.

Nordstedt, O. (1888). *Fresh-water algae collected by D: r S. Berggren in New Zealand and Australia*. (Vol. 22). PA Norstedt & söner.

O'Reilly, J. E., Maritorena, S., Mitchell, B. G., Siegel, D. A., Carder, K. L., Garver, S. A., Kahru, M., & McClain, C. (1998). Ocean color chlorophyll algorithms for SeaWiFS. *Journal of Geophysical Research: Oceans, 103*(C11), 24937-24953.

Odermatt, D., Gitelson, A., Brando, V. E., & Schaepman, M. (2012). Review of constituent retrieval in optically deep and complex waters from satellite imagery. *Remote sensing of environment, 118*, 116-126.

Ogashawara, I., Mishra, D. R., Mishra, S., Curtarelli, M. P., & Stech, J. L. (2013). A performance review of reflectance based algorithms for predicting phycocyanin concentrations in inland waters. *Remote Sensing, 5*(10), 4774-4798.

Oliver, R. L., Hamilton, D. P., Brookes, J. D., & Ganf, G. G. (2012). Physiology, blooms and prediction of planktonic cyanobacteria. In *Ecology of cyanobacteria II* (pp. 155-194). Springer.

Özkundakci, D., & Allan, M. G. (2019). Patterns and drivers of spatio-temporal variability of suspended sediment in the Waikato lakes, New Zealand. *New Zealand journal of marine and freshwater research, 53*(4), 536-554.

Paerl, H. (2008). Nutrient and other environmental controls of harmful cyanobacterial blooms along the freshwater–marine continuum. *Cyanobacterial Harmful Algal Blooms: State of the Science and Research Needs*, 217-237.

Paerl, H. W., & Otten, T. G. (2013). Harmful Cyanobacterial Blooms: Causes, Consequences, and Controls. *Microbial ecology, 65*(4), 995-1010.

Paul, W., Hamilton, D., Ostrovsky, I., Miller, S., Zhang, A., & Muraoka, K. (2012). Catchment land use and trophic state impacts on phytoplankton composition: a case study from the Rotorua lakes' district, New Zealand. *Hydrobiologia, 698*(1), 133-146.

Paul, W. J. (2010). Standard protocol for fluorometric determination of chlorophyll a pigments: Hamilton: The University of Waikato.

Peperzak, L., Colijn, F., Koeman, R., Gieskes, W. W. C., & Joordens, J. C. A. (2003). Phytoplankton sinking rates in the Rhine region of freshwater influence. *Journal of plankton research, 25*(4), 365-383.

Prescott, G. W. (1964). How to know the freshwater algae. *How to know the freshwater algae.*

Rahel, F. J. (2007). Biogeographic barriers, connectivity and homogenization of freshwater faunas: it's a small world after all. *Freshwater biology, 52*(4), 696-710.

Rasch, G. (1989). *Wildlife and wildlife habitats in the Bay of Plenty region*. Department of Conservation.

Reuter, W., & Müller, C. (1993). New trends in photobiology: Adaptation of the photosynthetic apparatus of cyanobacteria to light and co2. *Journal of Photochemistry and Photobiology B: Biology, 21*(1), 3-27.

Reyjol, Y., Argillier, C., Bonne, W., Borja, A., Buijse, A. D., Cardoso, A. C., Daufresne, M., Kernan, M., Ferreira, M. T., Poikane, S., Prat, N., Solheim, A.-L., Stroffek, S., Usseglio-Polatera, P., Villeneuve, B., & van de Bund, W. (2014). Assessing the ecological status in the context of the European Water Framework Directive: Where do we go now? *The Science of the total environment, 497-498*, 332-344.

Reynolds, C. (1998). What factors influence the species composition of phytoplankton in lakes of different trophic status? *Hydrobiologia, 369*, 11-26.

Reynolds, C. S., & Wiseman, S. W. (1982). Sinking losses of phytoplankton in closed limnetic systems. *Journal of plankton research, 4*(3), 489-522.

Rigosi, A., Marcé, R., Escot, C., & Rueda, F. J. (2011). A calibration strategy for dynamic succession models including several phytoplankton groups. *Environmental Modelling & Software, 26*(6), 697-710.

Roy, S., Llewellyn, C. A., Egeland, E. S., & Johnsen, G. (2011). *Phytoplankton pigments: characterization, chemotaxonomy and applications in oceanography*. Cambridge University Press.

Rutherford, J., Pridmore, R., & White, E. (1989). Management of phosphorus and nitrogen inputs to Lake Rotorua, New Zealand. *Journal of water resources planning and management, 115*(4), 431-439.

Sathyendranath, S., Lazzara, L., & Prieur, L. (1987). Variations in the Spectral Values of Specific Absorption of Phytoplankton. *Limnology and oceanography, 32*(2), 403-415.

Schaeffer, B. A., Schaeffer, K. G., Keith, D., Lunetta, R. S., Conmy, R., & Gould, R. W. (2013). Barriers to adopting satellite remote sensing for water quality management. *International journal of remote sensing, 34*(21), 7534-7544.

Schallenberg, M., & Sorrell, B. (2009). Regime shifts between clear and turbid water in New Zealand lakes: environmental correlates and implications for management and restoration. *New Zealand Journal of Marine and Freshwater Research, 43*(3), 701-712.

Schalles, J. F., & Yacobi, Y. Z. (2000). Remote detection and seasonal patterns of phycocyanin, carotenoid and chlorophyll pigments in eutrophic waters. *Ergebnisse Der Limnologie, 55*, 153-168.

Scholes, P. (2009). *Rotorua Lakes water quality report 2009*. Whakatane, N.Z. Environment Bay of Plenty.

Scholes, P., & Hamill, K. (2016). *Rotorua lakes water quality report 2014/2015.* Bay of Plenty Regional Council.

Scholes, P., & McIntosh, J. (2010). The tale of two lakes: managing lake degradation, Rotorua lakes, New Zealand. *Transactions on ecology and the environment, 135*, 157-168.

Schopf, J. W. (2000). The fossil record: tracing the roots of the cyanobacterial lineage. In *The ecology of cyanobacteria* (pp. 13-35). Springer.

Sharp, S., Forrest, A., Bouma-Gregson, K., Jin, Y., Cortés, A., & Schladow, S. (2021). Quantifying Scales of Spatial Variability of Cyanobacteria in a Large, Eutrophic Lake Using Multiplatform Remote Sensing Tools. Front. *Environ. Sci, 9*, 612934.

Simis, S. G. H., Peters, S. W. M., & Gons, H. J. (2005). Remote Sensing of the Cyanobacterial Pigment Phycocyanin in Turbid Inland Water. *Limnology and oceanography, 50*(1), 237-245.

Skulberg, O. M., Carmichael, W. W., Codd, G. A., & Skulberg, R. (1993). Taxonomy of toxic Cyanophyceae (cyanobacteria). *Algal toxins in seafood and drinking water*, 145-164.

Smayda, T. J. (1974). Some experiments on the sinking characteristics of two freshwater diatoms. *Limnology and oceanography, 19*(4), 628-635.

Stedmon, C. A., Markager, S., & Kaas, H. (2000). Optical Properties and Signatures of Chromophoric Dissolved Organic Matter (CDOM) in Danish Coastal Waters. *Estuarine, coastal and shelf science, 51*(2), 267-278.

Straile, D., Jochimsen, M. C., & Kümmerlin, R. (2015). Taxonomic aggregation does not alleviate the lack of consistency in analysing diversity in long-term phytoplankton monitoring data: a rejoinder to Pomati et al. (2015). *Freshwater biology, 60*(5), 1060-1067.

Stumpf, R. P., Davis, T. W., Wynne, T. T., Graham, J. L., Loftin, K. A., Johengen, T. H., Gossiaux, D., Palladino, D., & Burtner, A. (2016). Challenges for mapping

cyanotoxin patterns from remote sensing of cyanobacteria. *Harmful Algae, 54*, 160-173.

Sun, J. (2003). Geometric models for calculating cell biovolume and surface area for phytoplankton. *Journal of plankton research, 25*(11), 1331-1346.

Sverdrup, H. U., Johnson, M. W., & Fleming, R. H. (1942). *The Oceans: Their physics, chemistry, and general biology*. (Vol. 1087). Prentice-Hall New York.

Taiz, L., Zeiger, E., Møller, I. M., & Murphy, A. (2015). *Plant physiology and development*. Sinauer Associates Incorporated.

Tassan, S., & Ferrari, G. M. (2002). A sensitivity analysis of the TransmittanceReflectance method for measuring light absorption by aquatic particles. *Journal of Plankton Research, 24*(8), 757-774.

Tempero, G., & Ling, N. (2020). Spectrofluorometric determination of phycocyanin pigments from freshwater filtrate: Hamilton: University of Waikato.

Tempero, G. W., & Hamilton, D. P. (Compiler) (2019). *Final report: inflow monitoring of the Rotopiko lakes and Lake Mangakaware*: Environmental Research Institute, Faculty of Science and Engineering, The University of Waikato.

Tempero, G. W., Hicks, B. J., Ling, N., Morgan, D., Daniel, A. J., Özkundakci, D., & David, B. (2019). Fish community responses to invasive fish removal and installation of an exclusion barrier at Lake Ohinewai, Waikato. *New Zealand journal of marine and freshwater research, 53*(3), 397-415.

Tempero, G. W., Ling, N., Daniel, A. J., & Morgan, D. K. J. (2015). Removal of invasive fish and exclusion of koi carp from Lake Ohinewai. In K. J. Collier & N. P. J. Grainger (Eds.), *New Zealand Invasive Fish Management Handbook* (pp. 90-94). Hamilton, New Zealand: Lake Ecosystem Restoration New Zealand (LERNZ) & Department of Conservation.

Timperley, M. H. (1983). Phosphorus in spring waters of the Taupo Volcanic Zone, North Island, New Zealand. *Chemical geology, 38*(3), 287-306.

Tomlinson, M. C., Stumpf, R. P., Wynne, T. T., Dupuy, D., Burks, R., Hendrickson, J., & Fulton Iii, R. S. (2016). Relating chlorophyll from cyanobacteria-dominated inland waters to a MERIS bloom index. *Remote Sensing Letters, 7*(2), 141-149.

Trolle, D., Hamilton, D. P., Hendy, C., & Pilditch, C. (2008). Sediment and nutrient accumulation rates in sediments of twelve New Zealand lakes: influence of lake morphology, catchment characteristics and trophic state. *Marine & Freshwater Research, 59*(12), 1067-1078.

Trolle, D., Hamilton, D. P., Pilditch, C. A., Duggan, I. C., & Jeppesen, E. (2011). Predicting the effects of climate change on trophic status of three morphologically varying lakes: Implications for lake restoration and management. *Environmental modelling & software : with environment data news, 26*(4), 354-370.

Utermöhl, H. (1958). Methods of collecting plankton for various purposes are discussed. *SIL Communications, 1953-1996, 9*(1), 1-38.

Vincent, W. (1989). Cyanobacterial growth and dominance in two eutrophic lakes: review and synthesis. *Arch Hydrobiol Beih, 32*, 239-254.

Vincent, W. F., Gibbs, M. M., & Dryden, S. J. (1984). Accelerated eutrophication in a New Zealand lake: Lake Rotoiti, central North Island. *New Zealand Journal of Marine and Freshwater Research, 18*(4), 431-440.

Vincent, W. F., Gibbs, M. M., & Spigel, R. H. (1991). Eutrophication processes regulated by a plunging river inflow. *Hydrobiologia, 226*(1), 51-63.

Vincent, W. F., Spigel, R. H., Payne, G., Dryden, S., May, L., Woods, P., Pickmere, S., Davies, J., & Shakespeare, B. (1986). *The impact of the Ohau channel outflow from Lake Rotorua on Lake Rotoiti*. Taupo Research Laboratory, DSIR.

von Westernhagen, N., Hamilton, D. P., & Pilditch, C. A. (2010). Temporal and spatial variations in phytoplankton productivity in surface waters of a warm-temperate, monomictic lake in New Zealand. *Hydrobiologia, 652*(1), 57-70.

Waipa District Council. (2007). *A plan for the management of peat lakes and associated reserves administered by the Waipa District Council*. Te Awamutu: Waipa District Council.

Weller, D. (2011). Detection, identification and toxigenicity of cyanobacteria in New Zealand lakes using PCR-based methods. *New Zealand Journal of Marine and Freshwater Research, 45*(4), 651-664.

Whitton, B. A., & Potts, M. (2007). *Ecology of Cyanobacteria: Their Diversity in Time and Space*. Dordrecht: Springer Netherlands.

Wilding, T. (2001). *Rotorua Lakes blue green algae monitoring* Rotorua Lakes 2001.

Wildland Consulting. (2011). *Vegetation assessment of Lake Rotongaro Wildlife Management Reserve.* . Prepared by Wildland Consultants for the Department of Conservation, Hamilton.

Willén, E. (1976). A simplified method of phytoplankton counting. *British Phycological Journal, 11*(3), 265-278.

Wood, S. A. (2004). *Bloom forming and toxic cyanobacteria in New Zealand.* thesis, Victoria University.

Wood, S. A., Crowe, A. L. M., Ruck, J. G., & Wear, R. G. (2005). New records of planktonic cyanobacteria in New Zealand freshwaters. *New Zealand Journal of Botany, 43*(2), 479-492.

Wood, S. A., Heath, M. W., Holland, P. T., Munday, R., McGregor, G. B., & Ryan, K. G. (2010a). Identification of a benthic microcystin-producing filamentous cyanobacterium (Oscillatoriales) associated with a dog poisoning in New Zealand. *Toxicon, 55*(4), 897-903.

Wood, S. A., Holland, P. T., Stirling, D. J., Briggs, L. R., Sprosen, J., Ruck, J. G., & Wear, R. G. (2006). Survey of cyanotoxins in New Zealand water bodies between 2001 and 2004. *New Zealand Journal of Marine and Freshwater Research, 40*(4), 585-597.

Wood, S. A., Prentice, M. J., Smith, K., & Hamilton, D. P. (2010b). Low dissolved inorganic nitrogen and increased heterocyte frequency: precursors to Anabaena planktonica blooms in a temperate, eutrophic reservoir. *Journal of plankton research, 32*(9), 1315-1325.

Wood, S. A., Puddick, J., Hawes, I., Steiner, K., Dietrich, D. R., & Hamilton, D. P. (2021). Variability in microcystin quotas during a Microcystis bloom in a eutrophic lake. *Plos one, 16*(7), e0254967.

Wood, S. P., J. Thomson-Laing, G. Hawes, I. Safi, K. McBride, G. Hamilton, D. (2018). *Review of the 'New Zealand Guidelines for Cyanobacteria in Recreation Fresh Waters' - 2018.* . Prepared for the New Zealand Ministry for the Environment. Cawthron Report No. 3233.

Wu, N., Daniel, A. J., & Tempero, G. W. (2013). *Fish biomass and gonad development in the Rotopiko (Serpentine) lakes.* University of Waikato.

Xi, H., Hieronymi, M., Röttgers, R., Krasemann, H., & Qiu, Z. (2015). Hyperspectral Differentiation of Phytoplankton Taxonomic Groups: A Comparison between Using Remote Sensing Reflectance and Absorption Spectra. *Remote sensing (Basel, Switzerland), 7*(11), 14781-14805.

Zhang, Y., Jeppesen, E., Liu, X., Qin, B., Shi, K., Zhou, Y., Thomaz, S. M., & Deng, J. (2017). Global loss of aquatic vegetation in lakes. *Earth-Science Reviews, 173*, 259-265.

Zhou, Y., Zhang, Y., Li, F., Tan, L., & Wang, J. (2017). Nutrients structure changes impact the competition and succession between diatom and dinoflagellate in the East China Sea. *Science of the Total Environment, 574*, 499-508.

Zhu, W., Yu, Q., Tian, Y. Q., Becker, B. L., & Carrick, H. (2014). Issues and potential improvement of multiband models for remotely estimating chlorophyll-a in complex inland waters. *IEEE Journal of Selected Topics in Applied Earth Observations and Remote Sensing, 8*(2), 562-575.

Appendices

6.3 Appendix A: Biovolume Results

Table A1: Biovolume used for each phytoplankton taxa counted in all lakes.

Phytoplankton taxa	BV um^3
Cyanobacteria	
Aphanocapsa	1.9
Coelosphaerium	14.5
Dolichospermum (coil)	176.7
Dolichospermum (straight)	314.4
Microcystis sp *small*	24.6
Microcystis sp *large*	97
Microcystis wesenbergii	130.1
Diatom	
Acanthoceras	6361.7
Asterionella	502.3
Aulacoseira granulata var *angustissmia*	438.6
Aulacoseira granulata var *spiralis*	300.3
Aulacoseira granulata	3041.7
Cocconeis	2102.1
Cyclotella	2503.7
Cymbella	2520
Epithemia	375
Fragilaria	630.8
Navicula	551.8
Nitzschia	290.7
Rhizosolenia	1381.7
Synedra	135
Surirella	1178
Tabellaria	450
Diatom species # 1	
Euglenoids	
Euglena	637
Phacus	22205.2
Trachelomonas	2242.5
Yellow - brown	
Dinobryon	149

Phytoplankton taxa	BV um^3
Green algae	
Actinastrum	29
Ankistrodesmus	29.1
Ankyra	14.8
Botryococcus (colony)	15150
Chlamydomonas	205.4
Closterium	666.2
Coelastrum	78
Cosmarium	1099
Crucigenia	87
Desmidium	816.9
Dictyosphaerium	110.9
Elakatothrix	96.7
Eudorina	1282.5
Kirchneriella	84
Mougeotia	843.4
Nephrocytium	50.1
Oocystis	553.3
Pandorina	268
Pediastrum	226
Pseudokirchneriella	5
Quadrigula	51.5
Scenedesmus	99.1
Staurastrum	2503
Green species #1	229.8
Green species #2	235.9
Dinoflagellates	
Ceratium	28964
Peridinium	56506
Cryptophyceae	
Cryptomonas	1273
Non pigmented Protozoa/Pollen	
Protozoa sp. #1	46024
Protozoa sp. #2	8620.8
Pollen	118552.6

Table A2: Biovolume (BV mm^3 L^{-1}) per site and sampling month for all lakes sampled.

Lake Rotoma BV mm^3 L^{-1} TAXA	**Nov-19** Site 1	Site 2	**Dec-19** Site 1	Site 2	**Jan-20** Site 1	Site 2	**Feb-20** Site 1	Site 2	**May-20** Site 1	Site 2
Cyanobacteria										
Aphanocapsa										
Coelosphaerium										
Dolichospermum (coil)										
Dolichospermum (straight)										
Microcystis sp small										
Microcystis sp large										
Microcystis wesenbergii										
Total Cyano BV										
Diatom										
Acanthoceras										
Asterionella										0.0126
Aulacoseira granulata var angustissmia				0.0053						
Aulacoseira granulata var spiralis										
Aulacoseira granulata		0.0213								
Cocconeis	0.0252		0.0210						0.0063	
Cyclotella	0.0125	0.0075	0.0601		0.0451	0.0175			0.0075	
Cymbella										
Epithemia										0.0011
Fragilaria	0.0076	0.0202	0.1514	0.0896	0.0196	0.0713				0.0107
Navicula					0.0028					
Nitzschia	0.0009		0.0020	0.0026	0.0015	0.0009			0.0058	0.0032
Rhizosolenia	0.0166		0.0235	0.0345	0.0207	0.0566			0.0083	0.0111
Synedra						0.0004			0.0023	
Surirella										
Tabellaria										
Diatom species # 1										
Total Diatom BV	*0.0628*	*0.0490*	*0.2580*	*0.1320*	*0.0896*	*0.1467*			*0.0302*	*0.0387*
Green algae										
Actinastrum										
Ankistrodesmus										
Ankyra										
Botryococcus (colony)										
Chlamydomonas					0.0006				0.0105	0.0144
Closterium			0.0020	0.0060	0.0020					0.0040
Coelastrum										
Cosmarium		0.0011							0.0066	
Crucigenia										
Desmidium										
Dictyosphaerium	0.0008			0.0261	0.0023	0.0061				0.0324
Elakatothrix	0.0003		0.0060	0.0015	0.0010	0.0190				0.0021
Eudorina										
Kirchneriella										0.0018
Mougeotia										
Nephrocytium	0.0019	0.0014	0.0029	0.0155	0.0032	0.0004			0.0045	0.0010
Oocystis	0.0055	0.0039	0.0039	0.0326	0.0055	0.0077			0.0155	0.0033
Pandorina										
Pediastrum										
Pseudokirchneriella	0.0004	0.0002	0.0010	0.0004	0.0002	0.0004			0.0003	0.0003
Quadrigula					0.0016	0.0021				0.0011
Scenedesmus		0.0006	0.0041	0.0012	0.0026				0.0011	
Staurastrum	0.0050	0.0025			0.0250	0.0250				0.0150
green species #1	0.0103	0.0097			0.0154				0.0110	0.0136
green species #2				0.0038	0.0038					
Total Green BV	*0.0242*	*0.0194*	*0.0198*	*0.0870*	*0.0632*	*0.0607*			*0.0495*	*0.0890*
Euglenoids										
Euglena										
Phacus										
Trachelomonas					0.0067				0.0067	0.0067
Total Euglenoid BV					*0.0067*				*0.0067*	*0.0067*
Yellow - brown algae										
Dinobryon	0.0015	0.0016	0.0040	0.0088	0.0012	0.0097			0.0030	0.0109
Total Yellow BV	*0.0015*	*0.0016*	*0.0040*	*0.0088*	*0.0012*	*0.0097*			*0.0030*	*0.0109*
Dinoflagellates										
Ceratium										
Peridinium					0.1695					
Total Dino BV					*0.1695*					
Cryptophyceae										
Cryptomonas					0.0025				0.0038	
Total Crypto BV					*0.0030*				*0.0038*	
Total all groups	0.0885	0.0700	0.2819	0.2278	0.3265	0.2171			0.0865	0.1386
excl protozoa/pollen										
Non pigmented Protozoa/Pollen										
Protozoa species #1		0.0460	0.3222		0.6904					0.3682
Protozoa species #2									0.0517	0.0948
Pollen										
Total Protozoa/pollen BV		*0.0460*	*0.3222*		*0.6904*				*0.0517*	*0.4630*

Lake Rotoma BV mm^3 L^{-1} TAXA	Oct-20 Site 1	 Site 2	2nd Dec 20 Site 1	 Site 2	20th Dec 20 Site 1	 Site 2	Jan-21 Site 1	 Site 2	Feb-21 Site 1	 Site 2	Mar-21 Site 1	 Site 2
Cyanobacteria												
Aphanocapsa			0.0002	0.0002	0.0077	0.0018	0.0073	0.0042	0.0037	0.0051	0.0028	0.0052
Coelosphaerium												
Dolichospermum (coil)												
Dolichospermum (straight)												
Microcystis sp small												
Microcystis sp large												
Microcystis wesenbergii												
Total Cyano BV			*0.0002*	*0.0002*	*0.0077*	*0.0018*	*0.0073*	*0.0042*	*0.0037*	*0.0051*	*0.0028*	*0.0052*
Diatom												
Acanthoceras												
Asterionella	0.0427	0.0522							0.0020			
Aulacoseira granulata var *angustissmia*											0.0136	0.0061
Aulacoseira granulata var *spiralis*												
Aulacoseira granulata			0.0030		0.0152			0.0335				0.3741
Cocconeis			0.0021	0.0147	0.0063	0.0063	0.0084			0.0042	0.0084	
Cyclotella			0.0150	0.0050		0.0175			0.0025			
Cymbella			0.0025									
Epithemia							0.0015	0.0004	0.0004	0.0015	0.0008	0.0008
Fragilaria				0.0612	0.0050	0.0492	0.1009	0.0309	0.0196	0.0132	0.0366	0.1041
Navicula			0.0006	0.0006	0.0033	0.0022	0.0066	0.0017	0.0044	0.0077	0.0022	0.0033
Nitzschia			0.0003		0.0009	0.0026		0.0032	0.0009	0.0006		0.0006
Rhizosolenia			0.0041		0.0111	0.0041	0.0138	0.0193	0.0041	0.0055	0.0166	0.0221
Synedra				0.0001			0.0001					
Surirella											0.0024	0.0071
Tabellaria						0.0027						
Diatom species # 1												
Total Diatom BV	*0.0427*	*0.0522*	*0.0277*	*0.0816*	*0.0418*	*0.0847*	*0.1314*	*0.0889*	*0.0339*	*0.0328*	*0.0805*	*0.5182*
Green algae												
Actinastrum												
Ankistrodesmus												
Ankyra	0.00004	0.0036	0.0008	0.0008		0.0001	0.0001	0.0002	0.00004	0.0002	0.0001	
Botryococcus (colony)											0.0303	0.0303
Chlamydomonas					0.0023	0.0037		0.0014			0.0012	
Closterium	0.0033	0.0020								0.0013		
Coelastrum												
Cosmarium												
Crucigenia												
Desmidium												
Dictyosphaerium	0.0034		0.0032	0.0043		0.0029	0.0069	0.0035	0.0006	0.0045		
Elakatothrix				0.0011		0.0006		0.0011		0.0012	0.0015	0.0020
Eudorina												
Kirchneriella				0.0004								
Mougeotia												
Nephrocytium	0.0034	0.0016	0.0006	0.0006	0.0005	0.0001			0.0002	0.0003		
Oocystis	0.0083	0.0764	0.0238	0.0077	0.0028		0.0066	0.0017		0.0066	0.0044	
Pandorina												
Pediastrum												
Pseudokirchneriella	0.00002	0.00002	0.0001	0.0001	0.0002	0.0002	0.0005	0.0002	0.0003	0.0005	0.0007	0.0025
Quadrigula			0.0024		0.0016	0.0011		0.0003			0.0004	0.0015
Scenedesmus							0.0008					
Staurastrum		0.0075		0.0125				0.0075				
green species #1		0.0007	0.0014		0.0053	0.0074	0.0044	0.0034	0.0055	0.0018	0.0067	0.0062
green species #2												
Total Green BV	*0.0185*	*0.0917*	*0.0323*	*0.0275*	*0.0126*	*0.0159*	*0.0192*	*0.0193*	*0.0066*	*0.0165*	*0.0454*	*0.0425*
Euglenoids												
Euglena												
Phacus												
Trachelomonas			0.0224		0.0269	0.0404	0.0090	0.0157	0.0112	0.0269		
Total Euglenoid BV			*0.0224*		*0.0269*	*0.0404*	*0.0090*	*0.0157*	*0.0112*	*0.0269*		
Yellow - brown algae												
Dinobryon	0.0092	0.0058	0.0098	0.0121	0.0043	0.0122	0.0012	0.0021	0.0013	0.0018		
Total Yellow BV	*0.0092*	*0.0058*	*0.0098*	*0.0121*	*0.0043*	*0.0122*	*0.0012*	*0.0021*	*0.0013*	*0.0018*		
Dinoflagellates												
Ceratium												
Peridinium	0.2825					0.3390	0.1130			0.1130	0.1130	0.1130
Total Dino BV	*0.2825*					*0.3390*	*0.1130*			*0.1130*	*0.1130*	*0.1130*
Cryptophyceae												
Cryptomonas												
Total Crypto BV												
Total all groups	0.3529	0.1497	0.0700	0.1214	0.0664	0.4536	0.2721	0.1145	0.0455	0.1692	0.2417	0.6789
excl protozoa/pollen												
Non pigmented Protozoa/Pollen												
Protozoa species #1	1.0586	0.1381	0.1381	0.1381	0.4142	0.1381	0.2761			0.1841	0.4602	0.2761
Protozoa species #2							0.0345					
Pollen												
Total Protozoa/pollen BV	*1.0586*	*0.1381*	*0.1381*	*0.1381*	*0.4142*	*0.1381*	*0.3106*			*0.1841*	*0.4602*	*0.2761*

Lake Rotoiti BV mm^3 L^{-1} TAXA	Nov-19 Site 1	 Site 2	Dec-19 Site 1	 Site 2	Jan-20 Site 1	 Site 2	Feb-20 Site 1	 Site 2	May-20 Site 1	 Site 2
Cyanobacteria										
Aphanocapsa										
Coelosphaerium										
Dolichospermum (coil)			0.0055	0.0058		0.0023	0.0102		0.0110	0.0937
Dolichospermum (straight)	0.0069	0.0129	0.0138	0.0179	0.0063	0.0132		0.0283		
Microcystis sp small		0.0034	0.0027	0.0036		0.0049				0.0061
Microcystis sp large										
Microcystis wesenbergii						0.0066				
Total Cyano BV	*0.0069*	*0.0163*	*0.0220*	*0.0274*	*0.0063*	*0.0270*	*0.0102*	*0.0283*	*0.0110*	*0.0998*
Diatom										
Acanthoceras		0.0191						0.0191		
Asterionella										
Aulacoseira granulata var *angustissmia*	0.0197	0.0092		0.0154	0.0079			0.0075	0.0202	0.0061
Aulacoseira granulata var *spiralis*	0.2790	0.3399		0.0357		0.0021		0.0057	0.0078	
Aulacoseira granulata	0.0760	0.3194		0.0943	0.0122			0.0639	1.9315	1.0828
Cocconeis								0.0063		
Cyclotella	0.0150	0.0651	0.0025	0.0426					0.0125	0.0075
Cymbella										
Epithemia		0.0011			0.0008					
Fragilaria	0.0126	0.0681		0.1041	0.0902	0.0391	0.0183		0.2858	0.2246
Navicula	0.0017	0.0017	0.0017	0.0011	0.0221		0.0033	0.0083		
Nitzschia				0.0020	0.0052	0.0026	0.0006	0.0026	0.0015	0.0006
Rhizosolenia										
Synedra										
Surirella										
Tabellaria										
Diatom species # 1			0.0040	0.0130	0.0060	0.0100		0.0010	0.0090	
Total Diatom BV	*0.4041*	*0.8236*	*0.0082*	*0.3082*	*0.1443*	*0.0538*	*0.0222*	*0.1143*	*2.2682*	*1.3216*
Green algae										
Actinastrum										0.0008
Ankistrodesmus										
Ankyra										
Botryococcus (colony)							0.0606			
Chlamydomonas					0.0008	0.0162	0.0060	0.0105	0.0068	0.0113
Closterium	0.0040	0.0020	0.0020	0.0073	0.0087	0.0073	0.0040	0.0093		0.0013
Coelastrum	0.0041									
Cosmarium										
Crucigenia	0.0010				0.0008					
Desmidium					0.2557	0.0270				
Dictyosphaerium	0.0038	0.0051		0.0073		0.0039	0.0191	0.0258		0.0021
Elakatothrix				0.0004			0.0008		0.0017	
Eudorina					0.0231					
Kirchneriella						0.0028				
Mougeotia	0.0329	0.0236	0.0008	0.1569	0.0127	0.0127		0.0101		
Nephrocytium						0.0002	0.0016	0.0017		0.0011
Oocystis		0.0055	0.0022		0.1295	0.0205	0.0083	0.0077	0.0243	0.0077
Pandorina										
Pediastrum										
Pseudokirchneriella				0.00002				0.00002		
Quadrigula										0.0010
Scenedesmus										0.0024
Staurastrum	0.0200	0.2052	0.0851	0.0325	0.0050			0.0050		
green species #1	0.0018		0.0037	0.0080	0.0034	0.0041	0.0080	0.0011	0.0136	0.0159
green species #2			0.0316							
Total Green BV	*0.0676*	*0.2415*	*0.1254*	*0.2125*	*0.4396*	*0.0946*	*0.1083*	*0.0713*	*0.0464*	*0.0436*
Euglenoids										
Euglena										
Phacus										
Trachelomonas	0.0135		0.0022	0.0045			0.0090		0.0067	
Total Euglenoid BV	*0.0135*		*0.0022*	*0.0045*			*0.0090*		*0.0067*	
Yellow - brown algae										
Dinobryon	0.0247	0.0180		0.0079	0.0006					0.0010
Total Yellow BV	*0.0247*	*0.0180*		*0.0079*	*0.0006*					*0.0010*
Dinoflagellates										
Ceratium										
Peridinium			0.1695				0.3390	0.1695		
Total Dino BV			*0.1695*				*0.3390*	*0.1695*		
Cryptophyceae										
Cryptomonas					0.0025	0.0051				
Total Crypto BV					*0.0025*	*0.0051*				
Total all groups	0.5168	1.0994	0.3274	0.5604	0.5934	0.1806	0.4887	0.3835	2.3323	1.4660
excl protozoa/pollen										
Non pigmented Protozoa/Pollen										
Protozoa species #1			0.5983		0.1841	0.3222	0.7824	0.4142	0.1381	
Protozoa species #2		0.0690			0.0345	0.0345				
Pollen	0.3557									
Total Protozoa/pollen BV	*0.3557*	*0.0690*	*0.5983*		*0.2186*	*0.3567*	*0.7824*	*0.4142*	*0.1381*	

Lake Rotoiti BV mm^3 L^{-1} TAXA	Oct-20 Site 1	 Site 2	2nd Dec 20 Site 1	 Site 2	20th Dec 20 Site 1	 Site 2	Jan-21 Site 1	 Site 2	Feb-21 Site 1	 Site 2	Mar-21 Site 1	 Site 2
Cyanobacteria												
Aphanocapsa											0.0032	0.0003
Coelosphaerium												
Dolichospermum (coil)	0.0396	0.0601		0.0115	0.1145	0.0014			0.0021	0.0028	0.0399	
Dolichospermum (straight)	0.0368	0.0013	0.0069	0.0604	0.0849	0.1229	0.0163		0.0729		0.0079	
Microcystis sp small												
Microcystis sp large						0.0015				0.0020		
Microcystis wesenbergii												
Total Cyano BV	*0.0764*	*0.0613*	*0.0069*	*0.0719*	*0.1994*	*0.1258*	*0.0163*		*0.0751*	*0.0049*	*0.0510*	*0.0003*
Diatom												
Acanthoceras											0.1336	0.0763
Asterionella				0.0116	0.0080						0.0146	
Aulacoseira granulata var *angustissmia*		0.0009		0.0044			0.0114			0.0018		
Aulacoseira granulata var *spiralis*		0.0003		0.0009						0.0105	0.0309	0.0075
Aulacoseira granulata	0.1095		0.0183	0.0183			0.0487		0.0183	0.0243		0.2707
Cocconeis					0.0042		0.0021					
Cyclotella		0.0075		0.0050			0.0075				0.0401	
Cymbella												
Epithemia					0.0015	0.0019					0.0008	0.0015
Fragilaria	0.0637	0.0013	0.0038	0.0145	0.0063		0.0574			0.1426		0.2403
Navicula	0.0017				0.0011	0.0028	0.0022		0.0033	0.0022	0.0022	0.0011
Nitzschia	0.0006	0.0003	0.0003	0.0009	0.0061	0.0015	0.0009		0.0017	0.0073	0.0041	0.0035
Rhizosolenia												
Synedra							0.0001			0.0003		0.0003
Surirella												
Tabellaria												
Diatom species # 1	0.0010									0.0035	0.0360	0.0330
Total Diatom BV	*0.1764*	*0.0102*	*0.0223*	*0.0555*	*0.0273*	*0.0061*	*0.1303*		*0.0233*	*0.1924*	*0.2622*	*0.6343*
Green algae												
Actinastrum				0.0003							0.0003	
Ankistrodesmus												
Ankyra							0.0001		0.0003	0.0004		
Botryococcus (colony)							0.0455			0.0303		0.0303
Chlamydomonas	0.0053	0.0031	0.0010	0.0090	0.0088	0.0111	0.0010			0.0249	0.0739	0.0407
Closterium	0.0013	0.0013		0.0020	0.0127	0.0153	0.0047		0.0013	0.0027	0.0107	0.0107
Coelastrum												
Cosmarium												
Crucigenia												
Desmidium	0.0343			0.0082	0.0253	0.0760						
Dictyosphaerium	0.0035		0.0045	0.0014	0.0078		0.0053		0.0103	0.0073	0.0114	0.0395
Elakatothrix			0.0005				0.0008		0.0038	0.0052	0.0004	
Eudorina											0.0603	
Kirchneriella												
Mougeotia	0.1080	0.0169	0.0641	0.0464	0.0725	0.1695	0.0439			0.0034	0.0194	0.0101
Nephrocytium												
Oocystis		0.0039	0.1444	0.1007	0.0127	0.0083	0.0094		0.0083	0.0044	0.0089	0.0138
Pandorina						0.0088						
Pediastrum												
Pseudokirchneriella			0.00001							0.00002		
Quadrigula			0.0016	0.0023			0.0003			0.0004		
Scenedesmus					0.0004							
Staurastrum		0.0025					0.0025		0.0050			0.0100
green species #1		0.0037		0.0014	0.0085	0.0124	0.0074		0.0106	0.0103		0.0198
green species #2												
Total Green BV	*0.1525*	*0.0313*	*0.2162*	*0.1717*	*0.1487*	*0.3015*	*0.1207*		*0.0395*	*0.0894*	*0.1853*	*0.1748*
Euglenoids												
Euglena												
Phacus												
Trachelomonas		0.0022		0.0112	0.0224	0.0336	0.0157			0.0045	0.0090	0.0090
Total Euglenoid BV		*0.0022*		*0.0112*	*0.0224*	*0.0336*	*0.0157*			*0.0045*	*0.0090*	*0.0090*
Yellow - brown algae												
Dinobryon	0.0307	0.0021	0.0039	0.0113	0.0018	0.0215				0.0012		0.0024
Total Yellow BV	*0.0307*	*0.0021*	*0.0039*	*0.0113*	*0.0018*	*0.0215*				*0.0012*		*0.0024*
Dinoflagellates												
Ceratium												
Peridinium					0.2260		0.0565		0.1130	0.2260	0.1130	0.2260
Total Dino BV					*0.2260*		*0.0565*		*0.1130*	*0.2260*	*0.1130*	*0.2260*
Cryptophyceae												
Cryptomonas	0.0038	0.0025									0.0025	0.0025
Total Crypto BV	*0.0038*	*0.0025*									*0.0025*	*0.0025*
Total all groups	0.4398	0.1098	0.2493	0.3216	0.6256	0.4884	0.3395		0.2509	0.5183	0.6230	1.0494
excl protozoa/pollen												
Non pigmented Protozoa/Pollen												
Protozoa species #1	0.2301	0.0460	0.0460	0.0920	0.5523	0.4602			0.1841	0.2761	0.5523	0.2761
Protozoa species #2	0.0172			0.0172			0.0690			0.0172	0.1207	0.3017
Pollen												
Total Protozoa/pollen BV	*0.2474*	*0.0460*	*0.0460*	*0.1093*	*0.5523*	*0.4602*	*0.0690*		*0.1841*	*0.2934*	*0.6730*	*0.5779*

Lake Rotoehu BV mm^3 L^{-1} TAXA	Nov-19 Site 1	 Site 2	Dec-19 Site 1	 Site 2	Jan-20 Site 1	 Site 2	Feb-20 Site 1	 Site 2	May-20 Site 1	 Site 2
Cyanobacteria										
Aphanocapsa										
Coelosphaerium	0.002			0.0043			0.002204			
Dolichospermum (coil)	0.013	0.0102			0.0601	0.0122				
Dolichospermum (straight)				0.0566			0.017921	0.016034		
Microcystis sp small	0.003	0.0029			0.0051	0.0029				
Microcystis sp large										
Microcystis wesenbergii							0.346066	0.053601	0.066741	0.0290
Total Cyano BV	0.018	*0.0131*		*0.0609*	*0.0652*	*0.0150*	*0.366191*	*0.069636*	*0.066741*	*0.0290*
Diatom										
Acanthoceras										
Asterionella	0.498	0.4998								
Aulacoseira granulata var *angustissmia*	0.033	0.0329		0.0105	0.0066	0.0101		0.178072	0.008333	
Aulacoseira granulata var *spiralis*							0.025526			
Aulacoseira granulata	0.167	0.1247	0.0943	0.0274	4.3679	2.0197	0.705674	0.611382	0.10646	0.6357
Cocconeis					0.0168	0.0084				0.0063
Cyclotella					0.0200	0.0100				
Cymbella										
Epithemia								0.001875		
Fragilaria	0.363	0.3545	0.7866	0.5904	1.7625	0.3066			0.034063	0.0132
Navicula	0.008	0.0055	0.0033	0.0028					0.004414	
Nitzschia			0.0035		0.0067		0.002616	0.001454	0.007849	0.0020
Rhizosolenia										
Synedra				0.0012						
Surirella										
Tabellaria										
Diatom species # 1										
Total Diatom BV	1.069	*1.0174*	*0.8877*	*0.6323*	*6.1804*	*2.3548*	*0.733816*	*0.792782*	*0.161119*	*0.6573*
Green algae										
Actinastrum										
Ankistrodesmus										
Ankyra										
Botryococcus (colony)					0.1212		0.4242	0.3939		0.1061
Chlamydomonas	0.011	0.0105							0.031015	0.0134
Closterium	0.013	0.0067	0.0093	0.0093		0.0053			0.00533	0.0113
Coelastrum	0.003	0.0027		0.0034						
Cosmarium		0.0154								
Crucigenia										
Desmidium	0.297	0.7564		0.1748		0.2361				
Dictyosphaerium	0.011	0.0122	0.1324	0.0211		0.0150				
Elakatothrix				0.0009			0.00087	0.002031		
Eudorina			0.1937							
Kirchneriella				0.0096		0.0039				0.0012
Mougeotia	0.018	0.0202	0.0228		0.0067	0.0160	0.059881	0.060725		
Nephrocytium	0.001	0.0009	0.0011	0.0005		0.0006	0.001904	0.000501		0.0011
Oocystis	0.034	0.0360	0.1328	0.1289	0.1665	0.1450	0.068056	0.011619	0.021579	0.0116
Pandorina								0.005628		
Pediastrum										
Pseudokirchneriella					0.0001		0.00007	0.00005	0.00002	0.0001
Quadrigula						0.0008	0.000979			
Scenedesmus	0.003	0.0027	0.0055			0.0015				
Staurastrum	0.025	0.0075	0.0175	0.0476	0.0375	0.0100	0.035042		0.030036	
green species #1	0.012	0.0149	0.0142	0.0600	0.1312	0.0142	0.046879	0.023669	0.014248	0.0221
green species #2	0.003	0.0057	0.0050							
Total Green BV	0.432	*0.8917*	*0.5342*	*0.4559*	*0.4633*	*0.4484*	*0.637881*	*0.498123*	*0.102227*	*0.1667*
Euglenoids										
Euglena										
Phacus										0.0666
Trachelomonas	0.070	0.0314	0.1233	0.1480	0.0875		0.085215	0.069518	0.02691	0.0381
Total Euglenoid BV	0.070	*0.0314*	*0.1233*	*0.1480*	*0.0875*		0.085215	0.069518	0.02691	*0.1047*
Yellow - brown algae										
Dinobryon				0.0036						
Total Yellow BV				*0.0036*						
Dinoflagellates										
Ceratium										
Peridinium				0.5086	1.2996	0.2260	5.6506	10.17108	1.525662	3.2773
Total Dino BV				*0.5086*	*1.2996*	*0.2260*	*5.6506*	*10.17108*	*1.525662*	*3.2773*
Cryptophyceae										
Cryptomonas			0.0267	0.0484			0.0051	0.0064		
Total Crypto BV			*0.0267*	*0.0484*			*0.0051*	*0.0064*		
Total all groups	1.5883	1.9536	1.5720	1.8577	8.0961	3.0442	7.4788	11.6075	1.8827	4.2351
Non pigmented Protozoa/Pollen										
Protozoa species #1							0.4142			
Protozoa species #2							0.0776		0.0345	
Pollen										
Total Protozoa/pollen BV							*0.4918*		*0.0345*	

Lake Rotoehu BV $mm^3 L^{-1}$ TAXA	Oct-20 Site 1	 Site 2	2nd Dec 20 Site 1	 Site 2	20th Dec 20 Site 1	 Site 2	Jan-21 Site 1	 Site 2	Feb-21 Site 1	 Site 2	Mar-21 Site 1	 Site 2
Cyanobacteria												
Aphanocapsa											0.0008	0.0036
Coelosphaerium					0.0276							
Dolichospermum (coil)	0.2518	0.0739	0.1785	0.2663	0.3071	0.3891	0.1115	0.0659	0.3479	0.3601	0.0037	0.0051
Dolichospermum (straight)	0.0101	0.0113	0.0258	0.0519			0.0321	0.0047	0.1622	0.0531	0.0016	
Microcystis sp small			0.0048	0.0085	0.0269		0.0026		0.0474	0.0404	0.0642	0.0887
Microcystis sp large						0.1557	0.0094					
Microcystis wesenbergii	0.1309	0.0343		0.1183	0.1236	0.0468	0.1118	0.1492	0.4655	0.3609	0.0215	0.0688
Total Cyano BV	*0.3927*	*0.1195*	*0.2091*	*0.4449*	*0.4851*	*0.5916*	*0.2674*	*0.2198*	*1.0230*	*0.8145*	*0.0918*	*0.1662*
Diatom												
Acanthoceras								0.0763				
Asterionella				0.0151								
Aulacoseira granulata var *angustissmia*	0.0009		0.0039	0.0022			0.0246	0.0311	0.0781	0.1715		
Aulacoseira granulata var *spiralis*										0.0357		
Aulacoseira granulata	0.0061	0.0760	0.1612	0.3224	0.2160	0.9064			0.2099	0.0639	0.7604	0.9490
Cocconeis						0.0210						
Cyclotella	0.0175							0.0150	0.0275	0.0100		0.0075
Cymbella												
Epithemia							0.0030	0.0011	0.0015		0.0011	0.0011
Fragilaria	0.3671	0.0650	0.1949	0.3097	0.7727	4.9985	0.0170					0.0776
Navicula								0.0033	0.0022	0.0022	0.0011	0.0066
Nitzschia	0.0012	0.0020			0.0026		0.0055	0.0052			0.0006	
Rhizosolenia												
Synedra	0.0005						0.0007	0.0004				
Surirella												
Tabellaria												
Diatom species # 1												
Total Diatom BV	*0.3933*	*0.1430*	*0.3601*	*0.6494*	*0.9913*	*5.9259*	*0.0508*	*0.1326*	*0.3192*	*0.2833*	*0.7632*	*1.0419*
Green algae												
Actinastrum												
Ankistrodesmus												
Ankyra				0.0020	0.0025	0.0044		0.0001				
Botryococcus (colony)				0.0758								
Chlamydomonas			0.0008					0.0066	0.0014	0.0008		
Closterium	0.0027				0.0033		0.0053	0.0100	0.0047			
Coelastrum												
Cosmarium												
Crucigenia												
Desmidium		0.0506		0.0359		0.7564						
Dictyosphaerium		0.0040			0.1569	0.1780			0.0161	0.0035		0.0027
Elakatothrix	0.0004	0.0009			0.0064			0.0006			0.0016	0.0034
Eudorina	0.0590											
Kirchneriella												
Mougeotia			0.0017	0.0127		0.0953	0.0995	0.1611				
Nephrocytium							0.0008					
Oocystis	0.0077	0.0149	0.0160		0.2340	0.5179	0.0221	0.0343	0.0504	0.0891	0.1948	0.3480
Pandorina			0.0029	0.0054	0.0153	0.0386						
Pediastrum												
Pseudokirchneriella												
Quadrigula							0.0006	0.0006				
Scenedesmus												
Staurastrum							0.0075	0.0075		0.0200		
green species #1	0.0011		0.0025	0.0016	0.0055	0.0283	0.0129	0.0209	0.0818	0.0094	0.0067	
green species #2												
Total Green BV	*0.0709*	*0.0704*	*0.0240*	*0.1333*	*0.4240*	*1.6189*	*0.1487*	*0.2417*	*0.1543*	*0.1229*	*0.2031*	*0.3541*
Euglenoids												
Euglena												
Phacus												
Trachelomonas	0.0112	0.0179	0.0493	0.0224	0.0426	0.0224	0.0112	0.0269		0.0090	0.0202	0.0135
Total Euglenoid BV	*0.0112*	*0.0179*	*0.0493*	*0.0224*	*0.0426*	*0.0224*	*0.0112*	*0.0269*		*0.0090*	*0.0202*	*0.0135*
Yellow - brown algae												
Dinobryon												
Total Yellow BV												
Dinoflagellates												
Ceratium	0.1448		0.0579									
Peridinium	2.5993	3.5034	0.1130	0.1130	0.2825			0.3390				
Total Dino BV	*2.7441*	*3.5034*	*0.1709*	*0.1130*	*0.2825*			*0.3390*				
Cryptophyceae												
Cryptomonas											0.0025	0.0025
Total Crypto BV											*0.0025*	*0.0025*
Total all groups	3.6123	3.8543	0.8134	1.3631	2.2256	8.1589	0.4781	0.9600	1.4965	1.2297	1.0808	1.5782
Non pigmented Protozoa/Pollen												
Protozoa species #1		0.3222		0.0920							0.0920	0.5523
Protozoa species #2	0.0345	0.0345			0.0431	0.086208					0.0259	
Pollen												
Total Protozoa/pollen BV	*0.0345*	*0.3567*		*0.0920*	*0.0431*	*0.086208*					*0.1179*	*0.5523*